PETRO-CHEMICAL INVESTIGATIONS OF THE ROCKS OF GOLO DAS AND SURROUNDING AREAS GILGIT-BALTISTAN, PAKISTAN IN THE PERSPECTIVE OF GOLD AND BASE METALS MINERALIZATION

BY

LAWANGIN SHEIKH

Thesis submitted to the National Centre of Excellence in Geology, University of Peshawar for partial fulfillment of requirements for the Degree of M.S in Geology.

NATIONAL CENTRE OF EXCELLENCE IN GEOLOGY
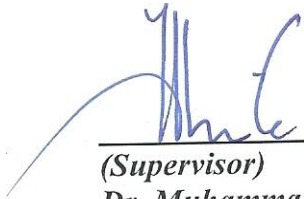
UNIVERSITY OF PESHAWAR, PAKISTAN

2013

APPROVED BY

(Examiner)
Dr. Muhammad Hassan Agheem
Associate Professor
Centre for Pure and Applied Geology
University of Sindh, Jamshoro

(Supervisor)
Dr. Muhammad Tahir Shah
Professor
National Centre of Excellence in Geology
University of Peshawar
Peshawar

(Director)
Prof. Dr. M. Asif Khan (T.I)
National Centre of Excellence in Geology
University of Peshawar
Peshawar

Dissertation Acceptance Certificate

I hereby declare that the work presented in this dissertation is original (excluding where referred) and has not been used for the award of any degree by any university or institution.

Lawangin Sheikh (Author)

National Centre of Excellence in Geology (NCEG)

University of Peshawar

2012-2013.

DEDICATION

THIS RESEARCH WORK IS DEDICATED TO MY LOVING PARENTS

LIST OF CONTENTS

LIST OF FIGURES

LIST OF TABLES

ACKNOWLEDGEMENT

ABSTRACT

The study area which includes Golo Das and surrounding areas is a part of Ghizar district of Gilgit-Baltistan province. Geologically it is located just south of the northern suture zone (NSZ), a mega thrust separating the rocks of Karakoram plate from the Kohistan island arc. The rocks exposed in the study area are mainly basalt-andesite sheet dominant (BASD) volcanics and Ishkoman volcanic centre (IVC) volcanics of Ghizar formation intruded by stage-2 diorites of Kohistan batholith. The IVC volcanics are usually undeformed or less deformed while the BASD volcanics are highly deformed. These rocks of the study area are explored for finding the geochemical and petrographic characteristics as well as to find out the concentration of gold and silver and base metals associated with altered/sulfide zones.

Detailed petrographic study shows that the basalt-andesite sheet dominant volcanics have well developed foliation and mainly comprised of phenocrysts of hornblende and plagioclase in a cryptocrytalline groundmass having abundant chlorite and epidote. The rocks are highly tectonized as the phenocrysts of plagioclase and hornblende show preferred orientation and the laths of tremolite/actinolite are winding around these phenocrysts. Quartz micro-veins are common in these rocks. The volcanics rocks of the IVC dominantly comprised of phenocrysts of clinopyroxenes (augite) and plagioclase embedded in the felsophyric groundmass containing chlorite epidote and opaque minerals. These phenocrysts are generally fresh looking but partially altered phenocrysts are also present. Diorites of the study area are medium to coarse-grained. On the basis of petrography, two varieties of diorites are distinguished, one is having major amount of plagioclase, hornblende and biotite while the other has dominantly plagioclase, biotite and augite along with minor amount of quartz, alkali feldspar and opaque minerals. Zircon, apatite and garnet in traces are present as accessory minerals.

On the basis of whole rock geochemistry, the studied BASD volcanics are basaltic in composition while the IVC volcanics are classified as basalt-andesites. Both the volcanics are olivine normative. Major and trace element data show smooth fractionation trend for IVC volcanics while no significant fractionation trend is found in BASD volcanics. This could be attributed to the greater alteration noticed in the latter. The spider diagrams of both BASD and IVC volcanics indicate enrichment in large ion lithophile elments (LILE) relative to high field

strength element (HFSE) with well-defined negative Nb and positive Sr anomalies. The diorites (SiO_2 in the range of 59.78 to 61.65 wt %) are quartz normative. The major and trace element data in the Harker diagrams represent well-defined fractionation trend. These diorites also show enrichment in LILE relative to HFSE with well-defined negative and positive anomalies for Nb and Sr respectively.

The altered/sulfide-bearing sheared zones present within IVC volcanics are studied for chemical concentration of gold and silver and other base metals like Cu, Pb, Zn, Ni, Cr, Co, and Cd. The gain and loss of various metals in these zones suggest that there is an enrichment of Cu, Co, Ag and Au and depletion of Pb, Zn, Ni and Cr occur due to the hydrothermal alteration along these sheared zones. However, the concentrations of gold, silver and base metals in these zones are not anomalous and are, therefore, of no economic significance.

Major and trace elements data of the studied Ghizar formation (i.e., BASD and IVC volcanics) and diorites are plotted on the discrimination diagrams. The data suggest that these rocks are akin to the fields defined for subduction related calc-alkaline rocks of island arc type of setting. These rocks are, therefore, displaying subduction related signature and are considered a part of the Cretaceous Kohistan island arc. On the basis of chemical characteristics, the rocks of the Ghizar formation, especially the IVC volcanics, are considered as the eastern extension of the Teru formation/Shamran volcanics.

CHAPTER 1

INTRODUCTION

1.1. Background

The northern areas of Pakistan are known for the occurrence of placer gold along the river beds for decades. However, the source rocks for these placer gold grains are still unknown. Various stream sediment surveys have been conducted in the past to delineate areas of interest for further detail work. The present study has been carried out in the Golo Das and surrounding areas of Gilgit-Baltistan region as follow up studies of the previous investigations. Panning of stream sediments for gold in northern Pakistan is an old technique used by gold washers along Gilgit, Chitral, Hunza and Indus rivers in northern Pakistan for decades. Mineralogy of stream sediments along these rivers was also described by Tahirkheli (1974). According to him gold and other heavy minerals concentrates in the stream sediments in these rivers show irregular pattern. Geochemical studies of the stream sediments carried out by the Austromineral in the northern areas of Pakistan confirmed occurrence of gold in Indus and Gilgit rivers (Austromineral, 1976; 1978).

Detailed geochemical survey of stream sediments in the northern areas of Pakistan was carried out by Australian Agency for International Development (AusAID) in collaboration with Sarhad Development Authority (SDA) and Pakistan Mineral Development Corporation (PMDC) under a project named as Gold Exploration and Mineral Analysis Project (GEMAP). They collected panned concentrates and minus 80 mesh (-80#) samples from different drainage cells and prepared geochemical base maps for most parts of the Gilgit-Baltistan (GB) region in the perspective of gold and base metals (Sweatman et al., 1995). Later on M/s MINORCO an Australian company re-analyzed already collected samples by SDA and PMDC for multi-element geochemistry and defined distribution patterns of elements, especially Au in the northern parts of Pakistan (Halfpenny and Mazzucchelli, 1999).

The occurrence of gold grains in the stream sediments is a clue that it is the result of weathering of rocks in the upper reaches of the Gilgit-Baltistan terrane. The study conducted under a project GEMAP suggests the relationship of the gold occurrence with the major tectonic zones present in this terrane. PMDC marked some of the areas in northern Pakistan, the rocks of

1

which have anomalous gold concentration including the study area. All the zones pointed out by PMDC are along the northern suture zone (NSZ) or main Karakoram thrust (MKT), a mega thrust separating the rocks of the Eurasian plate from that of the Kohistan island arc (KIA).

1.2. Gilgit-Baltistan province

The study area lies in the Gilgit-Baltistan province of Pakistan and is accessed from Islamabad, capital of Pakistan, through Karakoram highway. It was previously known as federally administrated northern areas (FANA) of Pakistan. The two main towns in this province are Gilgit and Skardu. It is bounded by three mountain ranges namely Karakoram, Himalayas and Hindukush. Geographically it is connected to Afghanistan in the northwest, to China in the northeast and Province of Khyber Pakhtunkhwa in the southwest. It is the home of many largest mountain peaks and five of the mountain peaks are more than 8000 m high.

1.3. Location of the study area

The study area, covering Golo Das and surrounding areas in the Ghizar district, is located at a distance of 70 km northwest of Gilgit, a capital city of Gilgit-Baltistan province, Pakistan. It is located north of Gahkuch town, a capital of the Ghizar district. Golo Das is not a town, but this is the area which got importance due to the occurrence of alteration zones having sulfide mineralization. This area has, therefore, been selected for the possible occurrence of gold mineralization as the gold particles have been reported by PMDC in the sediments of a stream flowing through this area. The study area is lying between latitude 36° 10' 20" N to 36° 27' 00" N and longitude 73° 45' 20" to 73° 55' 10" E on the survey of Pakistan toposheet No. 42 H/16 and 42H/15. It lies in the northwestern most part of the Kohistan Island arc, adjacent to the northern suture zone or main Karakoram thrust, a major thrust separating the Kohistan island arc from Karakoram plate (Figs.1.1 and 1.2).

1.4. Climate and topographic relief

The climatic conditions in this region are very extreme and the hottest months are June and July in which the temperature reaches upto 40°C and in winter the temperature reaches upto minus 20°C. It is a region where monsoon cannot reach and, therefore, this terrane is classified as high altitude desert environment with very steep slopes. The relief of this terrane is extreme. K2,

the second highest mountain (8611m) of the world is located in the northeast of Gilgit-Baltistan province, while the Rakaposhi mountain (7788m) is located between the towns of Gilgit and Skardu.

1.5. Previous work

Gilgit-Baltistan region has a very complex set up in the context of geology and tectonic. Therefore, many workers in the past carried out extensive work in the area. The earlier workers include Hayden (1914) who defined various geological units in the Gilgit and Chitral regions for the first time. Ivanac et al. (1956) studied the volcanic rocks in the northern Pakistan and assigned them different names. The northern areas of Pakistan were unmapped on the first geological map published by geological survey of Pakistan in 1964. After the construction of Karakoram Highway, which is the only on ground access to the Gilgit-Baltistan region of Pakistan. Detailed geological work was conducted by various workers and they demarcated an intra-oceanic island arc named as Kohistan island arc (Tahirkheli et al., 1979; Klootwijik et al., 1979; Bard et al., 1980; Bard, 1983). Their studies showed that this region is formed as a result of mega tectonic process which caused northward subduction of the Neo-Tethyan oceanic lithosphere. Petterson and Windley (1985, 1991) did work on the volcanic sequences and Kohistan batholith exposed in this region. Geological work along the northern suture zone, which separates the rocks of Kohistan island arc from the rocks of Eurasian plate, was conducted by Pudsey, (1986) and Pudsey et al. (1985). The other workers such as Searle (1991), Kazmi and Jan (1997), Khan et al. (1989), Coward et al. (1982, 1986, 1987), Khan et al. (1995, 1996, 2007, 2011), Rehman et al (2011) carried out detail work in the context of geology and geotectonic setting of this region.
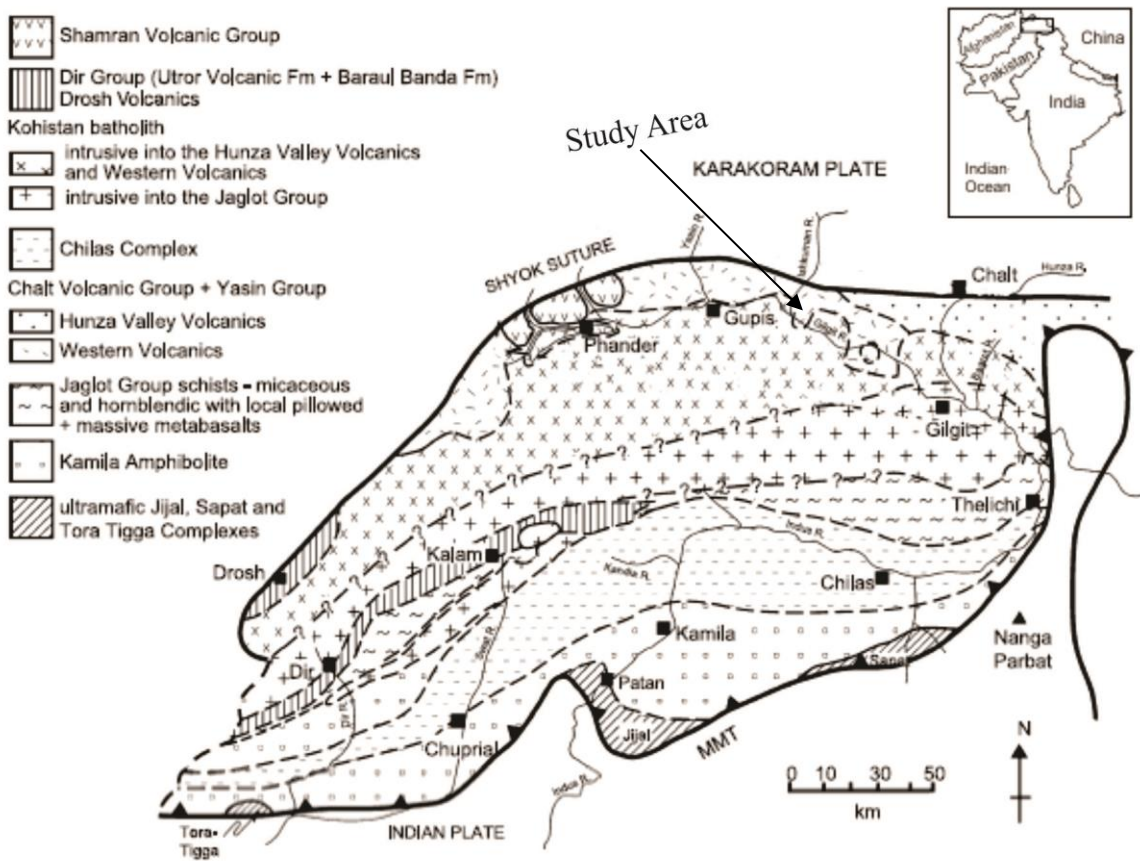
Fig.1.1. Geological map of Kohistan Island arc showing the location of study area (after Treloar et al., 1996).
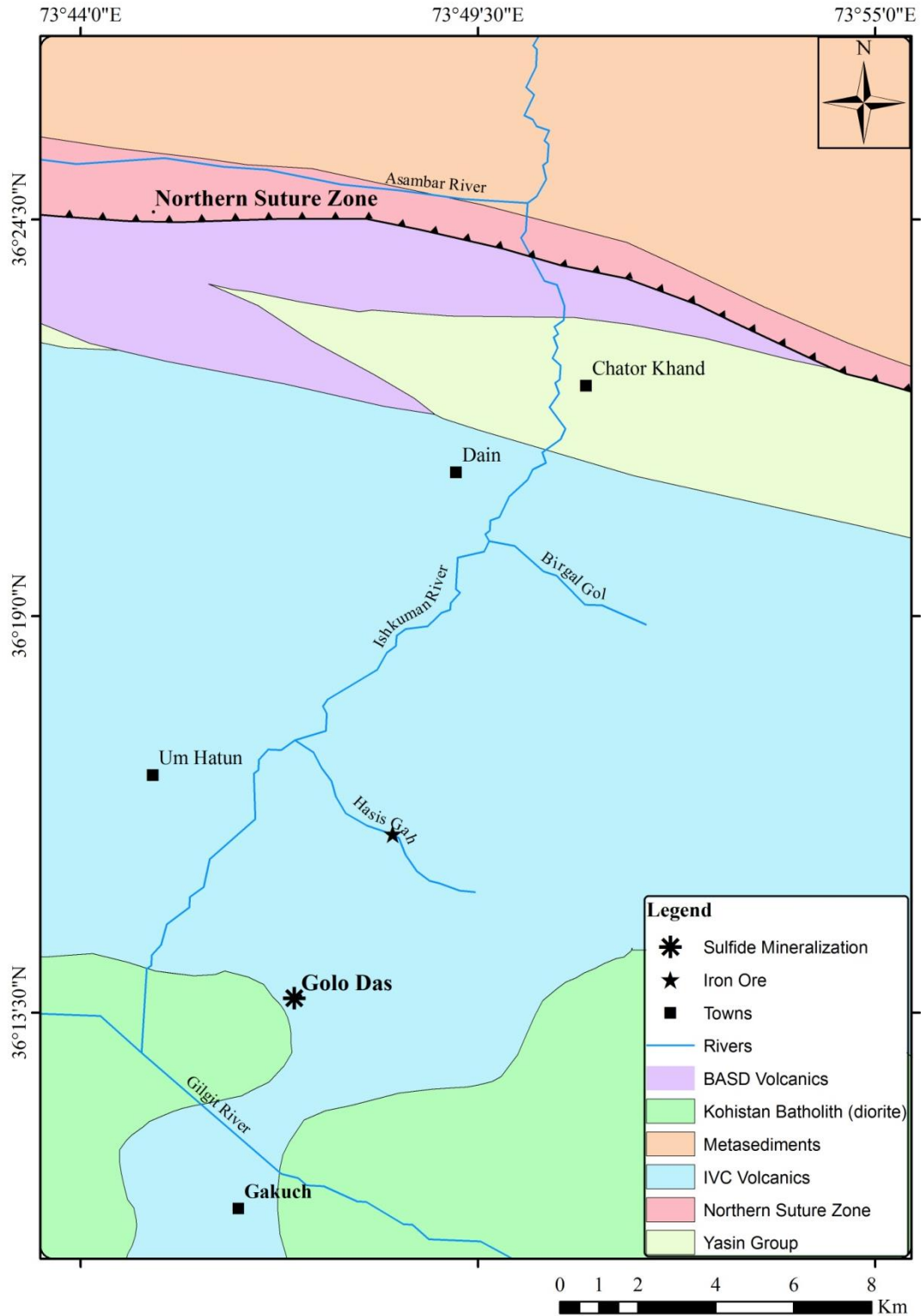
Fig.1.2. Geological map of the study area including Golo Das and surrounding areas. (compiled from Searle and Khan, 1996; Petterson and Treloar, 2004).

1.6. Present investigation

Considering the stream sediments surveys conducted so far, it is noted that the drainage system of the study area has the potential for Au and base metal concentration contributed by the weathering of bed rocks exposed in the drainage cells (catchment areas). The present study is, therefore, aimed at carrying out petro-chemical account of the rocks and associated alteration zone for the possibility of occurrence of gold and other base metals mineralization in the area. This study includes the collection of representative rock samples in the form of bulk (>10kg) and grab (<1kg) samples, their geochemical analysis in order to find out the source rock, if any, which contribute gold particles in the stream sediments of the area. This study will also help in finding out the geochemical affiliation of the rocks of the study area to the specific paleotectonic environments.

1.7. Aims and objectives

Following are the aims and objectives of this study:

- Identification of alteration/sulfide zone in the area
- Petrographic and geochemical investigations of the igneous rocks of the area in the context of their genesis
- Evaluation of gold, silver and base metal concentration in specific altered/sulfide zones
- Identification of source rocks for gold, if any, for further follow-up program

CHAPTER 2
REGIONAL GEOLOGY

The tectonic evolution of the Kohistan-Ladakh island arc (KLIA) in the Himalaya-Karakoram region is the result of collision of Indo-Pakistan and Asian plates with the closure of the Tethys. The KLIA is an intra-oceanic Cretaceous island arc which is welded to Indo-Pakistan plate along Southern suture and to Asian plate along Northern suture. The development of KLIA and the occurrence of suture zones on the northern and southern margins of KLIA is well understood and widely accepted. However, the timing of the collision of the KLIA with Indo-Pakistan and Asian plates, is still controversial. There are two groups of scientists who are proposing different timing of collision of KLIA with Indo-Pakistan and Asian plates. One group is suggesting the collision of KLIA first with Asian plate during 102-75Ma and then with Indo-Pakistan plate during 55-50Ma (Molnar and Tapponnier, 1975; Petterson and Windley, 1985; Treloar et al., 1989, 1996, 2003; Hanson, 1989; Beck et al, 1995; Rowley, 1996; Clift et al., 2002; Bignold and Treloar, 2003; Rehman et al., 2011). The second group of geoscientist is of the opinion that the KLIA first collided with Indo-Pakistan between 95-60Ma before its collision with Asian plate (Tahirkheli, 1979; Sharma and Gupta, 1983; Scharer et al., 1984; Reuber, 1986; Corfield et al., 1999, 2001, Yin and Harrison, 2000; Ziabrev et al., 2004; Ding et al., 2005, Yin, 2006, Khan et al., 2009; Chatterjee et al., 2013).

2.1. Geology of northern Pakistan

Gilgit-Baltistan region is covering most part of the northern areas of Pakistan. The northern areas of Pakistan are mainly comprised of three tectonic plates. From north to south, these are Karakoram plate, Kohistan island arc and Indo-Pakistan plate. Kohistan island arc is sandwiched between Karakoram and Indo-Pakistan plates by having two main thrusts the NSZ or MKT in the north and the Indus Suture zone (ISZ) or Main mantle thrust (MMT) in the south (Fig. 2.1) (Tahirkheli, 1979; 1982; Bard, 1983). The GB region is mainly composed of the rocks of the Karakoram plate (i.e., meta-sedimentary and meta-igneous complexes), northern suture zone (i.e., Ophiolitic melanges) and Kohistan island arc (i.e., mafic-ultramafic complex and batholithic plutons) (Pudsey et al., 1985). The timing of collision of Indian plate with the KIA along the ISZ is Eocene and the KIA collided with the Eurasian plate along the NSZ between 80

and 100 Ma (Searle, 1991; Treloar et al., 1989). The development of back-arc basin with the Kohistan island arc has been given for the first time by Khan (1994).

2.1.1. Karakoram plate

Karakoram plate represents the northern most part of Pakistan and is located on the northern side of NSZ or MKT. The rock bodies exposed here are highly deformed sedimentary, meta-sedimentary and igneous assemblages and they are ranging in age from Jurassic to Late Cretaceous and formed as a result of collision between KIA with Eurasian plate along NSZ or MKT (Tahirkheli, 1982). Karakoram plate is divided by Gaetani et al. (1996) into the following three geological units from north to south as:

1. The northern sedimentary belt
2. The Karakoram axial batholith
3. The southern metamorphic belt

2.1.1.1. The northern sedimentary belt: The northern sedimentary belt is the northern most unit of Karakoram block and it is mainly consisting of upto 7km thick sedimentary belt, which is transgressive on a pre-Ordovician crystalline basement rocks. The sedimentary belt is further divided into different thrust sheets in the Chitral and Hunza valley along the western and eastern margin of the Karakoram block. The rock bodies present within this block range in age from Permian to Paleozoic and most of the successions within eastern Karakoram along Hunza valley are of Permian age (Zanchi and Gaetani, 1994; Searle, 1999). The two sub groups Hunza and Batura plutonic units are also included in the northern Karakoram block. The Hunza plutonic unit includes calc-alkaline granodiorite which has both biotite and hornblende mineral phases and they represent the age of 105.7±0.5 Ma (Fraser et al., 1999) and the second group Batura plutonic unit consists of gabbros and diorites and it is younger than the Hunza plutonic unit which is more deformed. The Batura plutonic unit in the south intrudes the deformed and older Hunza granodiorites while in the north it intrudes Permian slates and marble (Debon et al., 1987; Rex et al., 1988; Crawford and Searle, 1992).

2.1.1.2. The Karakoram axial batholith: The Karakoram axial batholith is a large body of igneous rocks intruded in different times and the earliest magmatic episode is recorded earlier

than 100 Ma and can be correlated with the initial stages of intra-oceanic subduction. The extension of this batholith is upto Ladakh in the east and across the border into Afghanistan in west. The northern sedimentary belt in the northern part of Karakoram plate is separated from the marginal mass present in the southern part of the Karakoram plate by this axial batholith in the Hindukush and Karakoram ranges. The dominant rock phases of this batholith are granodiorite, granites and pegmatites which are readily intruded by sills and dykes mostly basic in nature (Tahirkheli, 1994).

At least three major tectonic episodes of magmatic intrusion were identified in this mega axial batholith. The earliest episode was in the mid-Cretaceous and mainly consisting of sub-alkaline and calc-alkaline intrusions. The second phase of intrusion consists of sub-alkaline granite of Eocene age (43±3Ma) having mainly biotite, amphibole-granite and andalusite. The last episode occurred in Miocene and is represented by leucogranitic sheets and intrusions of batholithic dimensions (see Searle, 1991; Crawford and Searle, 1992; Debon et al., 1987).

2.1.1.3. The southern metamorphic belt: The southern metamorphic belt of the Karakoram plate is developed as a hanging wall along the NSZ or MKT. The different groups included in this belt are variously named as we move from the western to the eastern margin (i.e., Chitral slate in Hindukush, Darkot group in the Yasin valley, Baltit group and Dumurdu Formation in the Hunza valley and Shigar group in the Baltistan region). The low grade metamorphic rocks in this belt are biotite-schist, chlorite-schist, quartz-schist, while the high grade metamorphism is demarcated by kyanite and silliminte schists. A marbalized bed is also present within this zone and mapped from shigar valley in the east upto Ishkoman valley in the west and the upper contact of this coarse white marble is with the axial Karakoram batholith (Gaetani et al., 1996; Tahirkheli, 1994).

2.1.2. Northern suture zone (NSZ) or main Karakoram thrust (MKT)

Main Karakoram Thrust or NSZ is a fault contact which seperates the rocks of Eurasian plate from that of KIA. This sutures zone is formed as a result of collision of KIA with Eurasian plate. NSZ is comprised of ophiolitic mélange containing rocks like serpentinite, volcanics and marine sediments in a slate. The different types of sedimentary and volcanic rocks present on the

northern side of KIA are separated from the slates and quartzites of the Eurasian plate by this mélange. The rock bodies are present along this 4km thick mélange are limestone, quartzite, volcanic greenstone and altered rocks like serpentine in a slate matrix (Pudsey, 1986).

2.1.3. Kohistan island arc

Kohistan island arc (Fig. 2.1) is formed as a result of intra-oceanic subduction of neo-Tethys beneath Eurasian plate in late Jurassic to Early Cretaceous times and covering an area of about 3600km^2 (Tahirkheli et al., 1979). KIA is separated from the Indian plate by MMT or ISZ in the south while its northern boundary is marked by MKT or NSZ which seperates it from the Eurasian plate. The main rock units within KIA are amphibolites, diorites, meta-norites and associated volcanic rocks (Tahirkheli et al., 1979; Bard et al., 1980; Bard, 1983). KIA consists of the following geological bodies of rocks as we move from north to south (a) Yasin group sediments (Tahirkheli and Jan, 1984), (b) Chalt volcanic group (Coward et al., 1982), (c) Kohistan batholith (Petterson and Windley, 1985), (d) Dir-Utror volcanic series (Shah, 1991; Sullivan, 1993), (e) Chilas complex (Khan et al., 1989; Hamidullah and Jan, 1986), (f) Southern amphibolites belt (Jan, 1988, 1990; Shah et al., 1992) and (g) Jijal mafic-ultramafic complex (Jan and Howie, 1981).

2.1.3.1. Yasin sedimentary group: Yasin sedimentary group (Fig. 2.1) represents the northern part of KIA and they are the youngest Tethyan remains comprised of mainly sedimentary and volcano-clastic rocks. The volcanic rocks are metamorphosed to greenschist facies due to collision of two tectonic plates. This group shows variable lithologies along different parts of the NSZ. In the eastern part along Hunza valley, this group contains volcanoclastics, terrigenous clastics and slates while in the western part along the Ishkoman valley, this group comprises of slates, silty quartzites and pebble-cobble conglomerates while limestone unit is absent in the ishkoman block. The rocks exposed in this group are Cretaceous in age that is confirmed from the fossils of Albian-Aptian age and the main rock bodies present in this group are limestone, basal conglomerates, slates, volcanic and volcanoclastics (Ivanac et al., 1956; Pudsey et al., 1985; Pudsey, 1986). The Yasin group sediments are bounded by two faults; the NSZ in the north while in the south, it has faulted contact with Rakaposhi volcanic complex now called chalt volcanic group (Tahirkheli, 1982).

2.1.3.2. Chalt volcanic group: The rocks of the Chalt volcanic group (Fig. 2.1) are exposed in the south of NSZ. Chalt volcanic group is composed of basalts, rhyodacites and andesites and are generally metamorphosed to greenschist facies. The volcanic rocks present in this zone are highly deformed and shows metamorphic grade from greenschist in the west to amphibolites facies in the south. The volcanic or meta-volcanics present in this group are divided into two types on the basis of their geochemical contents. One group is having MgO content between 15 and 6%, while, the other group shows MgO content less than 6%. The former group, having MgO content greater than 6%, are present in the Hunza valley and the latter group, with MgO content less than 6%, are present in the western side of this group (Petterson and Windley, 1985, 1991).

2.1.3.3. Kohistan Batholith: The presence of major belt of granitic rocks in the northern part of KIA were first described by Tahirkheli and Jan (1979). These were later on named as Kohistan batholith (Fig. 2.1) by Petterson and Windley (1985). The major component of KIA is represented by Kohistan batholith. The area covered by this series along E-W direction is 300km and along N-S direction is 60km. Different rock bodies found in this batholith are granodiorite, diorite, hornblendite, hornblend grabbro and lecogranite. Kohistan batholith is formed as a result of three stages of magmatic intrusions. The geochemistry of first stage is characterized by two magma types. The first type of magma is represented by medium to high -potassium diorites, while the second is low potassium trondhjemites. The medium to high –potassium diorite is enriched in MgO, MnO, Fe_2O_3, V, Cr and Ni and having low content of incompatible elements. The second type of rocks present in first stage has unique features having lack of enrichment in LREE relative to HREE, and LILE relative to HFSE. The age assigned to this intrusion is 102± 12 Ma. The stage two pluton within the KIA covers upto two thirds of the batholith. The silica content varies from low to high (44-77%) in these rocks. Most of the rock samples within this group are from medium to high potassium in composition. The rock types present within this group are enriched in large ion lithophile relative to high field strength elements. The age assigned to this stage of intrusion is 85-40 Ma. The stage three pluton present within the KIA forms the minor part of the batholith. The age assigned to this group is 30 Ma, which means that

they are intruded after the formation of ISZ or MMT. The rocks within this group are depleted in LREE relative to the stage two pluton of the KIA (for detail see Petterson and Windley, 1991).

2.1.3.4. Dir Group: The volcano-sedimentary rocks are exposed in the western KIA around Dir and Swat areas (Tahirkheli (1979; 1982). These were named as Dir group (Fig. 2.1). This group further divided into three units from base to top. These are Baraul Banda slate, Dir-Utror volcanic series and the Panakot meta-arkose. Volcanic rocks found around Dir and Utror towns are named Dir-Utror volcanic series. They are representing the west-central part of KIA. Rocks of this group consists of metamorphosed calc-alkaline and associated meta-sediments. The basaltic rocks found within this group can be divided into two on the basis of their geochemical data (Tahirkheli, 1979; Shah, 1991). The thickness of this volcano-sedimentary belt is variable and ranges from less than 1km in the SW and upto 3km in Gumadand village in the north east succession. More than 90% of these rocks are mafic metavolcanic rocks including basalts, basaltic-andesites and andesite. Almost all these rocks show porphyritic texture having plagioclase as a phenocryst, quartz and epidote veins are common in these rocks (Shah and Shervais, 1999). The volcanic rocks found within the Dir-Utror series are divided into two groups. One group with MgO content more than 9% while the other with MgO content ranges from 5-9%. The high MgO basalts are upto 12%, low MgO basalts are upto 23%, basaltic andesites upto 34%, andesites upto 37%, dacites upto 4% and rhyolites upto 4% by volume (Shah and Shervais, 1999).

2.1.3.5. Chilas complex: Chilas complex (Fig. 2.1) is representing the southern part of KIA and consisting mainly of pyroxene-diorites and gabbronorites with minor amount of gabbros, anorthosites, troctolites, peridotites, dunites, and mafic dykes. In the southern part of KIA, this complex is extending 300km along east-west and 40km along north-south. The rock group present in this extensive complex are in age from Late Jurassic to Cretaceous. In the southern part, Chilas complex has a tectonic contact with the Kamila/southern amphibolites. Most of the rocks exposed in this belt are undeformed and show intrusive contacts at the margins with the surrounding rocks including amphibolites of the Kamila complex. These rocks show calc-alkaline character showing tectonic setting in the island arc environment. The very large size of this complex suggests that this belt is not formed as a result of one continuous magma chamber

but formed from pulses of magma over time and detailed mapping is necessary to confirm this fact (Hamidullah and Jan, 1986; Khan et al, 1985; 1989; 1993).

2.1.3.6. Kamila amphibolites: The Kamila amphibolites (Fig. 2.1) belt lie south of the Chilas complex in the KIA and mainly consists of two varieties of amphibolites. One variety is medium to coarse-grained homogenous amphibolites while, the other one is fine- grained banded or homogenous amphibolites. Geochemical study carried out by Jan (1988) found that the fine-grained variety is derived from a volcanic protolith and the medium to coarse- grained homogenous variety is formed from plutonic gabbroic-diorite. Width of Kamila amphibolite is 10-40km and is present all along the southern Kohistan batholith. Structural data and their age (83-80Ma) suggest that the deformation and metamorphism occurred before the collision of the Kohistan island arc with the indian plate along indus suture zone (Coward et al., 1987; Treloar et al., 1989). Main lithologies present in this sequence consist of meta-volcanic and meta-plutonic oceanic rocks. Kamila amphibolite seperates the rocks of Chilas complex in the north from the rocks of Indian plate in the south along MMT. These rocks show very close resemblance with the Chilas complex gabbro-norites, and suggesting the same origin in which both rock types have depletion in the high field strength elements showing the subduction related environment of typical island arc setting (Khan et al., 1989; 1993).

2.1.3.7. Jijal mafic-ultramafic complex: Jijal complex, having basal cumulates, layered gabbros and ultramafic rocks (Fig.2.1) lies in the southern part of KIA consisting of about 150km^2 and represents the deepest part of the arc. Two distinct units in this complex are 1) ultramafic rocks, consisting of dunites, harzburgites, websterites, and clinopyroxenites and 2) garnet granulites. The granulites present in this complex are of two types, one having plagioclase and other is free of plagioclase. The plagioclase free variety is ultrabasic to basic and the other variety having plagioclase is basic to intermediate in nature (Jan and Howie, 1981) The two distinct lithological units exposed in this complex are the ultramafics covering an area of about 150 square kilometers and mainly consist of garnet granulites and ultramafic rocks.
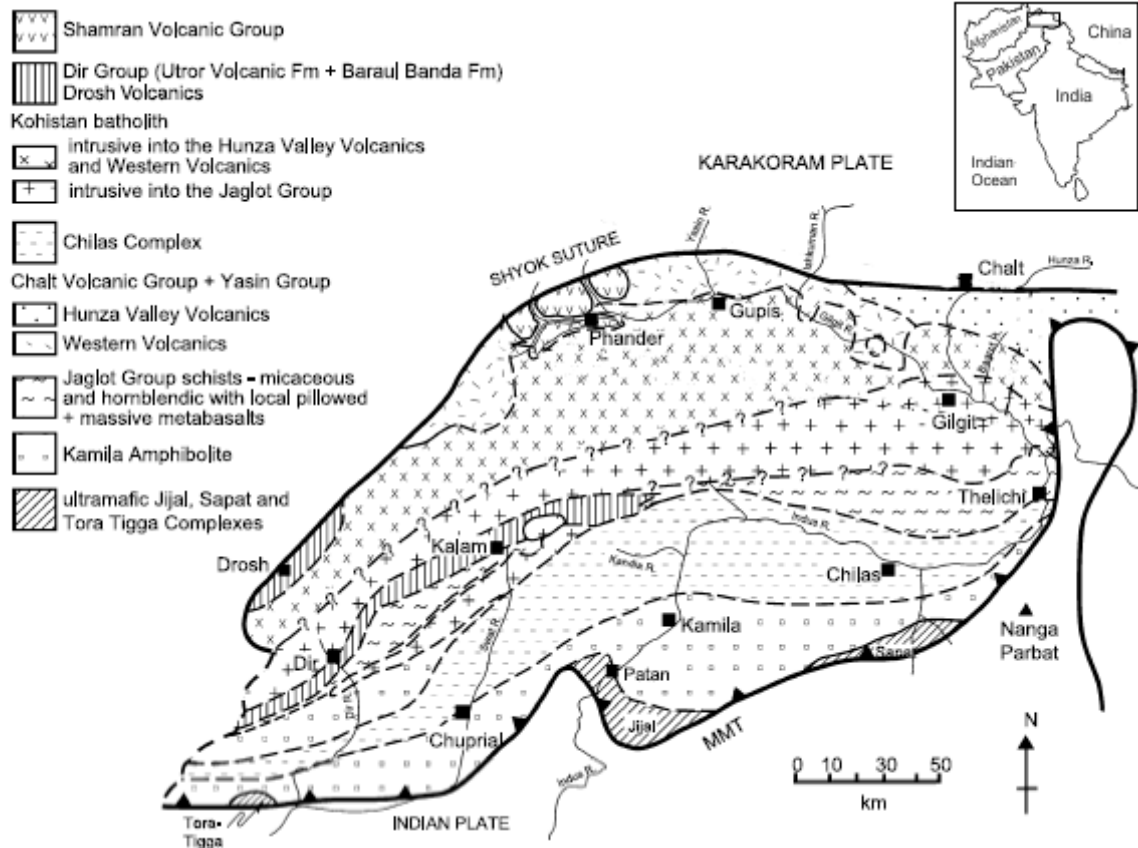
Fig.2.1. Regional geological map of Kohistan terrane, North Pakistan (after Treloar et al., 1996).

CHAPTER 3
LOCAL GEOLOGY

3.1. General

   The study area, Golo Das and its surroundings areas, lies in the northern most part of the Kohistan island arc and just south of northern suture zone or main Karakoram thrust, a tectonic zone separating the rocks of the KIA from that of Karakoram plate. Geologically the study area is very complex due to its involvement in regional scale tectonics. The rocks of the study area and its vicinity are mainly comprised of rocks of the Chalt volcanic group (CVG) and meta-sediments intruded by Kohistan batholiths. Volcanic rocks in the vicinity of Gilgit and Chitral areas were for the first time reported by Hayden, (1914). These were later named as greenstone complex by Ivanac et al. (1956). The greenstone complex was called as greenstone volcanics in Chitral region (Calkins et al., 1969). This greenstone complex is consisting of volcanics and sedimentary rocks. These rocks are metamorphosed to varying degrees as they are involved in regional tectonics. Different rock bodies occur in this complex are quartzites, mica schist, hornblende schist, hornblende gneiss, limestone, marble, andesite, rhyolite and basalt (Tahirkheli, 1979). The maximum thickness upto 4000m of these volcanics has been recorded by Tahirkheli (1982) in Hunza valley and are named as Rakaposhi volcanic group. The volcanic sequences are divided into two groups on the basis of their ages. The older group which is more deformed and metamorphosed is called Chalt volcanic group. Petterson and Windley (1991) differentiated these volcanics as 1) Hunza volcanics that crop out in the Hunza Valley and 2) Western volcanics which are exposed in the western part of Gilgit. Later on Petterson and Treloar (2004) named the Hunza volcanics as Hunza formation and the Western volcanics as Ghizar Formation. They have further divided the Ghizar formation in three types 1) Ishkoman Volcanic Centre (IVC), 2) basalt-andesite sheet dominant (BASD) and 3) tuff dominant (TD). The less deformed/undeformed younger volcanic rocks were first named as Shamran volcanics by Pudsey et al. (1985). The Shamran volcanics, consists mainly of basalt-rhyolite lava flows, are of Palaeocene age (Sullivan et al., 1993; Treloar et al., 1996). These volcanics were renamed as Teru volcanic Formation by Danishwar et al. (2001). Sullivan et al. (1991) have correlated the Western volcanics of Petterson and windley (1991) with the Shmaran volcanics on the basis of similarities in the petrographic and geochemical characteristics.

The local geological maps (Figs. 3.1 and 3.2) of the study area are showing the various geological units exposed in the area. The NSZ melange is separating the rocks of the Karakoram plate in the north from those of the KIA in the south. The rocks of the Karakoram plate are mainly composed of meta-sediments, while the rocks of the KIA in the study area are the volcanic rocks of the Ghizar formation, the meta-sediments of the Yasin Group and the diorites of Kohistan batholith. The contact between the Ghizar formation and the overlying Yasin group is sheared and tightly folded. The locations of both grab (<1kg) and bulk (>10kg) samples collected during field are shown in Figures 3.1 and 3.2 respectively. Description of different rock units, from north to south, and their field characteristics are explained below.

3.2. Meta-sediments of Karakoram plate

The meta-sediments occur just north of the NSZ and are representing the southern most part of the Karakoram plate. These rocks are present on the hanging wall of the NSZ and mainly consist of garnet-muscovite-schist, biotite schist, graphitic schist, staurolite schist, calc-schist, quratz-schist, chlorite schist and conglomerate with para-gneisses. The rock units present just north of NSZ were named differently along this mega thrust like Chitral slate in Hindukush along western Karakoram, Darkot Group in the Yasin valley along central Karakoram, Baltit group and Durmurdu formation in the Hunza valley along central Karakoram and Shigar group in Baltistan along eastern Karakoram (Tahirkheli, 1994).

In the study area the meta-sedimentary rocks mainly mica-schist and graphitic schist are the dominant rock bodies found in the northern most part of the study area. These rocks show layering (metamorphic bands) and schistocity along shear zones. The sulfide weathering along the shear zones in the form of yellowish-brown color due to oxidation of sulfide minerals, mainly pyrite, are well noticed during field. The sulfide zones present within these meta-sediments are shown in the (Figs. 3.3 and 3.4).

3.3. Melange zone rocks

The rocks in the form of chaiotic bodies present along the NSZ in the study area, are named as Shyok suture mélange by Pudsey et al. (1985). Shyok suture zone is a fault contact which separates the rocks of the Karakoram plate in the north from the rocks of KIA in the south.

The thickness of this mélange is variable and the maximum thickness up to 4km is recorded at Hunza valley (Pudsey et al., 1985). The Shyok suture mélange in the study area mainly contain slates with interbedded conglomerate and sandstone. It also contains chaiotic bodies of volcanics, serpentinites, limestone, red shale and quartzites.

3.4. Yasin Group

The meta-sedimentary rocks of the Yasin Group, exposed in the study area are variable proportion of limestone, slates and quartzites. These rocks are intensely sheared and exhibit boundinage structures and schistosity.

3.5. Ghizar formation

Searle and Khan (1996) have mapped the volcanic rocks of the southern part of the study area as Shamran volcanics. However, Petterson and Treloar (2004) have named these rocks as part of the Ghizar Formation. In order to avoid the confusion in adopting different nomenclatures for the rocks of the Chalt volcanic Group, the nomenclature used by Petterson and Treloar (2004) will be adopted here. The CVG in the study area is named as Ghizar formation which has been designated as 1) basalt-andesite sheet dominant (highly deformed) and 2) Ishkoman Volcanic Centre (less deformed/undeformed) volcanics. The basalt-andesite sheet dominant volcanics are exposed in the northern part of the study area while the rocks of the Ishkoman Volcanic Centre are covering most of the central and southern part of the study area. These volcanics are intruded by the diorites of Kohistan batholiths (Fig. 3.1).
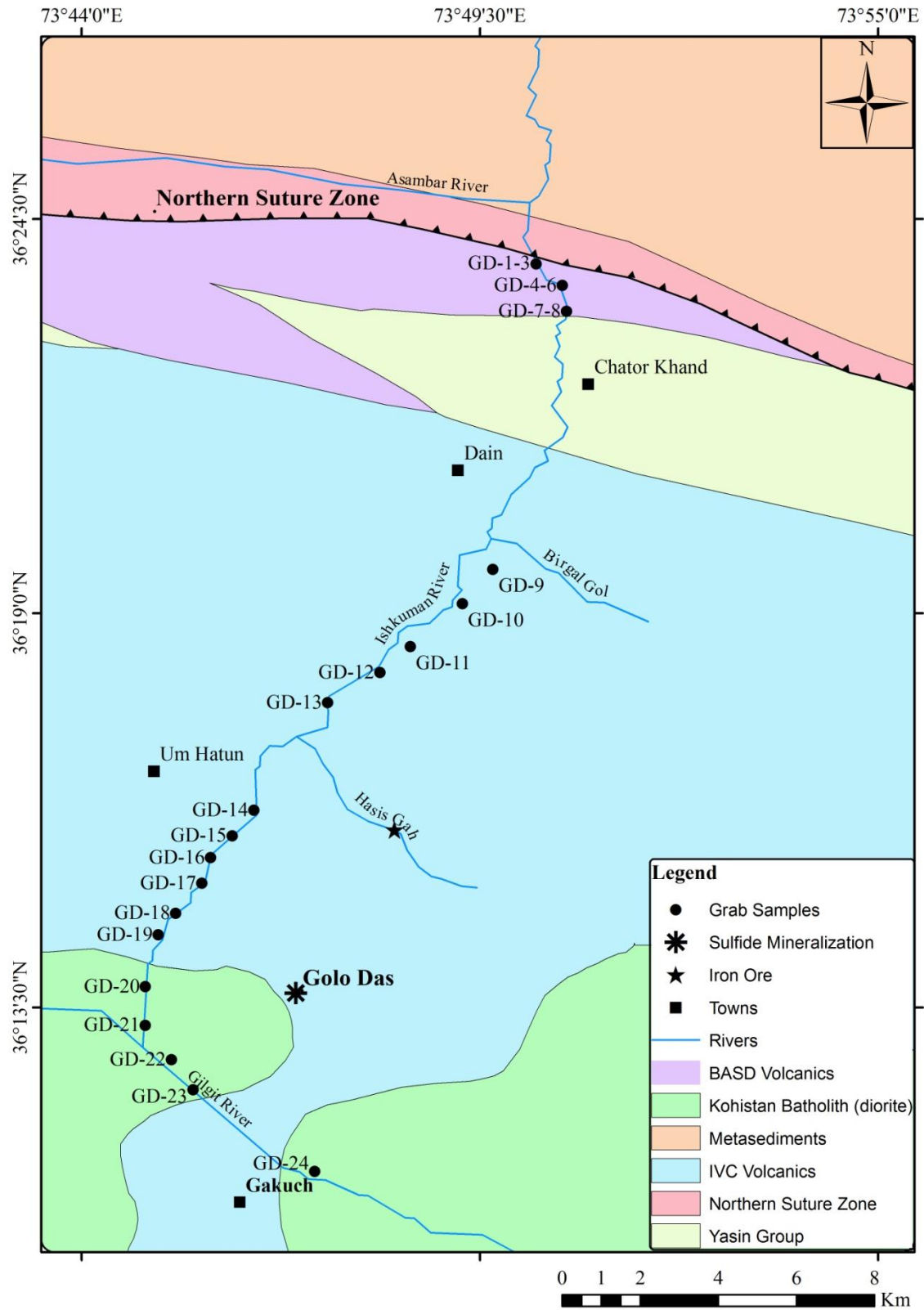
Fig.3.1. Geological map of Golo Das and surrounding areas showing grab sample locations (compiled from Searle and Khan, 1996; Petterson and Treloar, 2004).
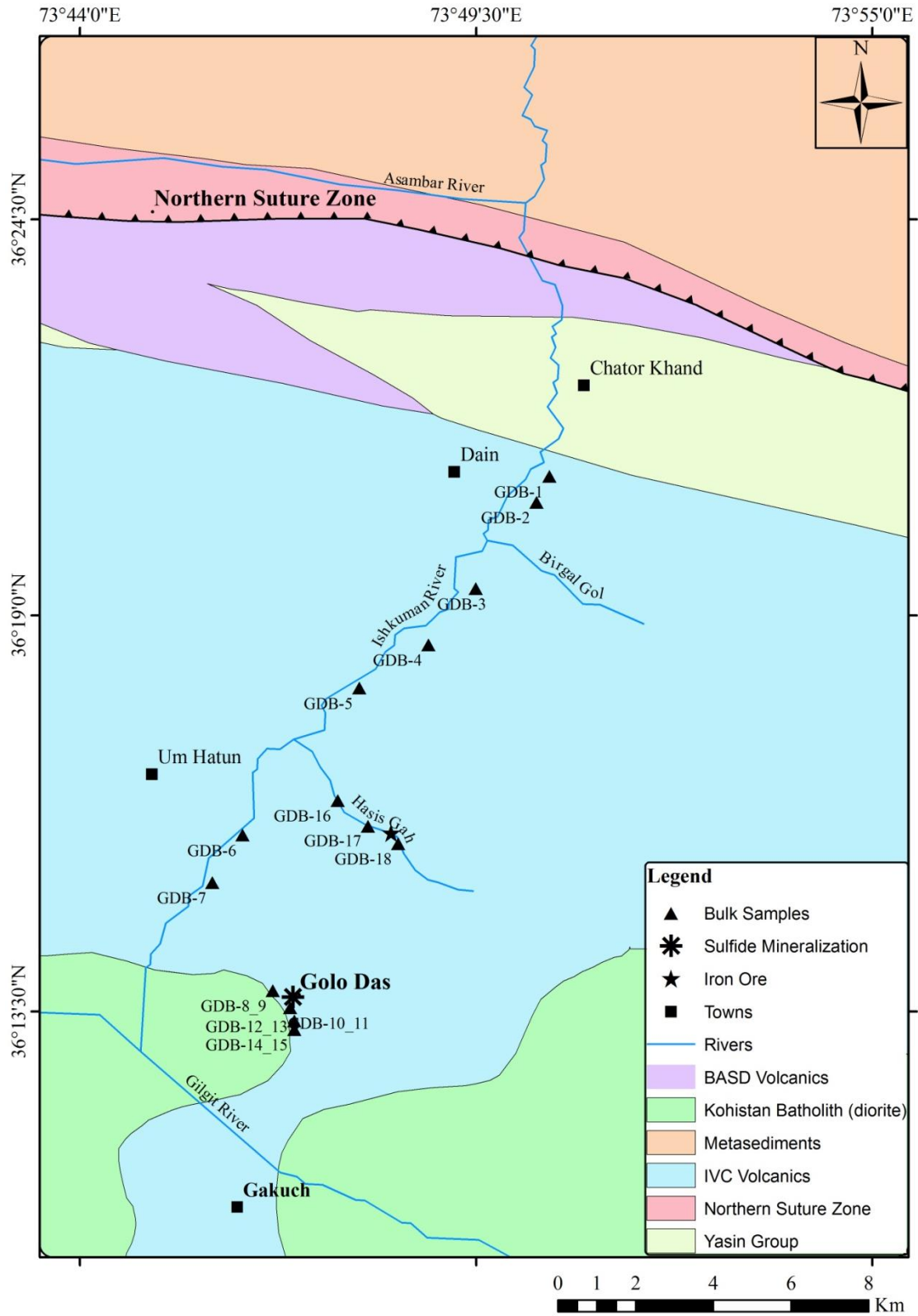
Fig.3.2. Geological map of Golo Das and surrounding areas showing bulk sample locations (compiled from Searle and Khan, 1996; Petterson and Treloar, 2004).

3.5.1. Basalt-andesite sheet dominant volcanics

This variety of Chalt volcanics is present south of the NSZ and occupy the northern most margin of KIA in the study area. Different types of rocks are present in this group. These are basalts, andesites and rhyolite flows, which are deformed and metamorphosed, ranging from greenschist facies to amphibolite facies. These volcanics are cleaved, thinly bedded to thickly laminated, and displaying green and grayish-green color on fresh surface and brown color on weathered surface. In the study area, these are generally foliated but at places also attain schistocity along shear zones. These rocks are characterized by chlorite, epidote, amphibole, sodic plagioclase, quartz-mica, carbonates and iron oxides. Quartz veining along shear zones is common in these rocks. These rocks also show brecciated appearance (volcanic breccia) and boundinage structures due to faulting and shearing (Figs. 3.5 & 3.6). The quartz veins within these volcanics are probably formed as a result of metamorphic or epithermal fluid.

3.5.2. Rocks of Ishkoman Volcanic Centre

These volcanics exhibit thrusted contact with the overlying meta-sediments of the Yasin Group and also with the BASD volcanics in the northern part of the study area. These rocks are compact, less deformed /undeformed and unmetamorphosed, dark-gray to greenish-grey in color. These rocks include basaltic-andesitic lavas, volcanoclastic and pyroclastic rocks. The lavas generally have porphyritic texture with phenocrysts of plagioclase, hornblende and pyroxene present in the greenish color chlorite mass. The volcanoclastic and pyroclastic rocks are generally matrix supported and containing angular volcanic clasts and bombs which represent proximity to sub-areal to subaqueous volcanic eruption centre. Quartz veins are noticed along the shear zones and local faulting. The weathering of sulfides are common along these shear zones where the malachite and azurite showings on the surface can be well observed. These showings are formed due to leaching of copper-bearing sulfides, mainly chalcopyrite (Fig. 3.7). The epidotization along fractures and shear zones are also common (Fig. 3.8). All the above mentioned weathering and alteration characteristics of these volcanics can be well noticed in the Golo Das area. In the Golo Das area calcareous rocks are present as more than 10m thick and 100-200m long beds within these volcanics. These beds show alteration/skarnification with the development of yellowish-brown surface weathering. These kinds of calcareous beds are also

exposed within these volcanics in the other parts of the study area, especially in the upper reaches of Hasis Gah.

3.6. Calcareous rocks

As pointed out earlier that the IVC volcanics have discontinuous beds of calcareous rocks exposed in the Golo Das area. The similar rocks are also exposed in the north of Golo Das along the Hasis Gah (stream). Calcareous rocks are present in the Hasis Gah (stream) hosting the iron ore, having magnetite, hematite, specularite and ilmenite (Fig. 3.9). The weathering of this ore to limonite is very common. The iron ore occurs as pods (>30m long and >2m thick) within the calcareous rock. These ores may have been formed due to skarnification probably due to dioritic intrusions at depth. The quartz vein cross cutting the calcareous beds are common where ever the iron ore is present (Fig. 10).This suggest skarnification due to metasomatization. There are many such type of discontinuous beds (<5m thick and >100m long) which can be recognized due to the reddish-brown weathered limonitic material on the surface from a distance (Fig. 11). However, beds with no iron ore can also be seen in the area.

3.7. Diorites

The dioritic intrusions in the study area are considered as part of the Kohistan batholith. These diorites are exposed in the southern part of the study area. These are medium to coarse-grained, having dark-gray color on fresh surface and brownish-gray color on weathered surface having intrusive contact with the IVC volcanics. The rocks are fresh looking, no fabrics observed however, angular fractures, local faulting and fractures are present. These are dominantly containing mica (biotite) with variable amount of amphibole along with the essential minerals such as plagioclase, easily distinguished in hand specimen. Due to the undeformed nature of these diorites these can be correlated with the stage 2 diorites of Petterson and Windley (1985, 1991).
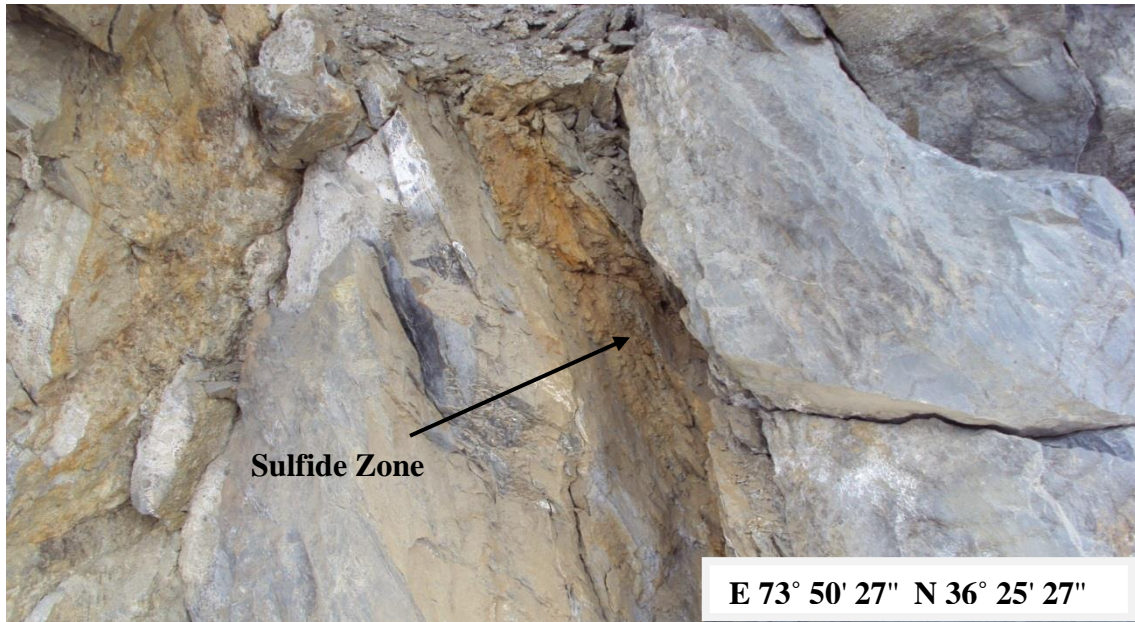
Fig.3.3. This photograph is showing about 30 cm wide sulfide zone highly weathered within meta-sediments. These kinds of sulfide zones and their leaching to yellowish-brown color are very common along the shear zone.

Fig.3.4. This photograph is showing a sulfide zone (=10m) within the meta-sediments of Karakoram plate. It is having spotted appearance due to leaching of and the formation of limonite.

Fig.3.5. Quartz vein along shear zone within BASD volcanics displaying boundage/augen structure.

Fig.3.6. This photograph showing brecciation in the BASD volcanics along local faults/shear zone.

E 73° 46' 42.3" N 36° 13' 47.6"
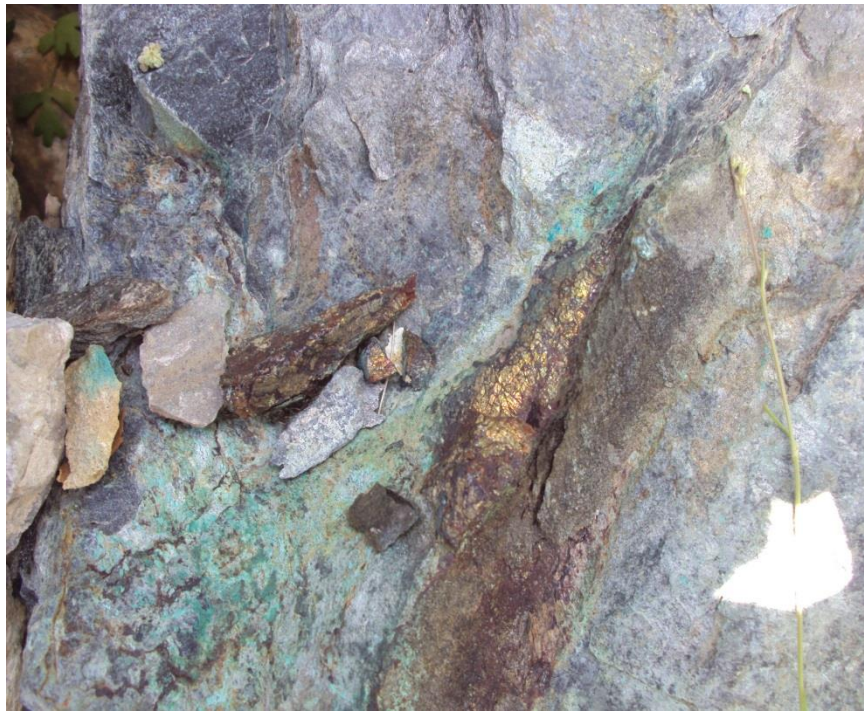
Fig.3.7. Block of IVC volcanics in the Golo Das area showing copper-bearing sulfide mineralization.

E 73° 46' 31.9" N 36° 16' 16.3"

Fig.3.8. Photograph showing slickenside and epidotization within the IVC volcanics.

E 73° 48' 19" N 36° 15' 49"

Fig.3.9. Photograph showing iron ore with limonitic material on the weathered surface in Hasis Gah.
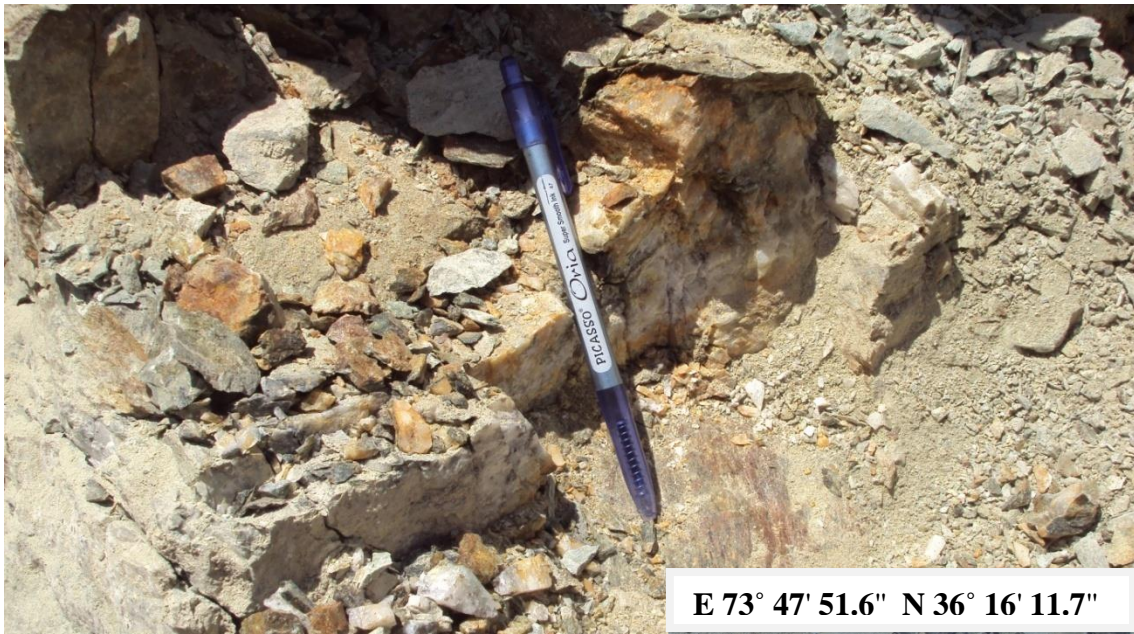
Fig.3.10. Photograph showing the intrusion of quartz veins associated with iron ore within the calcareous rock.

Fig.3.11. Photograph showing the western side of Ishkoman river opposite to Hasis village where a huge gossan can be seen within the IVC volcanics. This area is inaccessible.

CHAPTER 4

METHODOLOGY

4.1. Field work

A geological field work was conducted in July, 2011 in the Golo Das and surrounding areas. Various sulfide-bearing altered zones and host rocks have been identified and mapped. Rock samples in the form of bulk (> 10kg) and grab (1kg) were collected during field. Bulk samples were collected from the sulfide-bearing altered zones for the investigation of gold, silver and other base metals. While, grab samples were collected from the host rocks for the investigation of their petrographic and geochemical characteristics. During field the contacts between various rock units and their physical characteristics were noted and also photographed. Sample locations were marked by GPS. The bulk and grab samples collected in the field were properly arranged in the samples bags and numbered with permanent marker.

4.1.1. Bulk samples collection: A total number of eighteen bulk samples were collected during field for detail geochemical analysis of the research prospect. Seven bulk samples were taken from the road side along the Ishkuman valley where sulfide mineralizations were present along the shear zone. Eight bulk samples were also collected from alteration zones in the Golo Das area, where the IVC volcanics, hosting the copper mineralization along the calcareous beds, are exposed. The remaining three bulk samples were collected from the Hasis Gah-section. These samples were transported to the geochemistry laboratory of the National Centre of Excellence in Geology (NCEG), University of Peshawar for the analysis of gold, silver and base metals.

4.1.2. Grab samples collection: Twenty four representative grab samples were collected during field from IVC volcanics, BASD volcanics and dioritic intrusions exposed in the study area. These samples were transported to the NCEG for petrographic and geochemical studies in various laboratories.

4.2. Laboratory Work

4.2.1. Crushing and powdering of bulk samples

Bulk samples collected during field were crushed as a whole in the jaw crusher in the crushing and powdering lab of the NCEG. Each bulk sample was crushed to a smaller size

(<1cm). After crushing representative portion of each sample was obtained after proper spliting through spliter and also through quartering and conning techniques. This portion was then pulverized to -200 mesh size by the tungsten carbide ball mill. A representative portion of each powder sample was then collected by quartering and conning for further digestion and geochemical analysis.

4.2.2. Preparation of stock solution for gold

For the preparation of gold stock solution, 20g of sample was taken in 250ml graduated pyrex beaker, 50ml aqua regia (HNO_3: $3HCl$) was added to it and the beaker was cover with watch glass. After the addition of aqua regia it was heated on hot plate for 30 minutes at low heat. After 30 minutes the beaker was removed from the hot plate and cooled for a while. Then distilled water was added to the beaker. After the addition of distilled water, the solution was again heated until the required solution in the beaker reduced to 50ml and then it was filtered through Whatman 42 filter paper in the test tube. During filtration the pyrex beaker was washed with 6N HCl several times. The final solution was made to 50ml with distilled water. This solution was taken into separatory funnel and 50ml of distilled water was added to it and the separatory funnel was shaken for a while to mix the contents. Then 20ml Methyle Isobutyle Ketone (MIBK) was added to the funnel and then it was shaken for 10 minutes on automatic flask shaker. The lower layer was removed while the MIBK layer was retained in the funnel. 20ml of 2N HCl was added and again shaken for 10 minutes and again the lower layer was removed. The MIBK layer now contain the extracted gold. The MIBK was stored in the air tight brown color glass bottles until analyzed for gold. All the chemicals, acids and reagents used during the analytical process were of analytical grade.

4.2.3. Preparation of stock solution for base metals

For the preparation of stock solution for base metals about one gram sample was taken in teflon beaker and added 10ml hydrofluoric acid (HF) through plastic graduated cylinder by following the method of Jeffery and Hutchison (1986). After the addition of HF, that solution was heated for an hour on hot plate and then removed from the hot plate to cool down for few minutes. Then 20ml aqua regia was added in the beaker and heated until dried. 20ml of 2N HCl was added and heated it for few minutes. After that the required solution was diluted to 50ml

with distilled water and filtered through Whatmen No. 42 filter in a test tube. The test tube was covered with polyethylene film to avoid evaporation. All the samples along with the reference standards treated with the same method for the determination of Cu, Pb, Zn, Ni, Cr, Co, Cd and Ag.

4.2.4. Instrumental analysis

All the stock solutions were analyzed for Au and Ag and base metals such as Cu, Pb, Zn, Ni, Cr, Co and Cd using Perking Elmer graphite furnace atomic absorption spectrometer (AAS) modal AAS-PEA 700 under the standard operating condition. The instrumental conditions and analytical analysis of each element are described below.

4.2.4.1. Determination of Copper (Cu)

Instrumental conditions:

Mode	Absorption
Wavelength	324.8nm
Energy	68
Current	15
Slit width	0.7H
Air flow	17L/min
Fuel flow	2L/min

Standard stock solution of 1000ppm was prepared by dissolving 1g of Cu metal in (1:1) HNO_3 and diluted to 1L with distilled water in a volumetric flask. From this stock solution, working standard of 2.5, 5 and 10ppm were prepared and run on the atomic absorption as unknown. The instrument was calibrated with the working standards and after attaining the above mentioned condition the samples were aspired through AA one by one for the determination of Cu concentration in ppm. Further calculations were done for the determination of total Cu contents in the rock.

4.2.4.2. Determination of Lead (Pb)

Instrumental conditions:

Mode	Absorption
Wavelength	283.3nm
Energy	41
Current	10
Slit width	0.7H
Air flow	17L/min
Fuel flow	2L/min

Standard stock solution of 1000ppm for Pb was prepared by dissolving 1.598g of $Pb(NO_3)_2$ in 1% of HNO_3 and was made to the volume with distilled water. Working standards of 2.5, 5 and 10ppm were prepared from standard stock solution and the instrument was calibrated with the above given conditions by using the working standards. After calibration this working standards were run through AA as unknown. Once the working standard values were found similar to the actual concentration of the standards for Pb, the sample solutions were then aspirated in the flame of AA and the concentration of Pb was recorded in each sample. Further calculations for the total Pb contents in the rock were done.

4.2.4.3. Determination of Zinc (Zn)

Instrumental conditions:

Mode	Absorption
Wavelength	213.9nm
Energy	35
Current	15
Slit width	0.7H
Air flow	17L/min
Fuel flow	2L/min

1000ppm standard stock solution was prepared by dissolving 1g of Zn metal in minimum volume of HCl and was transferred to 1L volumetric flask. The volume was made to the mark with distilled water. Standard solution of 2.5, 5 and 10ppm were prepared from the standard stock solution. The atomic absorption was calibrated with the working standards under the above

mentioned instrumental conditions. After making sure that the instrument is properly calibrated and the Zn values of the working standards matched the actual concentration, the sample solutions were then run through the AA and the concentration of Zn was noted in each sample. The total content in each rock sample was then calculated.

4.2.4.4. Determination of Nickel (Ni)

Instrumental conditions:

Mode	Absorption
Wavelength	232nm
Energy	30
Current	25
Slit width	0.2H
Air flow	17L/min
Fuel flow	2L/min

Standard stock solution of 1000ppm for Ni was prepared by dissolving 1.273g of Ni_2O_3 in minimum volume of 10% (v/v) HCl and was made to the volume with distilled water. Working standards of 2.5, 5 and 10ppm were prepared from standard stock solution and the instrument was calibrated with the above given conditions by using the working standards. After calibration these working standards were run through AA as unknown. Once the working standard values were found similar to the actual concentration of the standards for Ni, the sample solutions were then aspirated in the flame of AA and the concentration of Ni was recorded in each sample. Further calculations for the total Ni contents in the rock were done.

4.2.4.5. Determination of Chromium (Cr)

Instrumental conditions:

Mode	Absorption
Wavelength	357.9nm
Energy	30
Current	25
Slit width	0.7H

Air flow	17L/min
Fuel flow	2.5L/min

1000ppm standard stock solution was prepared by dissolving 3.735g of potassium chromate (K_2CrO_4) and was transferred to 1L volumetric flask. The volume was made to the mark with distilled water. Standard solution of 2.5, 5 and 10ppm were prepared from the standard stock solution. The atomic absorption was calibrated with the working standards under the above mentioned instrumental conditions. After making sure that the instrument is properly calibrated and the Cr values of the working standards matched the actual concentration, the sample solutions were then run through the AA and the concentration of Cr was noted in each sample. The total content in each rock sample was then calculated.

4.2.4.6. Determination of Cobalt (Co)

Instrumental conditions:

Mode	Absorption
Wave length	240.7nm
Energy	36
Current	30
Slit width	0.2nm

Standard stock solution of 1000ppm was prepared by dissolving 1g of cobalt metal in a minimum volume of (1+1) HCl and diluted to 1L with 1% (V/V) HCl. From this stock solution, working standard of 2.5, 5 and 10ppm were prepared and run on the atomic absorption as unknown. The instrument was calibrated with the working standards and after attaining the above mentioned conditions, the samples were aspired through AA one by one for the determination of cobalt concentration in ppm. Further calculations were done for the determination of total Co contents in the rock.

4.2.4.7. Determination of Cadmium (Cd)

Instrumental conditions:

Mode	Absorption

Wavelength	279.5nm
Energy	39
Current	4
Slit width	0.2H46
Air flow	17L/min
Fuel flow	2L/min

Standard stock solution of 1000ppm for Cd was prepared by dissolving 1g of cadmium metal in minimum volume of HCl and diluted with 1% HCl was made to the volume with distilled water. Working standards of 2.5, 5 and 10ppm were prepared from standard stock solution and the instrument was calibrated with the above given conditions by using the working standards. After calibration this working standards were run through AA as unknown. Once the working standard values were found similar to the actual concentration of the standards for Cd, the sample solutions were then aspirated in the flame of AA and the concentration of Cd was recorded in each sample. Further calculations for the total Cd contents in the rock were done.

4.2.4.8. Determination of silver (Ag)

Instrumental conditions

Mode	Absorption
Wavelength	328.1nm
Lamp Energy	52
Lampe Current	10mA
Slit width	0.2nm
Air flow	17L/min

1000ppm of Standard stock solution was prepared by dissolving 0.787 g of $AgNO_3$ in 50ml of distilled water and diluted to one liter with 1 % (V/V) HNO_3. Standard solution of 2.5, 5 and 10ppm were prepared from the standard stock solution. The atomic absorption was calibrated with the working standards under the above mentioned instrumental conditions. After making sure that the instrument is properly calibrated and the Ag values of the working standards matched the actual concentration, the sample solutions were then run through the AA

and the concentration of Ag was noted in each sample. The total content in each rock sample was then calculated.

4.2.4.9. Determination of gold (Au)

Instrumental conditions

Mode	Absorption
Wavelength	242.7nm
Energy	14
Current	10mA
Slit width	0.2nm

1000ppm of standard stock solution was prepared by dissolving 1g of gold in aqua regia and was transferred to 1L volumetric flask. The volume was made to the mark with distilled water. From this stock solution working standards of 2.5, 5 and 10ppm were prepared in the 20 ml volume of Methyle Isobutyle Ketone by the method as described earlier for the extraction of gold. The instrument was calibrated with these working standard solutions. The standards prepared were run on the atomic absorption as unknown. After the instrument calibration and attaining of above mentioned condition for finding Au concentration, the certified standards were run. Once the values of the certified standards were within the confidence level the samples were run through atomic absorption and the concentration of Au in each sample was recorded in ppm. Further calculations were done for the total Au concentration in the rock.

4.2.5. Determination of loss on ignition

For the determination of loss on ignition of selected rock samples, 3g powder samples was taken in a porcelain crucible and kept in the furnace at 950˚C for at least four hours. After four hours the furnace temperature was gradually reduced to 500˚C. The crucible was transferred to the desicator from the furnace and was let to cool to the room temperature. The difference in weight before and after heating was noted, and heat loss was calculated in percent from these readings.

4.2.6. Thin sections preparation

Grab samples collected from the host rocks during field were mainly used for the preparation of thin sections. Thin section preparation was carried out in the rock cutting and polishing lab of NCEG. For the preparation of thin sections, a chip (5cmX2.5cm) was cut down by the rock cutter from the grab sample and smoothen it with grinding machine as well as by using different sizes of silicon carbide powder. The polished slab of rock was then mounted on the same size of polished glass slide with epoxy. The chip mounted on the glass slide was then cut and grinded until the thickness of 0.03mm was achieved by using different types of silicon carbide powder for grinding purpose.

4.2.7. XRF and ICP

Nine samples were selected for whole rock geochemistry and for that the X-ray fluorescence (XRF) and inductively coupled plasma (ICP) techniques were used for finding the major and trace elements at the Department of Earth and Atmospheric Science, University of Houston, USA.

CHPATER 5

PETROGRAPHY

To find out the volume percentages of minerals present in the rock samples, petrographic study under the polarized microscope is very useful. Rock identification on the basis of the mineral assemblages and their textural and mineralogical relationship is best studied in thin sections. For petrographic study of the research prospect, nineteen thin sections were prepared. Modal mineralogy in thin sections can be used to classify rocks. The grab samples selected for thin section study includes volcanics and dioritic intrusion within the vicinity of Golo Das and surrounding areas. The mineralogical and textural features observed in thin sections of these rocks are described below.

5.1. Ghizar formation

5.1.1. Basalt-andesite sheet dominant volcanics

These volcanics have developed fabrics due to the involvement in the regional tectonics. These rocks are generally porphyritic. The modal mineralogy of these volcanics is given in Table 5.1 whereas the textural features, the minerals associations, alteration and phenocryst to groundmass relationship are shown in Figures 5.1-5.3. The plagioclase and hornblende are the dominant mineral phases as phenocrysts in these rocks, whereas the groundmass is cryptocrystaline with chlorite and epidote. In few thin sections, fine-grained laths of tremolite/actinolite are found. Plagioclase as phenocryst ranges from (20-30%) and exhibit partial or complete alteration to sericite and epidotes. The plagioclase phenocrysts are tabular in with well-developed polysynthetic twinning. Some of the phenocrysts of plagioclase are so intensely altered that pseudomorphs after plagioclase are clearly seen. In some rocks, inclusions of biotite are present in plagioclase phenocrysts. The plagioclase phenocryts in these rocks have developed preferred orientation along the foliation plane and sometime the laths of tremolite/actinolite are winding around plagioclase phenocrysts. At places the deformed or broken plagioclase phenocrysts are also noticed. Epidotes and sericite are well observed in the groundmass which are the alteration product of plagioclase.

The second abundant mineral phase as phenocryst in these rocks is hornblende (7-30%) whereas at certain places hornblende phenocrysts are present with lesser amount of plagioclase

phenocrysts. Tremolite/Actinolite also occurs in the groundmass. As a phenocrysts the hornblende grains have well developed subhedral phases and exhibit alteration to chlorite and epidotes. At places the hornblende grains are deformed and the groundmass shows winding around hornblende grains (Fig. 5.2). Hornblende phenocryst is strongly pleochroic in different shades of green color. Quartz veins are commonly observed in these rocks which cut across the phenocryts of plagioclase and hornblende showing their later intrusion. Epidote (<5%) is present in the form of granular aggregates throughout these rocks while sometime epidote also occurs in the form of vein material. The rock shows well developed fabric as the plagioclase and amphiboles (both hornblende and tremolite/actinolite) show preferred orientation along the fabric direction. Opaque phase (<3%) is scattered in these rocks. It is mainly associated with hornblende grains both in the phenocryst as well as in the groundmass.

5.1.2. Rocks of Ishkoman Volcanic Centre

As mentioned earlier (Chapter 3), the rocks of IVC contain basaltic-andesite lava flow and volcanoclastic and pyroclastic rocks, but in order to understand the magma composition the samples of basaltic-andesite lava are selected for petrographic studies. These lavas have well-developed porphyritic texture having phenocrysts of plagioclase, augites, and hornblendes ranging from medium to coarse-grained embedded in the fine-grained (cryptocrystalline) groundmass. The modal mineralogy of these rocks is given in (Table 5.2) and the textural behavior, minerals association, alteration and phenocryst to groundmass relationships are shown in figures 5.4 to 5.8.

These rocks have dominantly augite and plagioclase in the form of phenocrysts, set in a partially chloritized felsophyric matrix with scattered epidote and opaque phases (Fig. 5.5). Clinopyroxene is augite in composition, having euhedral shape. At places it shows alteration to chlorite along micro-fractures (Fig. 5.5). The augite phenocrysts range from 5% to 35% and attained larger size as compared to the plagioclase phenocrysts. The augite phenocrysts are generally fresh but in some samples these show alteration to chlorite along margins and micro-fractures (Fig. 5.5). The prismatic grains of amphibole (hornblende) phenocryst (up to 30%), having well developed twinning are noticed in some thin sections (Fig. 5.6).

Table. 5.1. Modal mineralogy of BASD volcanics. The various mineral phases are in volume %.

Minerals	Basalt GD-4	Basalt GD-5	Basalt GD-6	Basalt GD-7	Basalt GD-8
Plagioclase	25%	30%	25%	20%	30%
Alkali-feldspar	3%	5%	-	5%	5%
Amphibole (Hornblende/ tremolite/ Actinolite)	30%	7%	30%	25%	15%
Groundmass	38%	52%	40%	45%	42%
Epidote	<1%	Traces	Traces	Traces	5%
Chlorite	2%	3%	3%	2%	1%
Opaque	2%	3%	2%	3%	2%
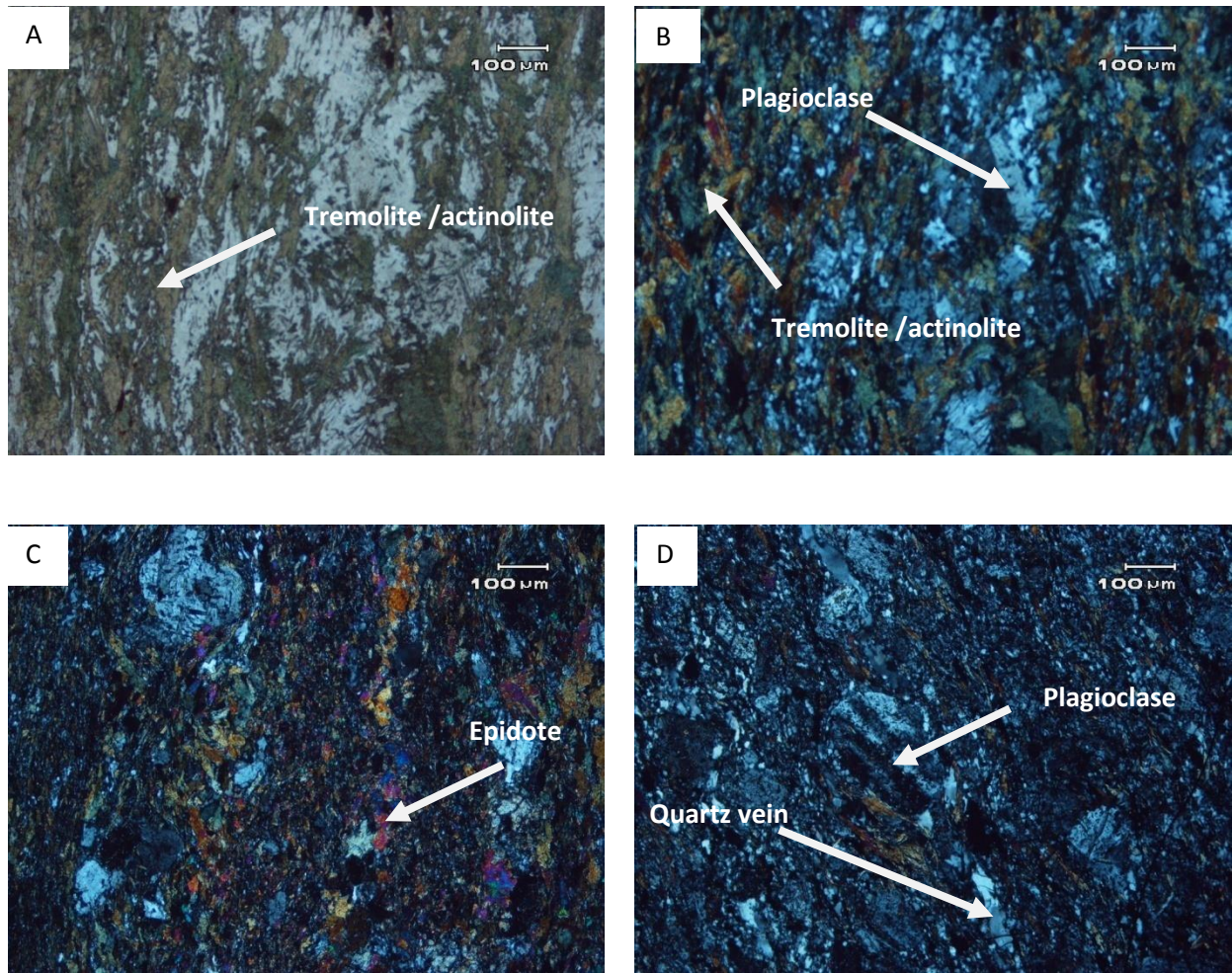
Fig.5.1. Photomicrographs: (A: PPL and B: XPL) Phenocryst of plagioclase is present while in groundmass flakes of tremolite/actinolite are visible which have preferred orientation, (C: XPL) Abundant epidotes are present in the groudmass of these volcanics, (D: XPL) Deformed plagioclase phenocryst is embedded in felsic groundmass having quartz microvein.
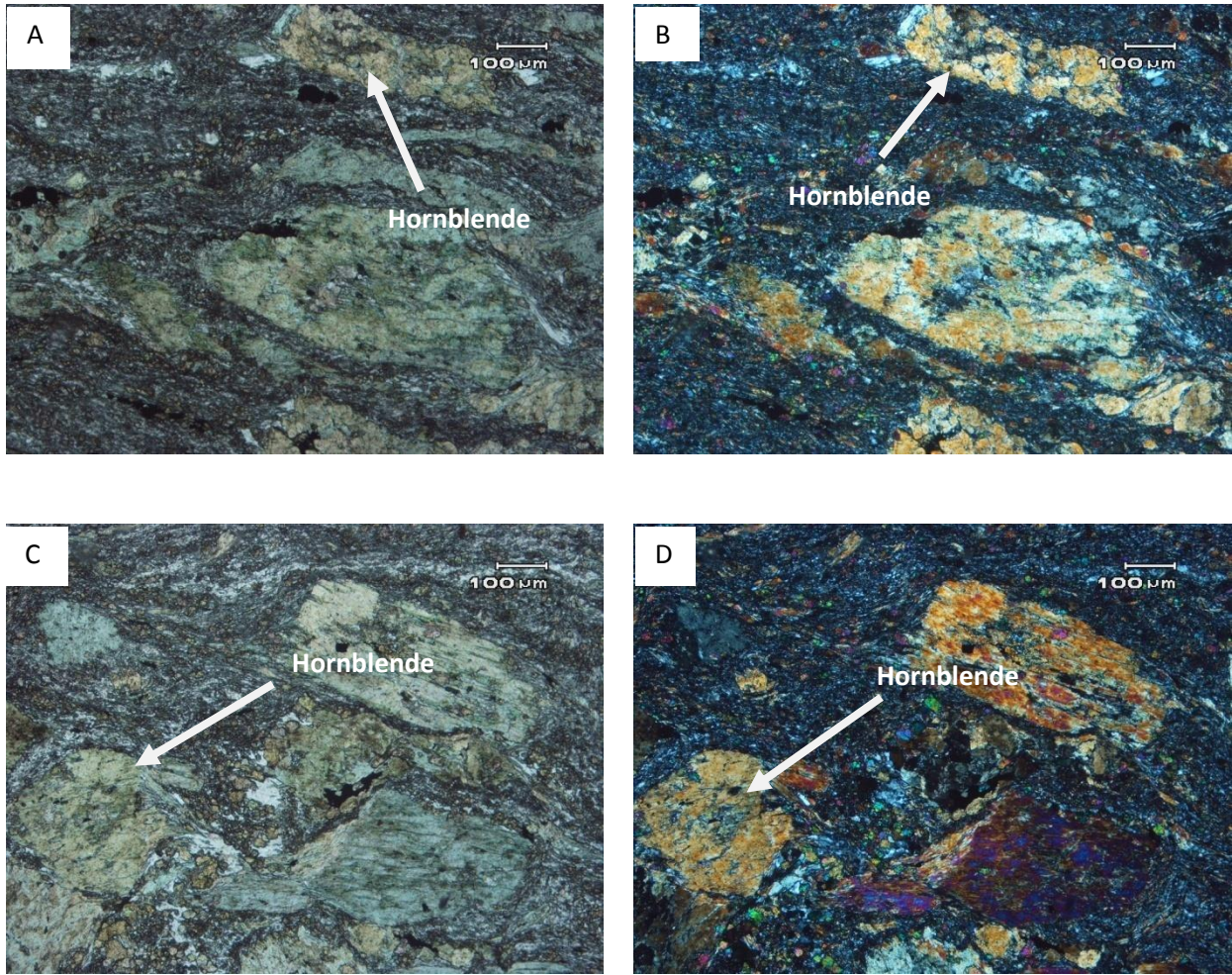
Fig.5.2. Photomicrographs: (AC: PPL; BD: XPL) Deformed phenocrysts of hornblende showing preferred orientation and the alteration product epidote is abundantly present in the groundmass. The groundmass exhibit winding around hornblende grains, appearing as augen structure.
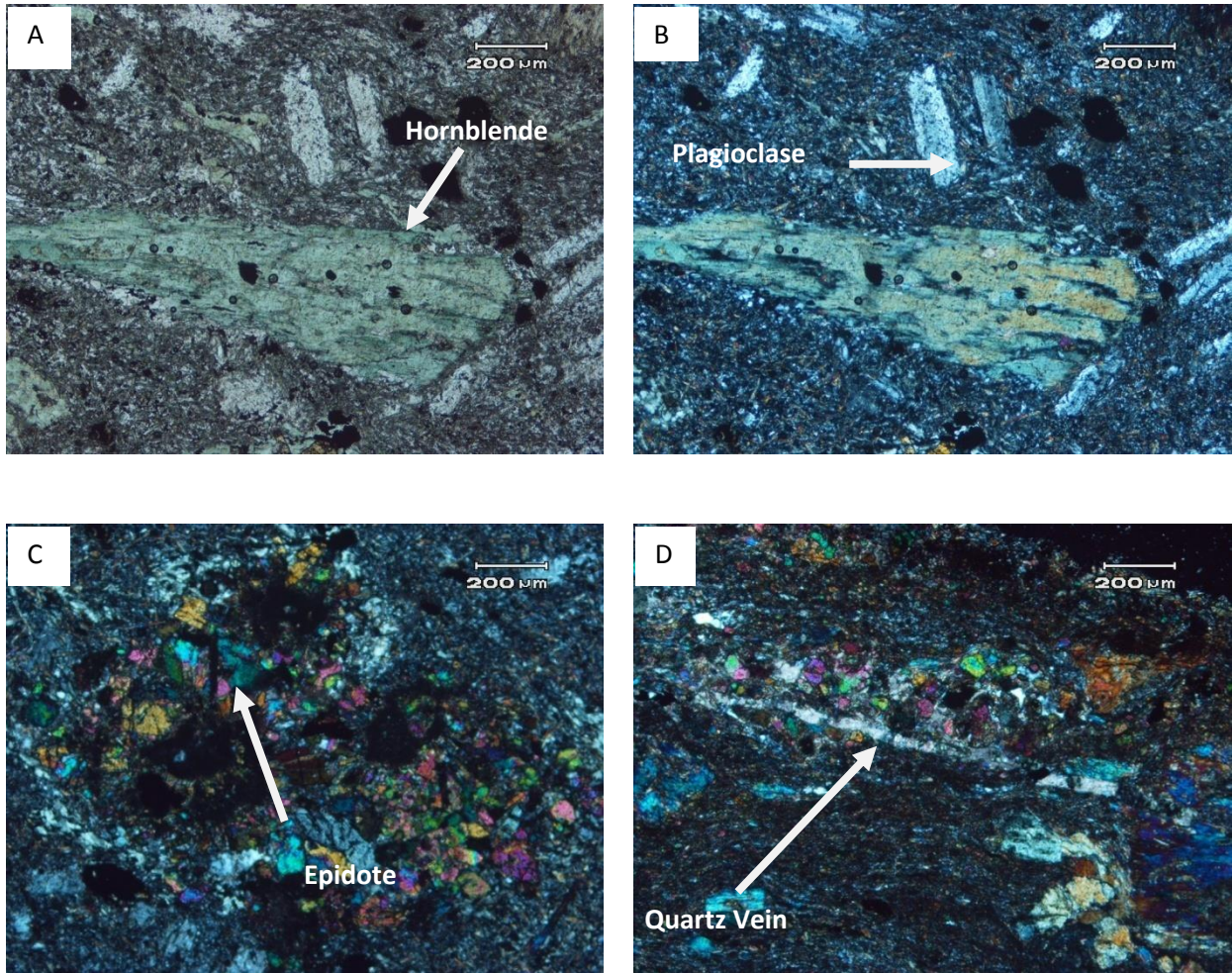
Fig.5.3. Photomicrographs: (A: PPL and B: XPL) Phenocrysts of plagioclase and hornblende are embedded in the groundmass having scattered fibrous tremolite/actinolite, epidote and opaque phases, (C: XPL and D, XPL) Groundmass is abundantly cryptocrystaline with scattered epidote and opaque phases. A microvein of fine-grained quartz is also visible.

In some thin sections, plagioclase is the dominant mineral phase, ranging from 20 to 35% with lesser amount of alkali-feldspar and quartz as phenocryst. The plagioclase and alkali-feldspar are generally fresh looking but partial alteration to epidote, carbonates, sericite and a dirty mass is also noticed. In some cases the groundmass has fine-grained granular aggregates of epidote. The fracture filled microveins of fine-grained felsic material are very common. These microveins are usually cutting the plagioclase phenocryst suggesting later filled veins. The quartz in the form of phenocrysts has been noticed in small amount (3%) in two thin sections (Table 5.2 and Fig. 5.4).

5.2. Diorites

On the basis of thin section study, the studied diorite can be divided into two groups: one group consists of major proportion of plagioclase, hornblende and biotite while the other group is having plagioclase, biotite and clinopyroxene (augite) in abundance. The minor amount of other minerals like quartz, alkali feldspar and opaque minerals are present in all of these rocks, whereas zircon, apatite and garnet occur in trace amount as accessory minerals. Texturally these rocks are medium to coarse-grained, with inequigranular, hypidomorphic texture. These rocks are partially altered to sericite and epidote which are observed on the surface of plagioclase grains, while the greenish color chlorite is present in the vicinity of biotite, hornblende and opaque phases. The modal mineralogy of these rocks is given in the Table 5.3 and the textural features, type of minerals and their alteration phases have been shown in figures 5.9 to 5.13.

Table. 5.2. Modal mineralogy of IVC volcanics. The various mineral phases are in volume %.

Minerals	Basaltic-andesite	Basaltic-andesite	Basaltic-andesite	Basaltic-andesite	Basaltic-andesite	Basaltic-andesite	Basaltic-andesite	Basaltic-andesite	Basaltic-andesite
	GD-9	GD-10	GD-11	GD-12	GD-14	GD-15	GD-16	GD-17	GD-18
Quartz	3%	2%	3%	3%	-	-	-	-	-
Plagioclase	35%	35%	30%	32%	20%	25%	25%	20%	25%
Alkali-feldspar	6%	5%	10%	10%	5%	-	3%	5%	-
Augite	10%	5%	5%	5%	30%	35%	-	25%	30%
Amphibole (Hornblende)	-	-	-	-	-	-	30%	-	-
Epidote	Tr	3%	2%	Tr	Tr	Tr	2%	Tr	Tr
Opaque	1%	Tr	Tr	Tr	Tr	Tr	<1%	Tr	<1%
Groundmass	45%	50%	50%	50%	45%	40%	40%	50%	45%
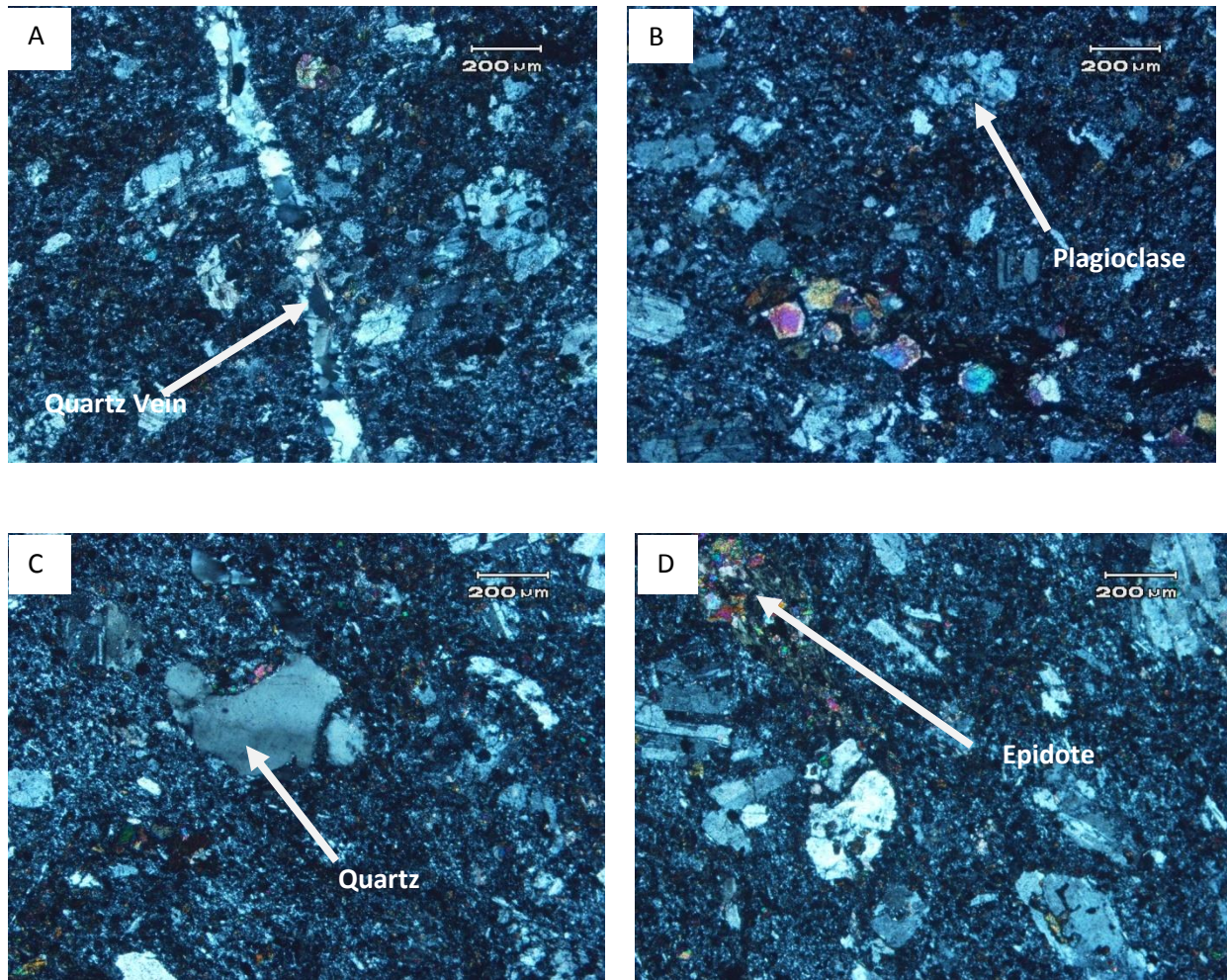
Fig.5.4. Photomicrographs (XPL): (A and B) Plagioclase phenocryst set in felsic groundmass; quartz microvein is also visible, (C) Phenocryst of quartz set in felsophyric groundmass (D) Phenocrysts of plagioclase, quartz and alkali-feldspar are set in the groundmass having granular epidote.
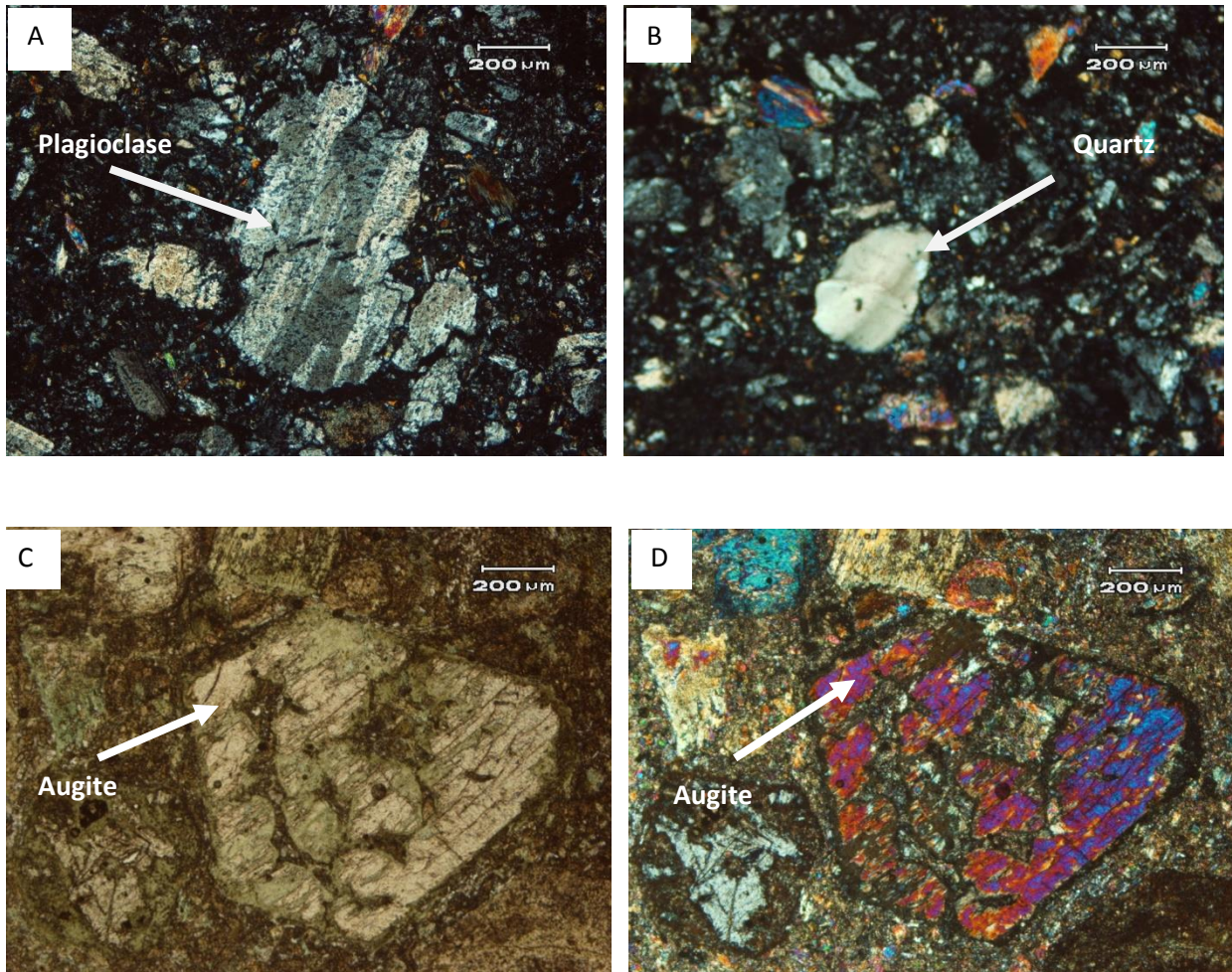
Fig.5.5. Photomicrograph (XPL): (A) Phenocryst of altered plagioclase, (B) Phenocryst of quartz in the felsic groundmass having scattered epidote, (C) (PPL) phenocryst of augite altered to chlorite along cleavage planes, (D) (XPL) phenocryst of augite showing high interference colors.
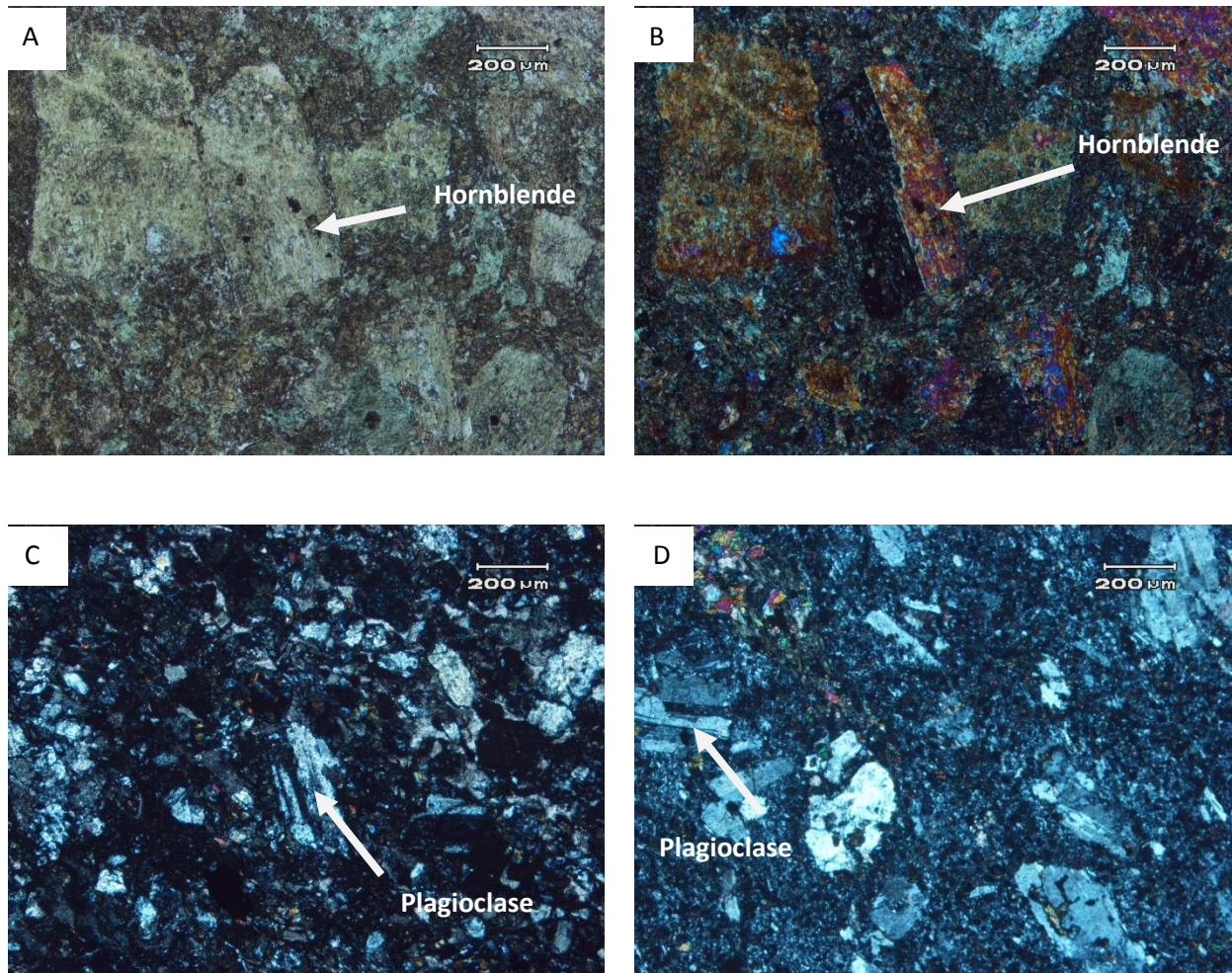
Fig.5.6. Photomicrograph (XPL): (A, B) phenocrysts of euhedral to subhedral hornblende showing simple twinning, (C, D) Phenocrysts of plagioclase set in a felsphyric groundmass.
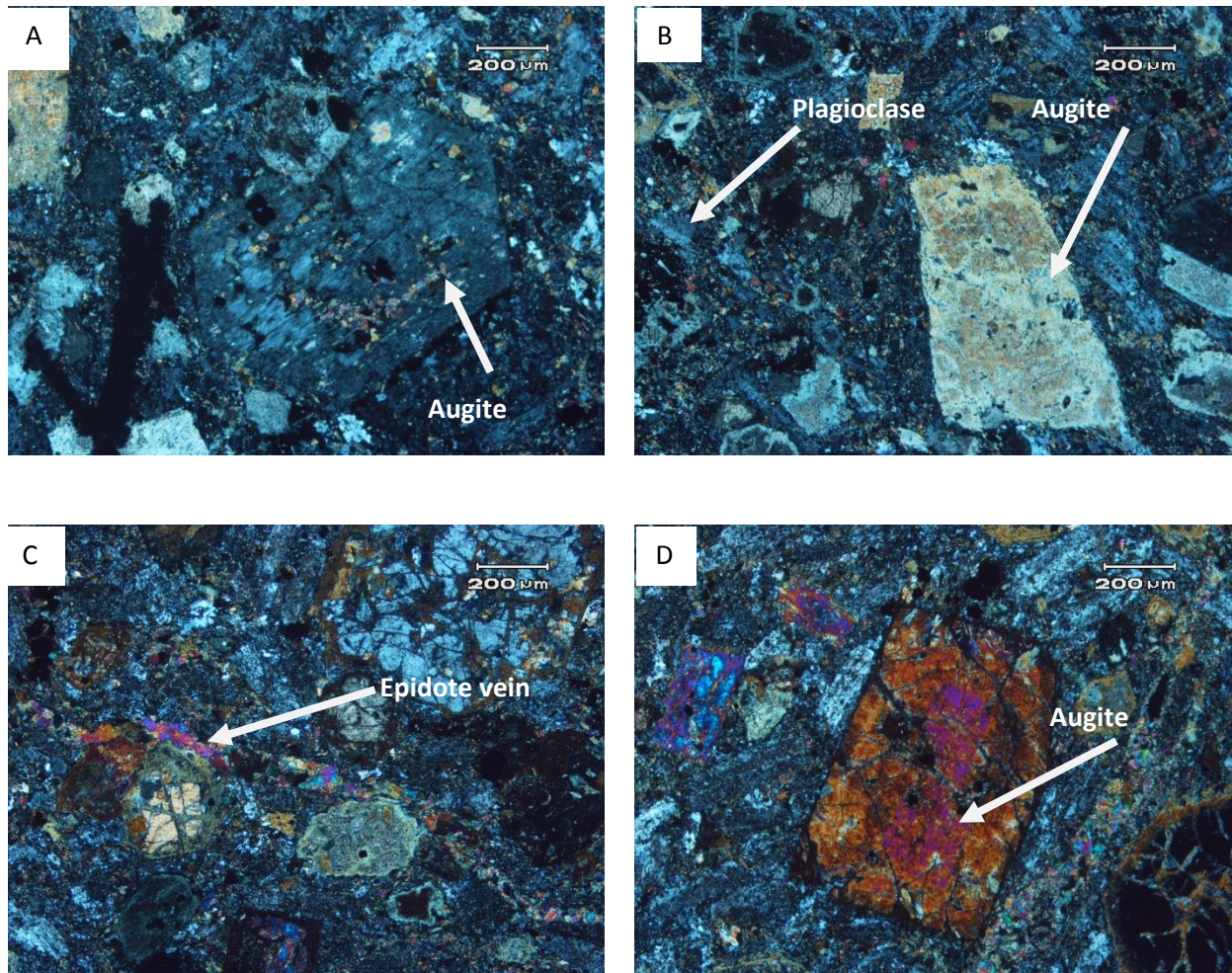
Fig.5.7. Photomicrographs (XPL): (A) Euhedral grain of augite showing alteration to epidote, (B) Large size phenocryst of augite along with small size plagioclase set in felsic groundmass, (C) Epidote vein crossing through the margins of augite phenocryst while the pseudomorphs of plagioclase can also be seen, (D) Phenocrysts of augite and plagioclase, set in felsic groundmass having scattered granular aggregates.
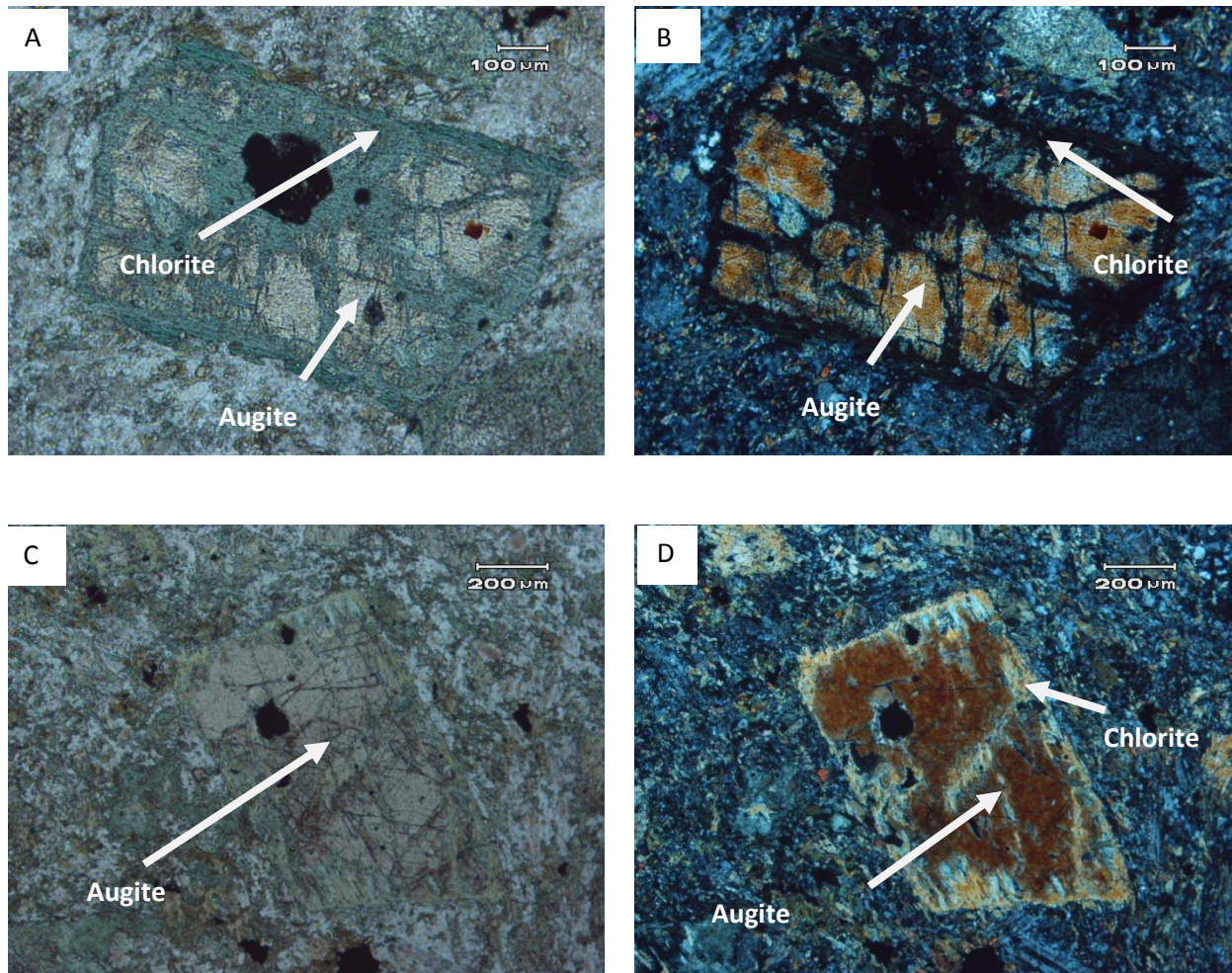
Fig.5.8. Photomicrographs (A, PPL): Phenocryst of augite showing alteration along margins and fractures to chlorite, (B, XPL): Chlorite an alteration product of augite at extinct position, (C, PPL; D, XPL) Phenocryst of augite embedded in groundmass.

The dominant mineral phase in all of these samples is plagioclase which is ranging from 40-60% and has tabular form, good polysynthetic twinning and partially altered to clay (sericite) and epidotes (Figs. 5.9 and 5.10). The anorthite content is ranging from 15-25% (An_{15-25}) indicating their sodic nature. Vermicular texture in feldspar is observed in almost all the samples, which is the result of co-precipitation of feldspar and quartz usually in crystallizing residual melts.

Hornblende is the second most abundant mineral phase ranges from 15 to 22% and the grains have subhedral to anhedral form and readily altered to chlorite and epidote along weak zones and margins (Figs. 5.10 and 5.11). Hornblende is strongly pleochroic from light-green to dark-green and where it is altered to chlorite that part is weakly pleochroic in green color. Some of the grains of hornblende showing simple twinning and at places it is intensively altered to chlorite and few crystals are also altered to epidotes. Inclusions of plagioclase are present within hornblende grains. Some of the hornblende grains have well developed rhombic cleavages.

Biotite (10-20%) is present in abundance in these rocks having well developed flaky form and strongly pleochroic. Biotite is altered to chlorite at grain boundaries, along fractures and birds eye extinction can be easily detected in biotite grains. Ore minerals are also present within biotite grains, especially along fracture planes. At places, titanium bearing opaque phases have developed coronas of leucoxene (Fig.5.12). Alkali-feldspar is generally orthoclase showing grid twinning with subhedral shape and is showing partial alteration to sericite at place. At places the alteration is so intense that the whole grain appears as dirty mass. Few grains of microcline are observed in some of these rocks which have well developed hatched twinning. Quartz grains are in minute amount (up to 5%) and grain size is smaller look like space filling material. The undulose extinction present within quartz grains suggests that rocks have subjected to stress condition either locally or regionally.

In two thin sections anhedral grains of augite were noticed (Table 5.3), showing partial alteration to chlorite. Chloritization usually occurs along cleavage within augite grains. Some of the augite grains exhibit intensive alteration while the others also have inclusions of plagioclase.

Table. 5.3. Modal mineralogy of diortic rocks. The various mineral phases are in volume %.

Minerals	Diorite GD-20	Diorite GD-21	Diorite GD-22	Diorite GD-23	Diorite GD-24
Quartz	5%	5%	5%	5%	5%
Plagioclase	60%	50%	55%	50%	60%
Alkali-feldspar	15%	8%	8%	10%	10%
Hornblende	-	15%	22%	20%	-
Biotite	10%	20%	10%	15%	10%
Augite	10%	-	-	-	15%
Apatite	-	-	Traces	Traces	Traces
Zircon	-	-	Traces	Traces	Traces
Opaque	<1%	<1%	<1%	<1%	<1%
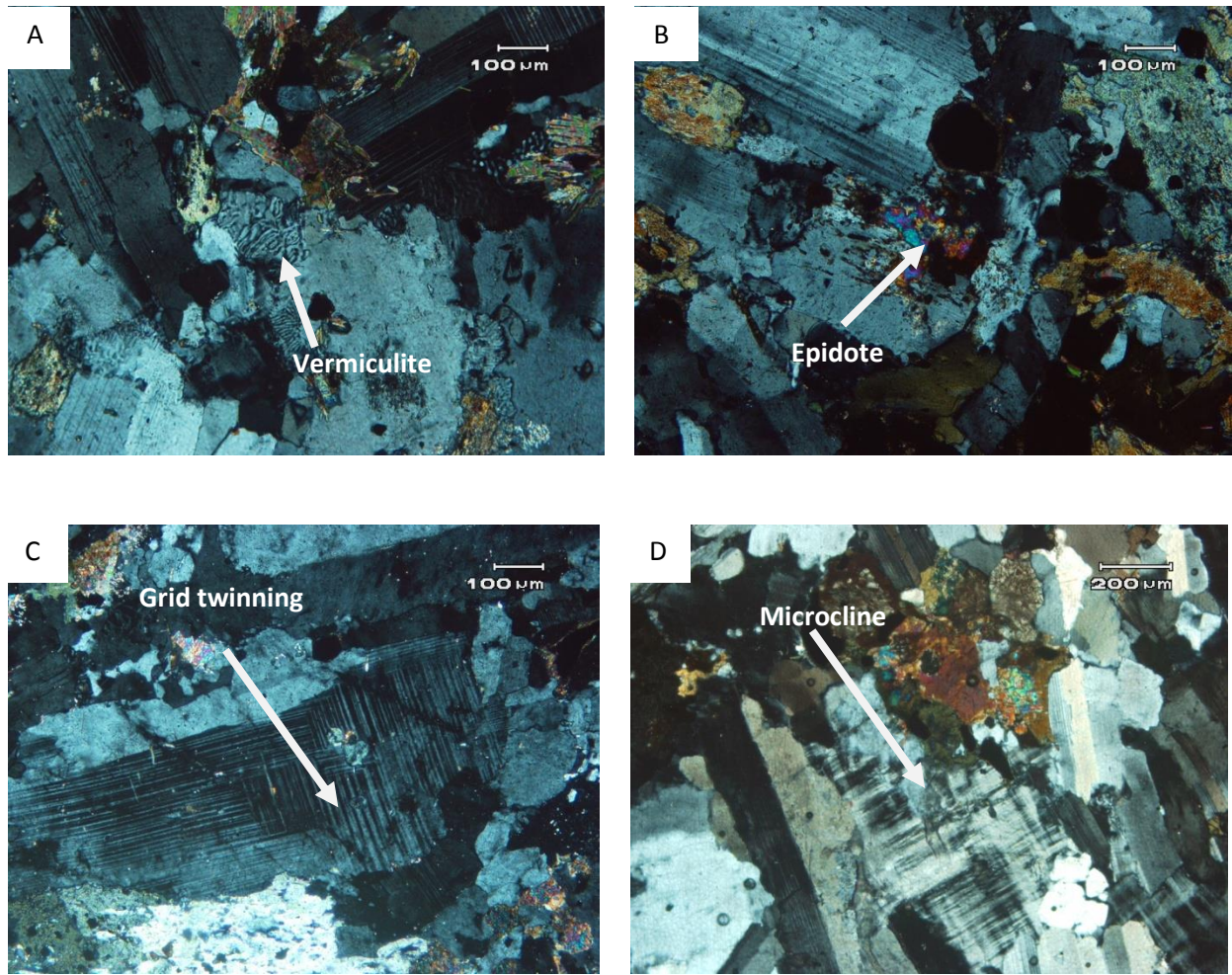
Fig.5.9. Photomicrographs (XPL): (A) Vermicular texture is visible, (B) Alteration of plagioclase to epidote, (C) Grid twinning in alkali feldspar, (D) Cross hatched twinning in microcline.
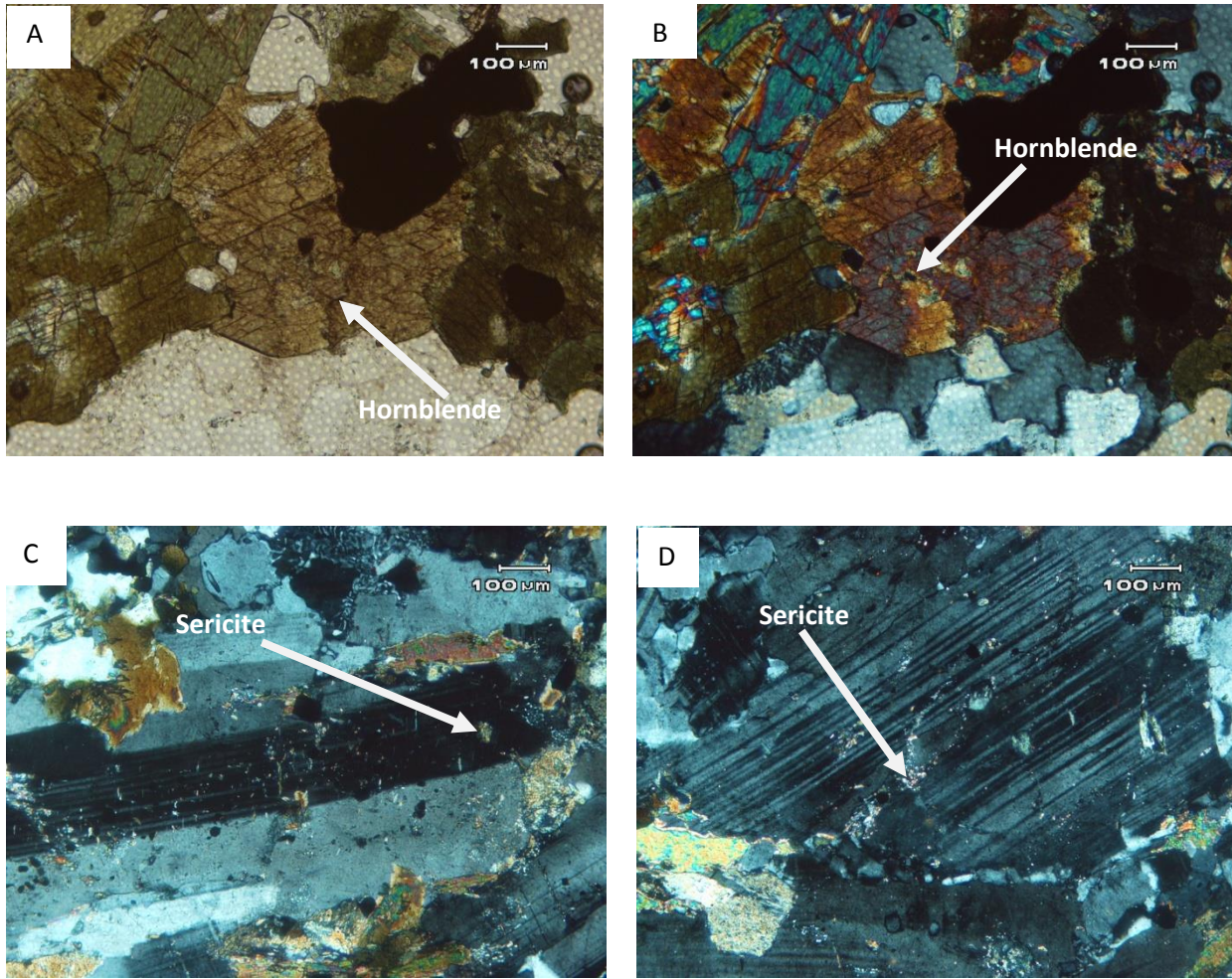
Fig.5.10. Photomicrographs: (A: PPL and B: XPL) Anhedral to subhedral hornblende grain surrounded by quartz in the lower side, the opaque grains are visible, (C: XPL and D: XPL) Sericite, the alteration product of plagioclase is present at normal direction to the polysynthetic twinning within plagioclase grains.
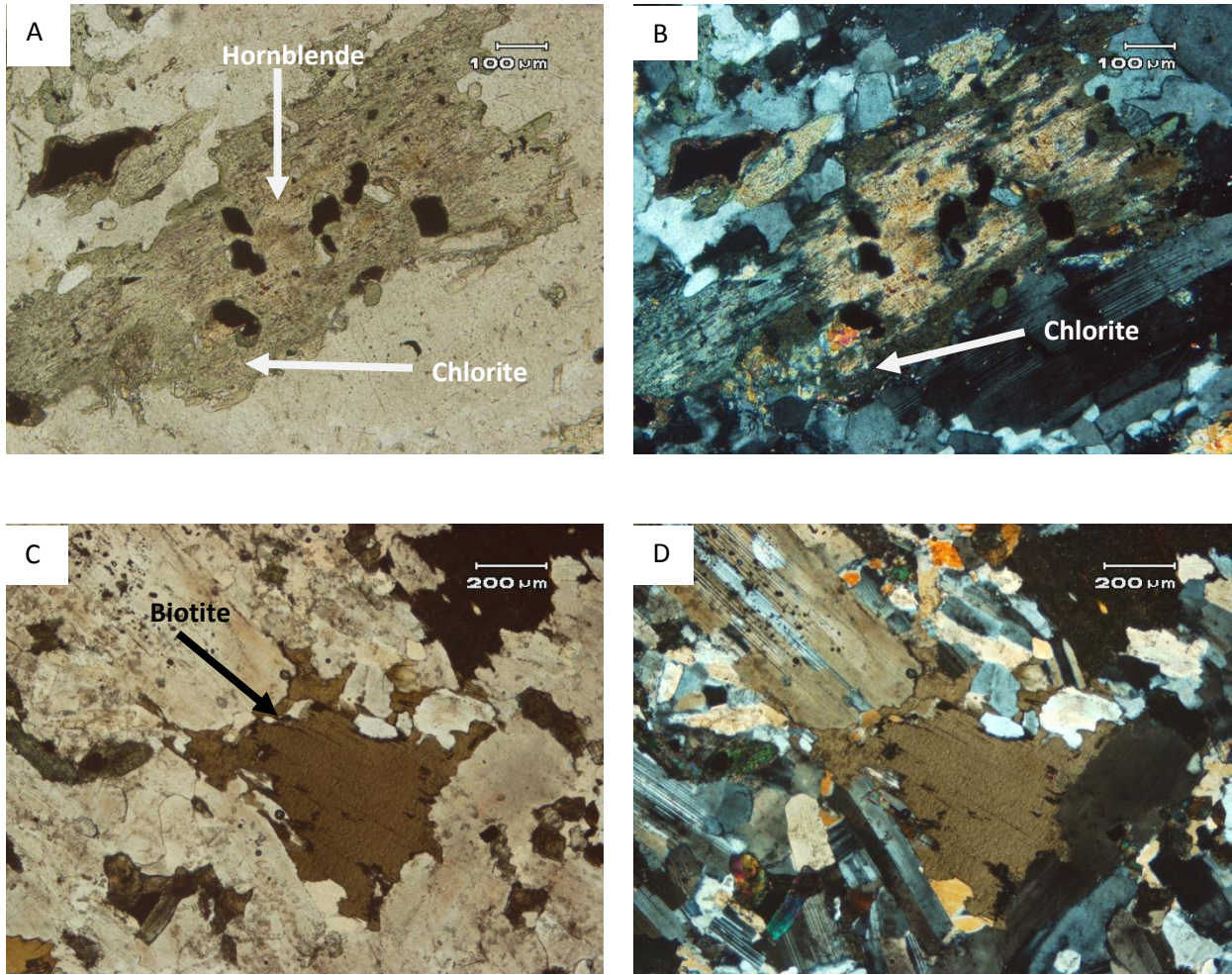
Fig.5.11. Photomicrographs: (A: PPL and B: XPL) Alteration of anhedral grains of hornblende to chlorite, inclusions of opaque minerals are also visible present, (C: PPL and D: XPL) Flakes of biotite surrounded by alkali-feldspar quartz and plagioclase.
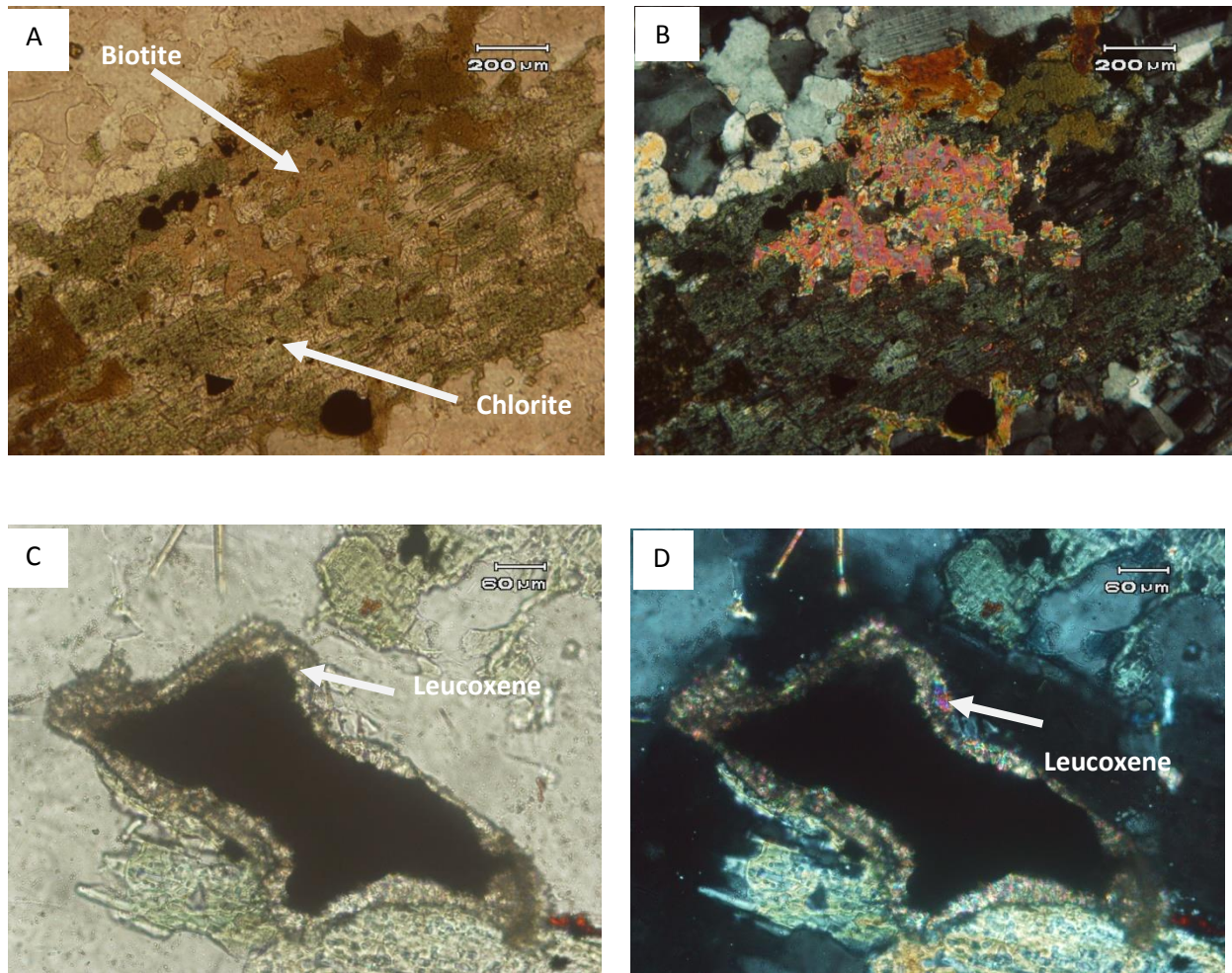
Fig.5.12. Photomicrographs: (A: PPL and B: XPL) Alteration of biotite to chlorite surrounded by small grains of quartz, (C: PPL and D: XPL) A thin border of leucoxene around an opaque mineral.
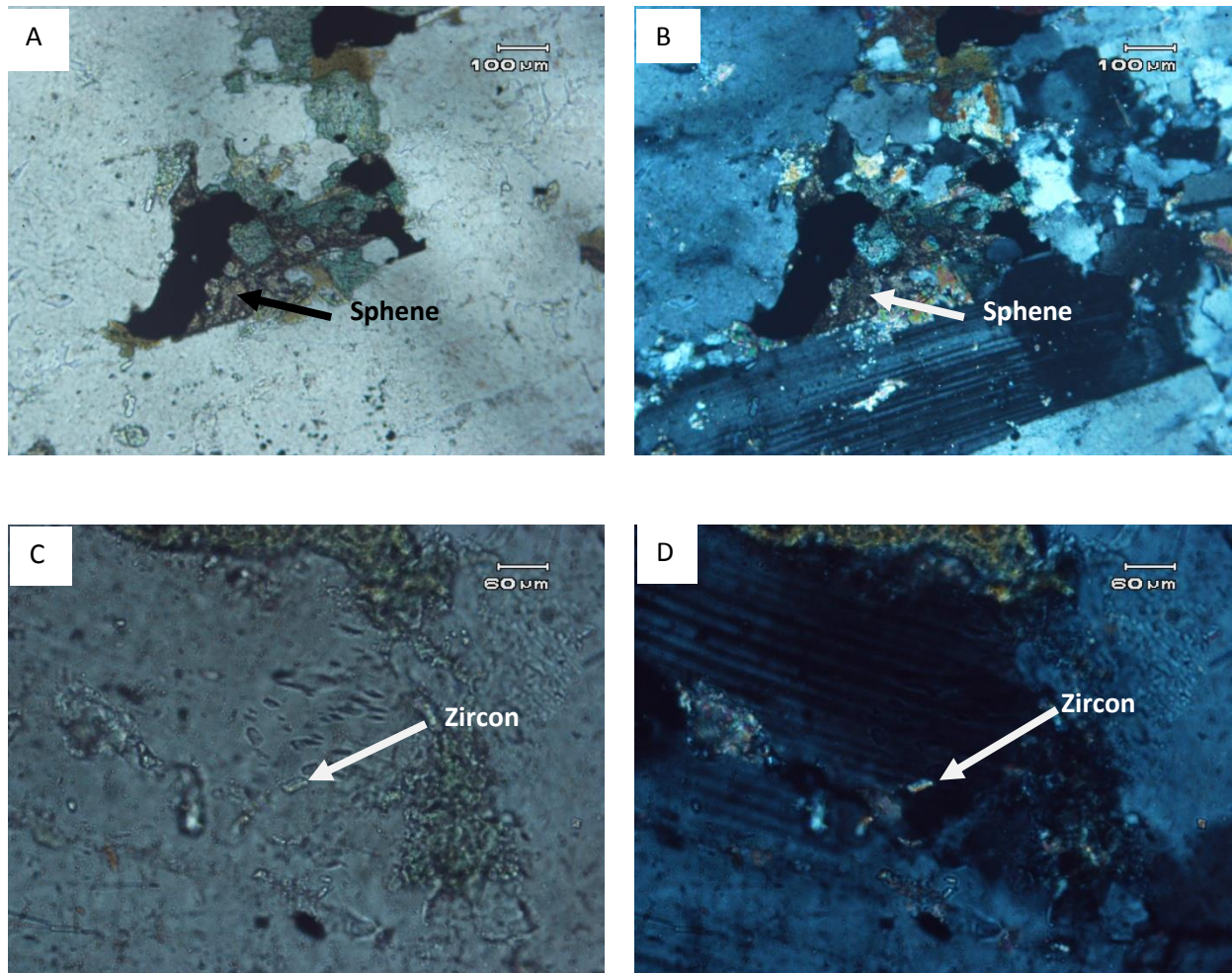
Fig.5.13. Photomicrographs: (A: PPL and B: XPL) Accessory mineral sphene formed adjacent to opaque mineral phase, (C: PPL and D: XPL) Inclusion of small size zircon within plagioclase grain.

CHAPTER 6

GEOCHEMISTRY

Geochemistry is defined as absolute and relative abundances of elements in the earth, and the lavas governing the distribution of these elements. Geochemical study of the study area was conducted by using different tools of geochemical analysis including whole rock geochemistry through XRF and bulk samples analysis for finding concentrations of gold and base metals using atomic absorption spectroscopy techniques (see Chapter 4). Petrogenetic studies are helpful in the characterization of source rocks from the magma chamber and condition under which the rocks are crystallized from the source magma. Petrogenetic studies of rocks are done by finding out the whole rock geochemistry of both major oxides and trace elements (Wilson, 1989). For the geochemical studies nine representative samples (3 samples each of BASD volcanics, IVC volcanics and diorites) were selected for whole rock geochemistry including the trace and major elements analysis whereas, eighteen bulk samples were selected for gold and base metals concentration in the study area. The geochemical data was obtained for two purposes, first to find out the tectonic setting of the study area and second to find out the concentration of base metals and gold associated with the altered/sulfide zones in the study area. Tectonic setting of the study area has been identified using different discrimination diagrams during this study.

6.1. Whole rock geochemistry

The data obtained as a result of the whole rock geochemistry was used in the plotting of different types of plots. These plots include Harker diagrams and discrimination binary and ternary plots. These binary and ternary discrimination plots are used for finding the geological setting of a tectonic zone and magma origination and its involvement in the formation of different variety of rocks.

Major element whole rock chemistry is generally based on ten elements (i.e., Si, Ti, Al, Fe, Mn, Mg, Ca, Na, K and P) which are usually reported as oxides. These are applied in the classification and nomenclature of igneous rocks. It is also used in construction of variation diagrams both bivariate and trivariate plots. These diagrams are useful in understanding the interrelationship between elements in the data set and from this relationship the geochemical process can be inferred. The major element data can also be used to calculate the CIPW norms.

During this calculation process chemical composition of igneous rocks is converted to an ideal mineral composition which is expressed as normative mineralogy. The normative mineralogy is usually different from the modal mineralogy based on visual estimates.

Trace element whole rock geochemistry has attained greater importance after the advancement in analytical instrumentation as the detection of trace elements in the rocks can be achieved more reliably. The trace elements play a vital role in the modern petrology and are very useful in discriminating between petrological processes. The trace elements are usually studied in groups and their behavior within the same group or in different groups can indicate the changes in the petrological process. The trace elements are generally classified as rare earth elements (REE), the platinum group elements (PGE), noble metals which include Au and transition metals, high field strength cations (HFS) and large ion lithophile elements (LILE).

Trace elements geochemistry is used mainly for tectonic setting and as well as the generation of magma and its crystallization. In many cases the major elements geochemistry is not helpful for finding the tectonic setting and thus trace elements are used for the study of igneous processes. The trace elements representing the largest group of discrimination diagrams are very helpful and used in a variety of binary, ternary and spider diagrams to distinguish between different types of magmas as well as their tectonic environment. The widely used trace element includes Ti, Zr, Y, Nb and P from the high field strength elements because they are immobile and remain in the magma melt till the last stages. The whole rock major and trace element chemistry of the studied rocks is evaluated for the variation in chemical behavior of major and trace elements and also deciphering the paleotectonic history of these rocks in the following section.

6.1.1. Ghizar formation
6.1.1.1. Basalt-andesite sheet dominant volcanics

Major element: The major element composition of the BASD volcanics are presented in Table 6.1. These volcanics plot in the compositional field of basalt (Fig. 6.1) when plotted in the SiO_2 vs Na_2O+K_2O classification diagram of Le Bas et al. (1986). The SiO_2 (46.67-47.89 wt%), Al_2O_3

(17.34-17.56 wt%), and Na_2O (2.95-3.32 wt%) exhibit no greater variation while rest of the oxides have a relatively wide range as TiO_2 is ranging from 0.49 to 0.72 wt%, Fe_2O_3t from 8.31-10.05 wt%, MnO from 0.10 to 0.19 wt%, MgO from 3.11 to 5.77 wt%, CaO from 11.12-11.78 wt%, K_2O from 0.10 to 0.71 wt% and P_2O_5 from 0.14 to 0.27 wt%. The loss on ignition (LOI) is ranging from 4.90 to 5.43 wt%. The high values of LOI suggest that these rocks might have suffered post magmatic secondary alteration. There could be the possibility that these rocks have been subjected to elemental mobilization especially the alkalis which are highly mobile. The CIPW norms calculated on anhydrous basis, using MINPET program, have been given in Table 6.1. The normative composition suggests that these rocks are olivine (0.59-3%) normative with high concentration of plagioclase (62.14-64.15%) and highly variable amount of diopside (8.57-22.22%) and hypersthene (1.29-19.1%). The other normative phases are orthoclase (0.65-4.49), ilmenite (1.01-1.48%), magnetite (3.9-4.7%) and apatite (0.35-0.65%). The Mg # $[100 \times MgO/(MgO+Fe_2O_3^t)]$ of all the samples is low, ranging from 0.27% to 0.36%.

The major element oxides have been plotted in Harker diagram (Fig. 6.2) to see their variation trends during differentiation. It is clear from these plots that $Fe_2O_3^t$, MgO and CaO show smooth negative line of descent while Al_2O_3, MnO and TiO_2 have poorly defined negative trend and P_2O_5 and Na_2O+K_2O a weak positive trend against SiO_2. These weakly defined trends can be attributed to the post-magmatic secondary alteration as discussed above. These kind of variation trends are comparable with the calc-alkaline rocks. These rocks are plotted on the AFM diagram (Fig. 6.3) of Irvine and Baragar (1971) which differentiate the tholeiitic rocks from the calc-alkaline rocks. All the three samples of the BASD volcanics plot on the dividing line indicating both tholeiitic and calc-alkaline characteristics.

Trace element: The trace element compositions of the BASD volcanics are given in Table 6.1. This table shows that the large ion lithophile elements (LILE) such as Sr (356-1961ppm), Ba (10-123ppm), Th (1-3ppm) and Rb (1-14ppm) and the High field strength elements (HFSE) such as Nb (1-4ppm), Pb (3-9ppm), Cr (45-164ppm), Zr (38-59ppm) and Y (19-26ppm) display a variable concentration. However, it can be envisaged from this table that the BASD volcanics though displaying heterogeneity but still these are enriched in LILE as compared to HFSE. Selected trace elements were plotted against SiO_2 in the Harker diagram (Fig. 6.4). Due to less

number of samples the clear trends cannot be obtained in these plots. The sample No GD-2 is deviating from the line of descent which indicates either the analytical error or the effects of post-magmatic alteration. However, the poorly defined positive and negative trends can be observed for Sr, Rb and Y and V, Zr and Sc respectively (Fig. 6.4). Cr is, however, showing greater scatter. The variation trends of the trace elements also favor the calc-alkaline magmatism for the BASD volcanics.

The use of trace elements in the interpretation of igneous rocks is used with great care as there is the involvement of weakly mobile and immobile element such as Ba, Sr, Zr and Ce. Various trace elements (i.e., Nb, La, Nd, P, Sm, Ti and Y) are considered insensitive to any changed environment such as weathering, alteration, metamorphism and other secondary process. These trace elements have been used for discriminative purposes (e.g., Pearce and Cann, 1973; Smith and Smith, 1976; Wood et al., 1979; Shervais, 1982; Saunders and Tarney, 1991).

The LILE and HFSE are plotted in the primodial mantle, chondrite and MORB normalized spider diagrams of Taylor and Mclennan (1985) (Fig. 6.5) Thompson (1982) and Sun (1980) (Fig. 6.5) and Bevins et al. (1984) (Fig. 6.5). The two samples of BASD volcanics in these diagrams generally show enrichment in LILE/HFSE ratios, therefore, have decreasing trend towards right while one sample exhibit very low Ba and Rb (may be due to alteration/leaching), due to which the trend is not well defined. These diagrams also display the negative Nb and positive Sr anomalies suggesting the role of calc-alkaline magmatism.

Table. 6.1. Whole rock geochemical data of the study area.

	BASD Volcanics			IVS Volcanics			Diorites		
Sample	GD-1	GD-2	GD-3	GD-13	GD-16	GD-18	GD-23	GD-21	GD-22
SiO_2	46.7	47.3	47.9	52.67	53.78	53.1	59.78	60.23	61.7
Al_2O_3	17.6	17.3	17.5	17.22	16.53	16.9	16.89	16.34	16
TiO_2	0.59	0.72	0.49	0.45	0.31	0.39	0.65	0.56	0.49
Fe_2O_3	10.1	8.75	8.31	9.22	8.32	8.78	6.56	6.12	4.89
MnO	0.19	0.1	0.14	0.19	0.22	0.13	0.09	0.13	0.12
MgO	5.77	3.33	3.11	7.2	5.8	6.21	2.94	2.54	2.78
CaO	11.8	11.6	11.1	9.34	8.13	8.42	5.8	5.73	5.68
Na_2O	2.95	3.23	3.32	1.92	2.74	2.37	3.42	3.89	3.82
K_2O	0.1	0.71	0.42	0.78	0.94	0.85	2.81	3.12	3.32
P_2O_5	0.14	0.27	0.26	0.3	0.38	0.44	0.37	0.33	0.42
L.O.I	4.9	4.67	5.43	1.57	1.8	2.83	0.8	0.92	0.84
Total	**101**	**98**	**97.9**	**100.86**	**98.95**	**100**	**100.11**	**99.91**	**100**
C.I.P.W. Norms									
Q	-	-	0.59	6.83	7.82	10	12.25	10.2	13.3
Pg	63.7	62.1	64.2	43.88	54.7	56.4	51.84	51.4	50.5
Or	0.65	4.49	2.66	13.65	5.73	0.65	16.72	18.6	17.4
Di	8.57	22.2	20.8	6.67	6.53	3.08	2.42	6.94	6.6
Hy	19.1	1.29	5.63	22.9	19.2	23	11.3	7.91	7.01
Ol	0.94	3	-	-	-	-	-	-	-
Il	1.22	1.48	1.01	0.72	0.82	0.76	1.25	1.08	1.71
Mg	4.7	4.07	3.9	4.03	3.73	4.35	2.89	2.68	2.15
AP	0.35	0.65	0.65	0.7	0.9	1.04	0.86	0.76	0.97
Trace elements (ppm)									
As	5	11	4	9	8	8	4	4	5
Sc	23	24	18	31	22	25	14	14	10
V	221	237	187	245	230	214	137	115	113
Co	32	17	15	50	50	36	18	16	23
Cr	45	164	45	402	226	198	65	79	55
Ni	23	76	20	110	82	61	39	35	15
Cu	85	17	127	18	66	71	100	145	138
Pb	3	9	6	6	4	6	14	14	11
Zn	96	71	78	105	116	79	81	89	58
Sr	356	1961	640	570	675	670	669	789	795
Rb	1	14	10	10	28	16	77	68	79
Ba	10	123	107	164	195	173	340	378	467
Th	2	3	1	4	3	3	10	9	12
U	1	1	2	2	1	1	1	1	2
Nb	2	4	1	1	1	1	8	7	6
Y	22	19	26	15	17	16	22	23	25
Zr	46	59	38	17	27	35	96	103	115
Hf	2	15	5	8	3	5	7	4	5
Ag	<0.05	<0.05	<0.05	<0.05	<0.05	<0.05	<0.05	<0.05	<0.05
Au	<0.05	<0.05	<0.05	<0.05	<0.05	<0.05	<0.05	<0.05	<0.05
Mg#	36	28	27	44	41	41	31	29	36
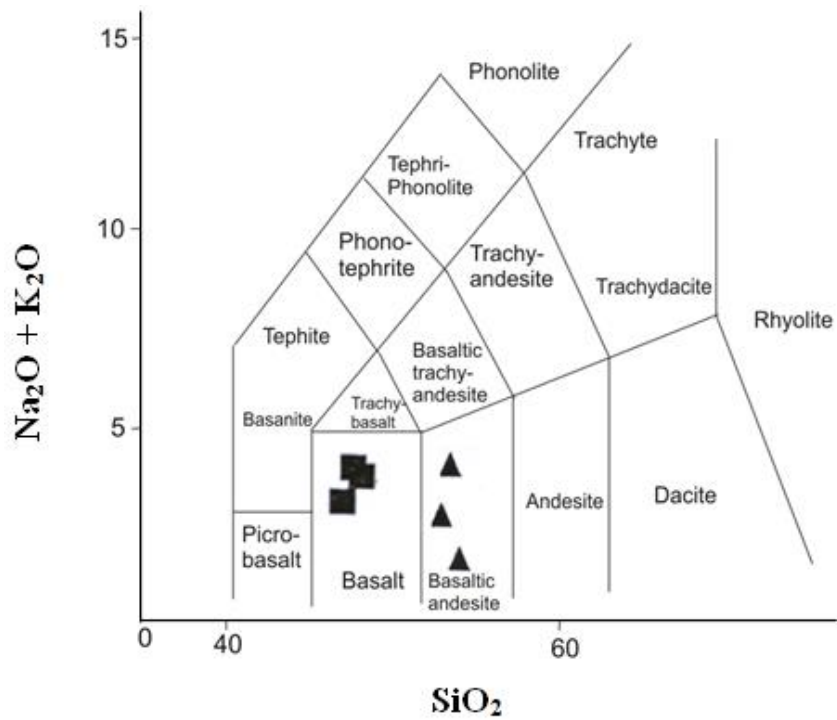
Fig.6.1. Plotting of volcanics rocks of the study area in a chemical classification of silica versus total alkalis diagram of Le Bas et al. (1986). ■ = Basalt-andesite sheet dominant volcanics, ▲ = Rocks of Ishkoman volcanic centre.
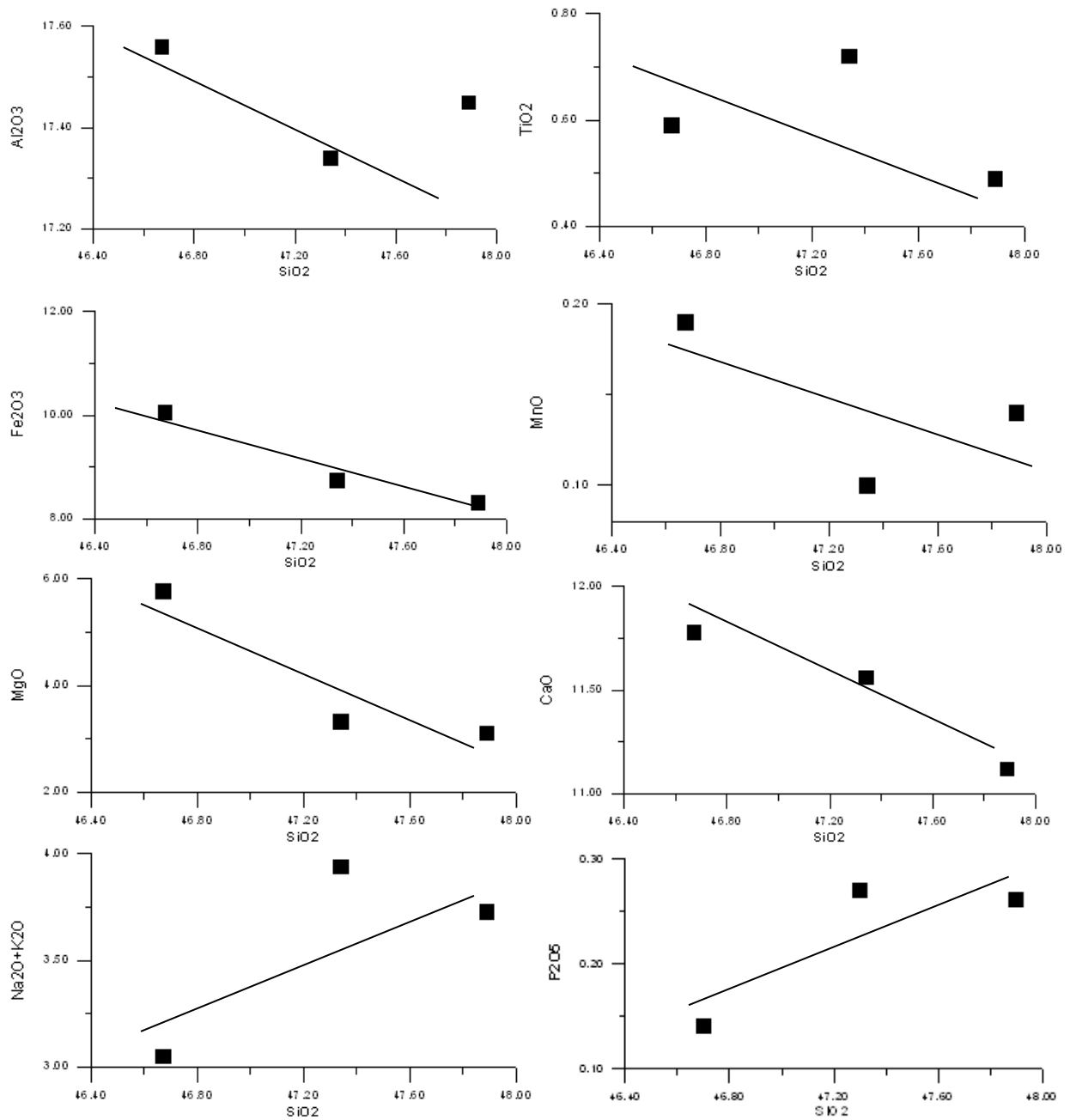
Fig.6.2. Silica versus major oxide Harker diagrams for BASD of the study area.
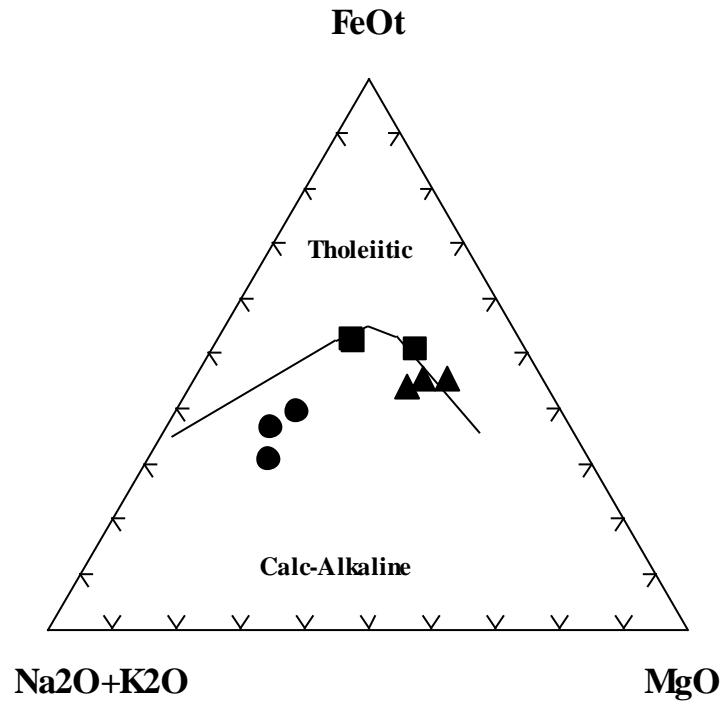
Fig.6.3. Plotting of rocks of the study area in alkalis-FeO-MgO ternary diagram differentiating fields of calc-alkaline and tholeiitic rocks (after Irvine and Barager, 1971). ■= Basalt-andesite sheet dominant volcanics ▲= Rocks of Ishkoman volcanic centre and ●= Diorites.

Fig.6.4. Silica versus trace elements Harker diagrams for BASD volcanics of the study area.
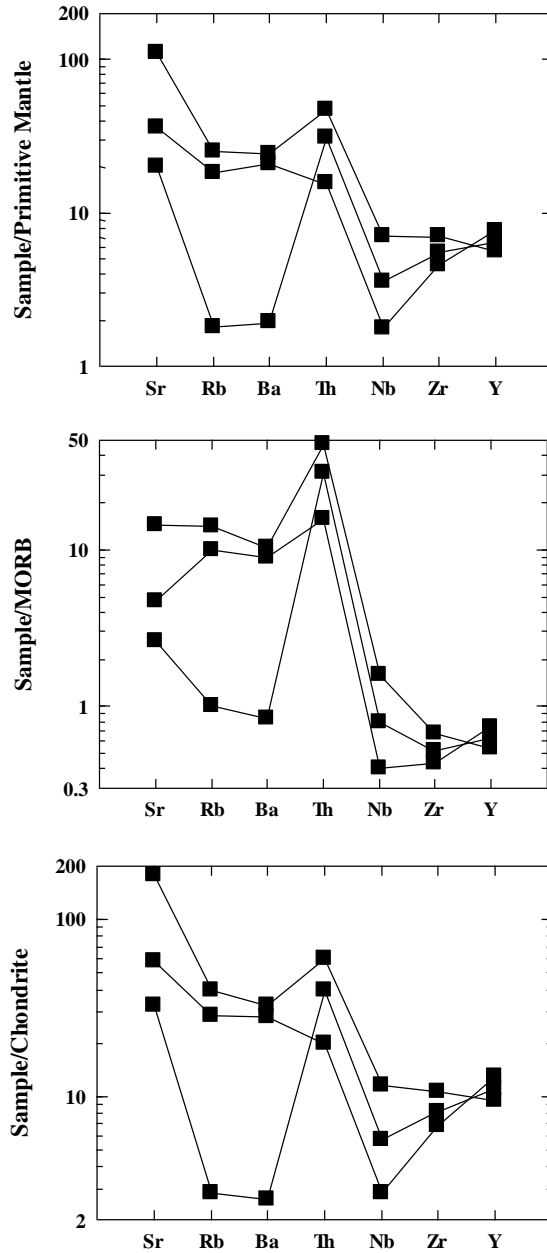
Fig.6.5. Spider variation diagram of BASD volcanics of the study area normalized to primitive mantle, MORB and Chondrite after Taylor and Mclennan (1985), Thompson (1982), Sun (1980) and Bevins et al. (1984) respectively.

6.1.1.2. Ishkoman Volcanic Centre volcanics

Major elements: The major element data of the IVC volcanics are given in Table 6.1. The rock samples fall in the field of basaltic-andesite on the basis of alkali vs SiO_2 diagram (Fig. 6.1) of Lebas et al (1986) and can also be classified on the basis of SiO_2 as basaltic-andesite (53-57%) (Gill, 1980). These rocks have narrow range of major element oxides having SiO_2 in the range of 52.67-53.78 wt%, Al_2O_3: 16.53-17.22 wt%, TiO_2: 0.31-0.45 wt%, Fe_2O_3: 8.32-9.22 wt%, MnO: 0.13-0.22 wt%, MgO: 5.80-7.20 wt%, CaO: 8.13-9.34 wt%, Na_2O: 1.92-2.74 wt%, K_2O: 0.78-0.94 wt% and P_2O_5: 0.30-0.44 wt%. The CIPW norms for these volcanics have been calculated on anhydrous basis and are presented in Table 6.1. These volcanics are quartz (6.83-10.83%) normative with dominant normative plagioclase (43.68-56.41%) and sub-ordinate normative hypersthene (19.17-22.99%). The other normative phases with lesser amount are orthoclase (0.65-13.65%), diopside (3.08-6.67%), ilmenite (0.72-0.76%), magnetite (3.73-4.35%) and apatite (0.70-1.04%). The Mg # of IVC volcanics ranges from 41 to 44% (Table 6.1).

The major element oxides are plotted against SiO_2 (considered as the differentiation index) in the Harker variation diagram (Fig. 6.6). It is clear from this diagram that the Al_2O_3, Fe_2O_3, MgO, CaO and TiO_2 display systematic decreasing trend while alkalis (Na_2O+K_2O), MnO and P_2O_5 show systematic increasing trend during differentiation. This indicates that fractionation could be the only process in evaluation of these rocks. This is compatible with typical calc-alkaline rocks. All the samples of the IVC volcanics when plotted in the AFM diagram, these are akin to the field of calc-alkaline rocks which is indicative of the rocks of subduction related environment.

Trace elements: The trace elements concentrations in the IVC volcanics are presented in Table 6.1. It is clear from this table that the LILE such as Sr, Ba, Th and Rb are ranging from 570 to 675ppm, 164 to 195ppm, 3 to 4ppm and 10 to 28ppm respectively while the HFSE such as Pb, Cr, Nb, Zr and Y varies from 4 to 6ppm, 55 to 79ppm, up to 1ppm, 17 to 35ppm and 15 to 17ppm respectively. This is indicative of enrichment of LILE as compared to the HFSE.

The samples are plotted on silica variation Harker diagram (Fig. 6.7). There is a negative correlation between silica and the compatable elements (Cr, V, Sc). Cr, Ni, V and Sc all decrease

with increasing SiO_2. The incompatible elements (Rb, Ba, Sr) show positive correlation against SiO_2. Zr and Y also show positive trend when plotted against SiO_2 (Fig. 6.7). The trends shown by most of the trace elements are consistent with the operation of fractional crystallization which is typical of calc-alkaline rocks.

The negative correlation of compatible elements shows that they are involved in the crystallization of minerals in the initial stages and their concentration decreased with the silica enrichment. The incompatible elements like Rb, Ba and Sr showing positive correlation with silica, which is the result of their incompatible nature and are not involved in the initial stages of crystallization and, therefore, their concentration increases with the enrichment of silica. The incompatible trace elements remain in the magma melt till the last stages of magma crystallization and thus its behavior shows the tectonic history under which different rocks form from the melt.

The LILE and HFSE of the three samples of IVC volcanics are normalized to primodial mantle, chondrite and MORB values and are plotted in Figure 6.8. The patterns obtained in this figure suggest that there is a decreasing trend from LILE to HFSE with the well defined negative anomaly for Nb and positive anomaly for Sr. The enrichment of LILE and depletion of HFSE and the depletion in the Nb can be attributed to the formation of these rocks in island arc type setup (Stolz et al., 1996).

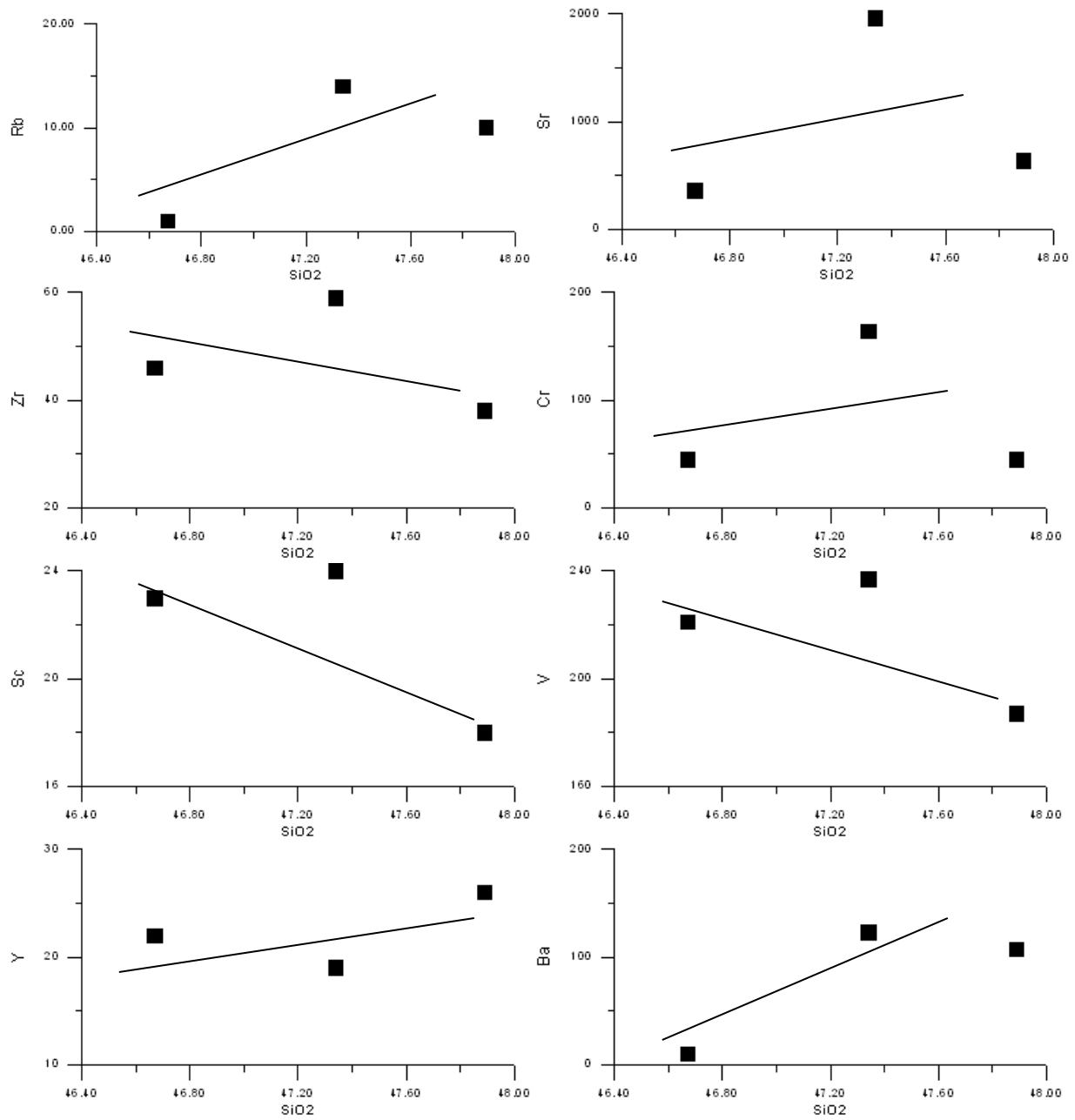Fig.6.6. Silica versus major oxide Harker diagram for IVC volcanics of the study area.

Fig.6.7. Silica versus trace elements Harker diagram for IVC volcanics of the study area.
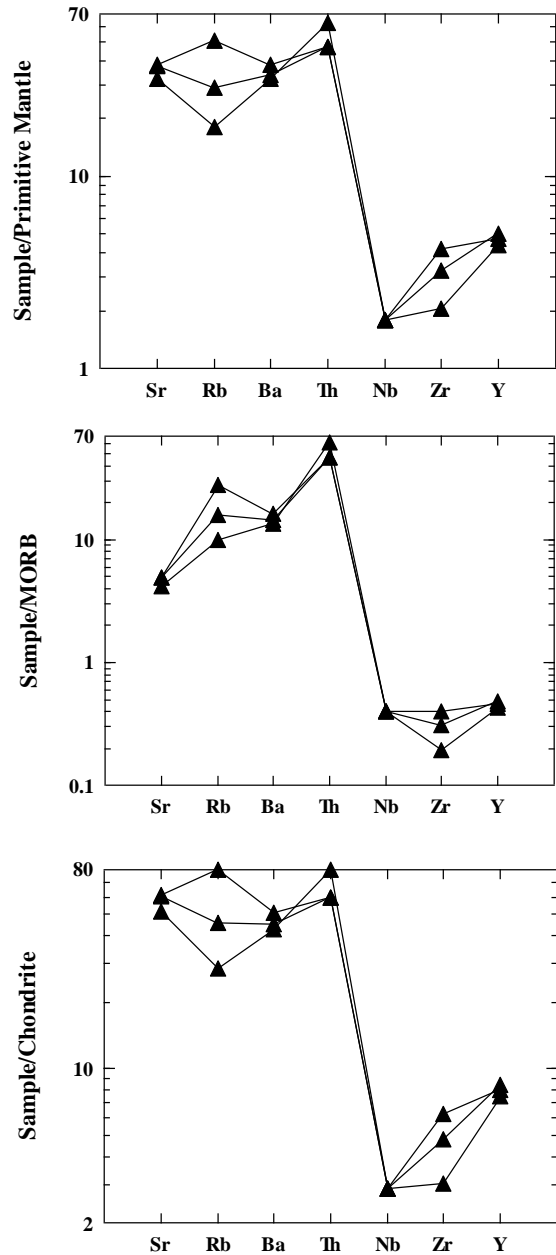
Fig.6.8. Spider variaition diagram for IVC volcanics normalized to primitive mantle, MORB and Chondrite after Taylor and Mclennan (1985), Thompson (1982) and Sun (1980) and Bevins et al. (1984) respectively.

6.2. Diorites

Major elements: The major element oxides data of the studied diorites have been given in Table 6.1. The data show that SiO_2 is ranging from 59.78 to 61.65 wt%, Al_2O_3 from 15.98 to 16.89 wt%, TiO_2 from 0.49 to 0.65 wt%, MnO from 0.09 to 0.13 wt%, MgO from 2.54 to 2.94 wt%, CaO from 5.68 to 5.80 wt%, Na_2O from 3.42 to 3.89 wt%, K_2O from 3.12 to 2.81 wt% and P_2O_5 from 0.33 to 0.42 wt%. The major oxide data of these rocks when plotted in the classification diagram (Fig. 6.9) of Cox et al., (1979), these rocks akin to the field of diorite and hence confirming their dioritic composition. The CIPW norms of these diorites are calculated on anhydrous basis and the results are presented in Table 6.1. It is clear from this table that these diorites are quartz (10.21-13.31%) normative. The plagioclase (50.54-51.84%) is a dominant normative phase with subordinate amount of orthoclase (16.72-18.62%) and hypersthene (7.91-11.30%). The other normative phases are diopside (2.42-6.94%), ilmentite (1.08-1.71%), magnetite (2.15-2.89%) and apatite (0.76%-0.97%). Mg # of these diorites is low ranging from 29 to 36%.

The studied diorite samples when plotted on the Harker variation diagram (Fig. 6.10) where the SiO_2 is the index of differentiation. It is clear from this diagram that like the IVC volcanics, the Al_2O_3, Fe_2O_3, MgO and CaO exhibit the decreasing trends while the total alkalis (Na_2O+K_2O), MnO and P_2O_5 show increasing trends with the increasing SiO_2 in these diorites These characteristic are compatible with those of calc-alkaline rocks. The calc-alkaline nature of these diorites is also clear from the AFM diagram (Fig. 6.3).Where all the diorite samples plot in the calc-alkaline field.

Trace elements: The trace element data of the studied diorites have been presented in Table 6.1. Among the LILE, Sr varies from 669 to 795ppm, Ba from 340 to 467ppm, Th from 9 to 12ppm and Rb from 68 to 79ppm. The HFSE such as Nb, Pb, Cr, Zr and Y have a range of 6-8ppm, 11-14ppm, 55-79ppm, 96-115ppm and 22-25ppm. It is clear from the Table 6.1 that the studied diorites are enriched in LILE relative to HFSE. The trace element data has been plotted against SiO_2 in the Harker variation diagram (Fig. 6.11). This diagram shows that Cr, V and Sc are decreasing with the increase in silica while Sr, Rb, Zr and Y are increasing with the increase in

silica. This is in consistence with the process of magma differentiation and can be correlated with the calc-alkaline magmatism.

The LILE and HFSE data of the studied diorites are normalized to primordial mantle, chondrite and MORB values and plotted on the spider diagram (Fig. 6.12). The trace element patterns indicate that there is a decreasing trend from left to right, showing the enrichment of LILE as compared to HFSE with negative anomaly for Nb and positive anomaly for Sr. This type of pattern is consistent with the calc-alkaline rocks originated in island type of environment (Stolz et al., 1996).
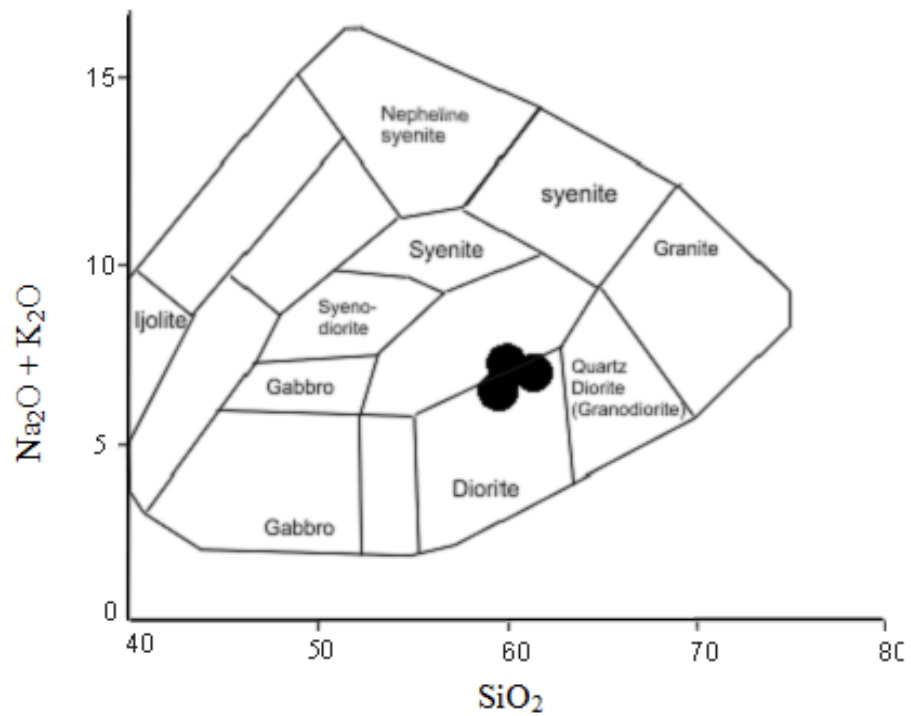
Fig.6.9. Plotting of rocks of the study area in the plutonic rocks classification diagram on the basis of SiO_2 versus total alkalis content (after Cox et al., 1979).
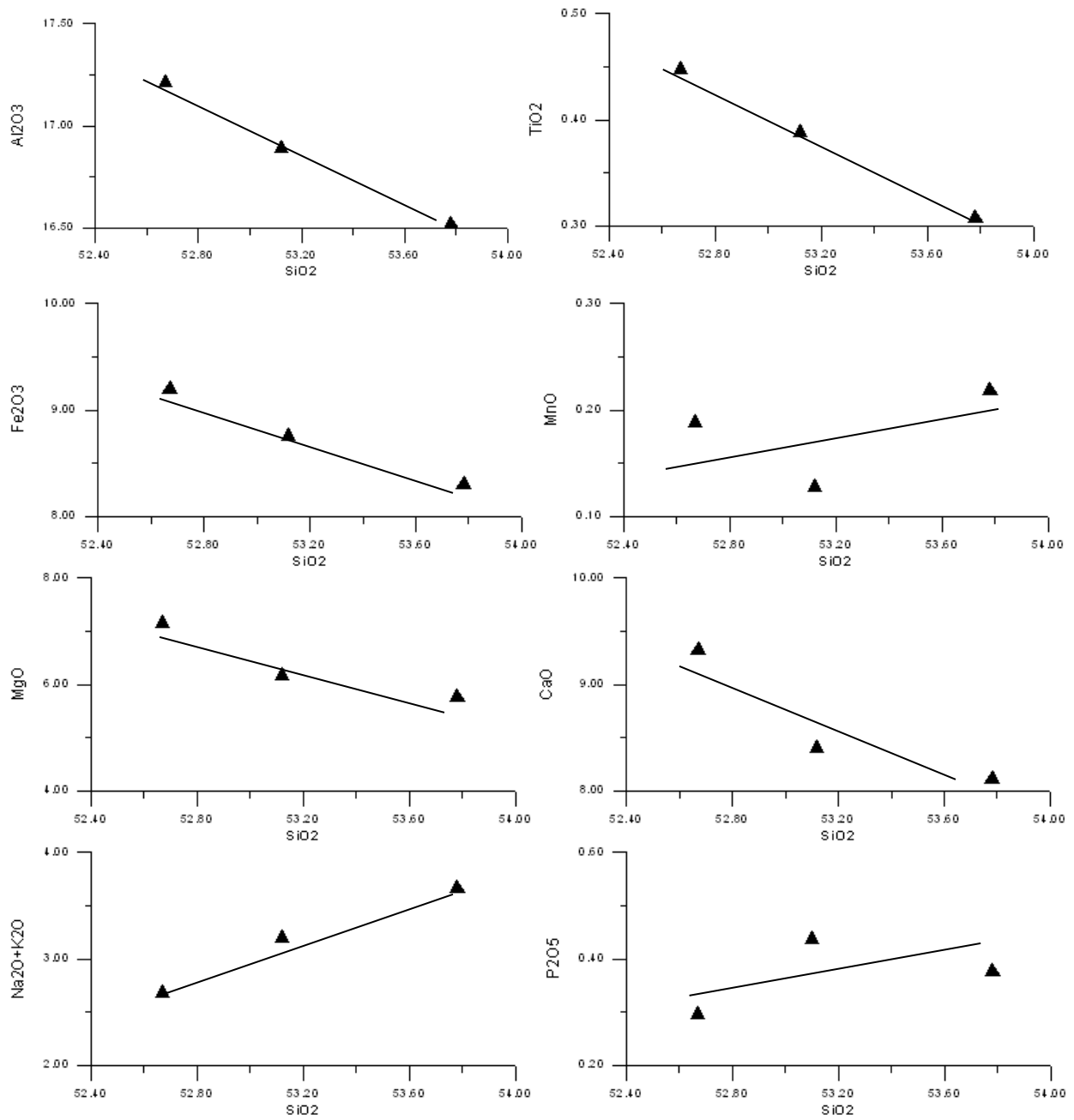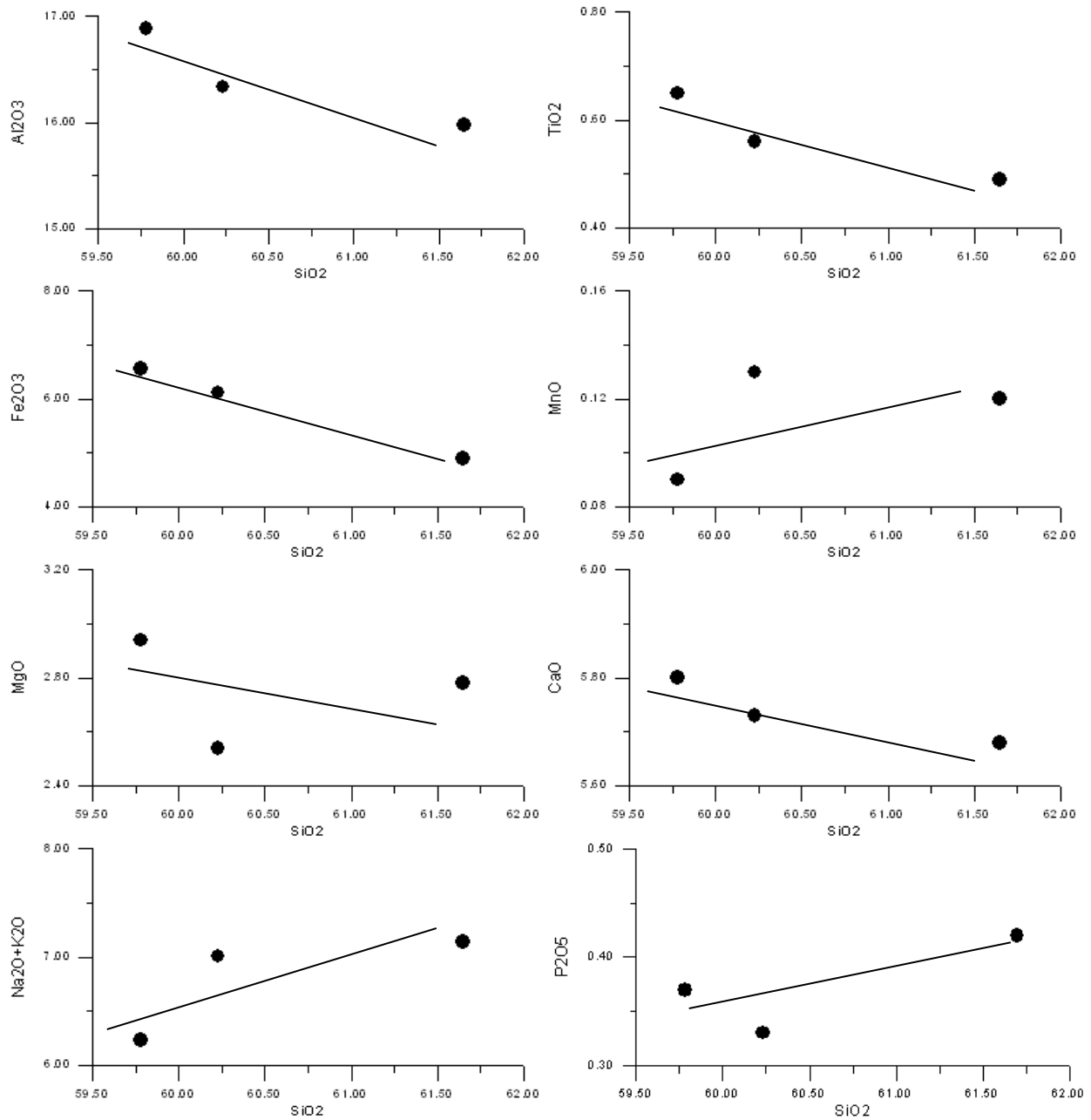
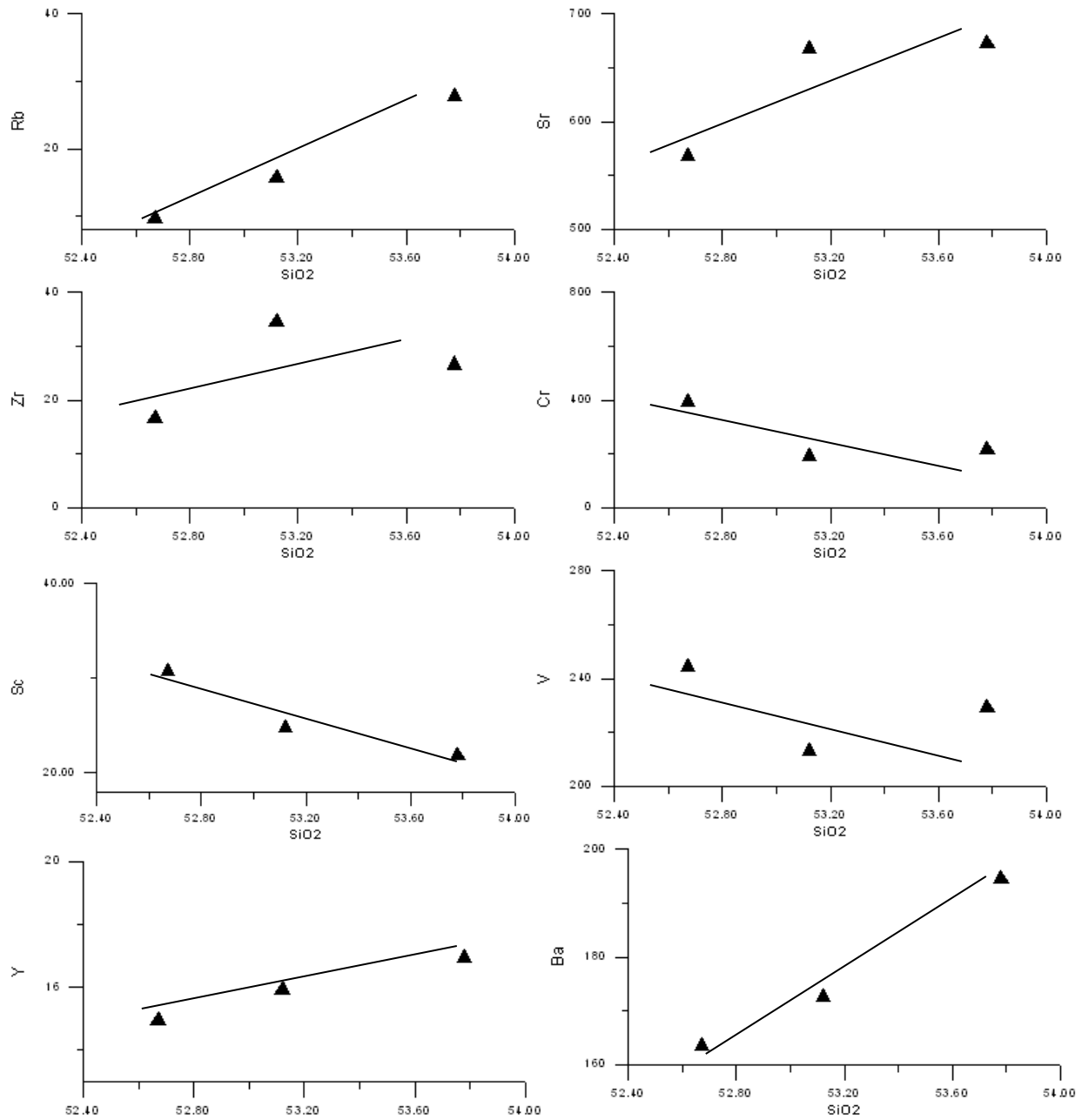Fig.6.10. Silica versus major oxides Harker diagram for diorites of the study area.
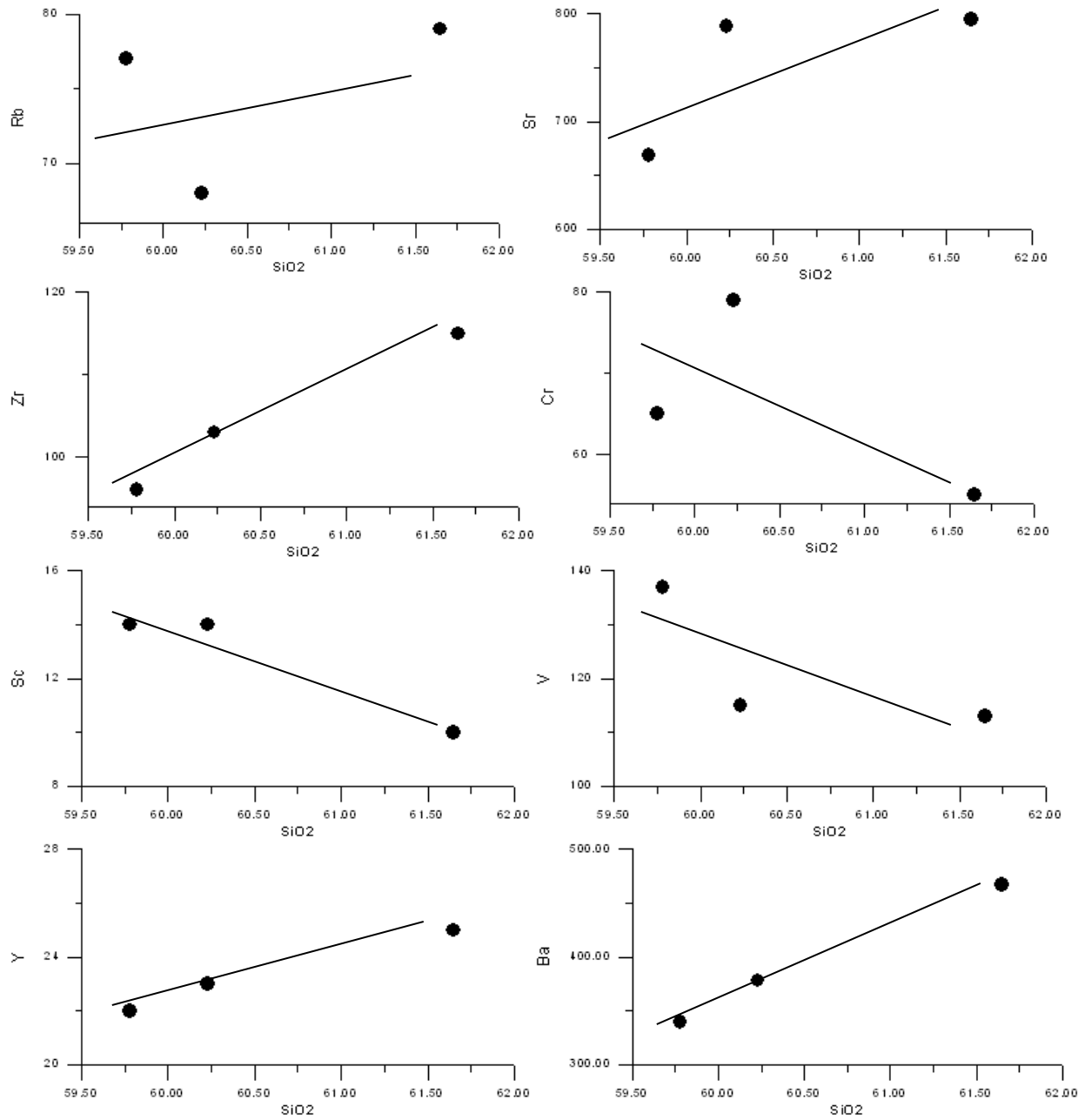
Fig.6.11. Silica versus trace elements Harker diagrams for diorites of the study area.
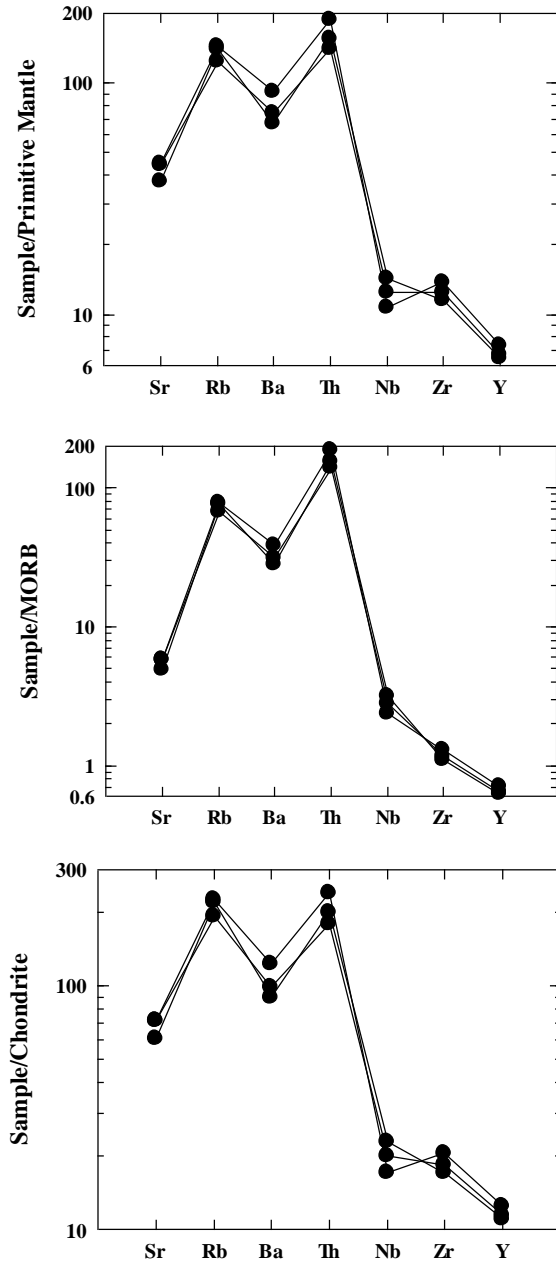
Fig.6.12. Spider variaition diagram for diorites normalized to primitive mantle, MORB and Chondrite after Taylor and Mclennan (1985), Thompson (1982), Sun (1980) and Bevins et al. (1984) respectively.

6.2. Gold, silver and base metals scenario in the altered sulfide zones

As already mentioned in the local geology of the study area in Chapter 3 that the sulfide-bearing alteration zones are present along the shear zones within the IVC volcanics. Wherever the shearing has been noticed the yellowish-brown color staining, due to leaching of sulfide phases, on the surface has been seen. The quartz veining along these shearing zones is also an important feature of these zones. This is suggestive of involvement of hydrothermal fluid in the alteration along these shear zones.

The sulfide-bearing altered zones in the Golo Das and surrounding areas have been identified during field. A major zone of alteration at a high altitude, difficult to access, was identified and associated with the carbonates rocks, the area of interest for this study in regard to precious metals (i.e., Au and Ag) and base metal (i.e., Cu, Pb, Zn, Ni, Cr, Co and Cd) mineralization. However, other small scale sulfide leaching zones identified during field were also sampled. The Golo Das area was first visited and the bulk samples (>10kg) from the major Golo Das alteration zone and the other such zones in the surrounding areas were collected for the geochemical concentration of Au, Ag and base metals for finding out the source rock for these metals in the area of study. The sample preparation and the analytical work has been discussed in Chapter 4 in detail. The concentration of precious metals such as Au and Ag and the base metals such as Cu, Pb, Zn, Ni, Cr, Co and Cd in the samples of sulfide-bearing altered zones are given in Table 6.2 and the average concentration are graphically presented in Fig. 6.13. In the analyzed samples, among the base metals Cu concentration varies from 1-3496ppm with an average amount of 424ppm, Pb varies from 0.2-5.75ppm with an average concentration of 3.45ppm, Zn varies from 5-52ppm with an average concentration of 30ppm, Ni varies from 2-48ppm with an average concentration of 10ppm, Cr varies from 4-182ppm with an average concentration of 49ppm, Co varies from 3-56ppm with an average concentration of 24ppm and Cd varies from 1-6ppm with an average concentration of 3ppm (Table 6.2). Among the precious metals analyzed, Au is ranging from 0.012-0.166ppm with an average amount of 0.083ppm and Ag is ranging from 0.4-2.9ppm with an average amount of 1.565ppm.

In order to see the gain and loss of the alteration zones relative to the unaltered rocks, the enrichment and depletion factors [(altered rocks-unaltered rocks/unaltered rocks)×100] for the

average composition of analyzed precious and base metals have been calculated and plotted in the Figure 6.14. As the alteration zones are found along the local faults within the IVC volcanics therefore, the calculations of enrichment and depletion factors are based on the assumption that the altered and unaltered rocks had identical composition priorer to alteration. It is clear from the Figure 6.14 that there is multifold increase in the concentration of Cu, Co, Ag and Au in the sulfides-bearing altered zones. While the Pb, Zn, Ni and Cr show depletion in the sulfide-bearing altered zones relative to the unaltered IVC volcanics. This is suggesting that the Cu-Fe sulfide phases such as chalcopyrite, pyrite have been precipitated along the shear zones by the hydrothermal solution which has altered the host rocks and also precipitated quartz veins along the shear zones. As no native gold and or gold and silver bearing phases have been observed in these altered rocks, therefore, it can be suggested that Au and Ag may have been incorporated in the sulfide phases. However the depletion of Pb, Zn, Cr, and Ni suggest that these may have been leached out during alteration or the hydrothermal solution was devoid of these elements.

The GIS based elemental distribution maps of the bulk samples, collected from sulfide-bearing alteration zones, have been prepared (Fig. 6.15a-i). It is clear from these maps that Cu, Zn, Ni, Co, Ag and Au show anomalous concentration in the shear zones in Golo Das area and also along the Hasis Gah. To find out the nature of gold anomaly whether native, in the form of fine particles (<0.3mm) or in sulfides and or in tellurides, each bulk samples was crushed to -80 mesh size and then panned to the last weight of about 20 grams. Each panned concentrate was studied under the stereoscopic microscope. No any fine grained particle was noticed in any sample, suggesting that the gold is not present in the native form but if present is mostly in the sulfide or telluride form.

The very low range of gold concentration (0.012-0.166ppm) in the studied alteration zones is suggesting that there are no promising occurrences of gold in the area. Therefore, the source rock for gold which was aimed in the proposed study is not present in the study area.

Table 6.2.Gold, silver and base metals concentration in Golo Das and surrounding areas.

S.No	Cu (ppm)	Pb(ppm)	Zn (ppm)	Ni (ppm)	Cr (ppm)	Co (ppm)	Cd (ppm)	Ag (ppm)	Au (ppm)
GDB-1	6.65	<0.02	34.9	19.75	50.55	19.3	2.6	1.75	0.084
GDB-2	1.3	4.2	21	22.2	64.05	33.55	3.5	2.9	0.097
GDB-3	73	3.85	12.9	<0.02	12.85	2.8	2	<0.05	0.112
GDB-4	60.5	<0.02	34.5	9.1	24.9	15.05	2.65	<0.05	0.103
GDB-5	72.75	5.75	49.8	6.8	49.05	29.7	2.8	<0.05	0.058
GDB-6	51.1	<0.02	34.95	5.75	52.4	24.9	1.2	<0.05	<0.05
GDB-7	2156.25	<0.02	43.2	3.95	40.55	23.6	3.2	<0.05	0.097
GDB-8	53.25	<0.02	34.15	10.95	59.2	29.8	1.7	<0.05	0.092
GDB-9	748	<0.02	4.9	<0.02	42.05	15.05	3.6	1.1	0.166
GDB-10	3496.25	<0.02	24.85	5.4	56.55	32.05	2.55	2.8	0.079
GDB-11	24.55	4.6	36	6.45	<0.02	27.75	3.95	1	0.031
GDB-12	8.35	4	<0.02	2.4	<0.02	3.8	2.55	1.6	0.082
GDB-13	11.55	0.55	<0.02	2.35	34.75	14.7	1.65	1.2	0.012
GDB-14	102.55	1.45	35.85	47.95	181.8	26.35	1.2	0.85	0.043
GDB-15	613.75	0.3	52.3	5.65	40.8	39.35	2.3	<0.05	0.111
GDB-16	14.85	6.45	<0.02	2.3	16.3	8.65	2.65	1.25	0.057
GDB-17	138.75	6.7	<0.02	8.8	21.3	44.6	5.55	1.2	0.112
GDB-18	4.85	0.2	4.6	7.2	33.9	37.45	2.5	<0.05	0.086
Average	424.347	3.45909	30.2786	10.4375	48.8125	23.8028	2.675	1.565	0.08365
Minimum	1.3	<0.02	<0.02	<0.02	<0.02	2.8	1.2	<0.05	0.012
Maximum	3496.25	6.7	52.3	47.95	181.8	44.6	5.55	2.9	0.166
Standard deviation	927.32	2.45141	14.9198	11.5042	38.6256	11.9921	1.04982	0.72688	0.03614
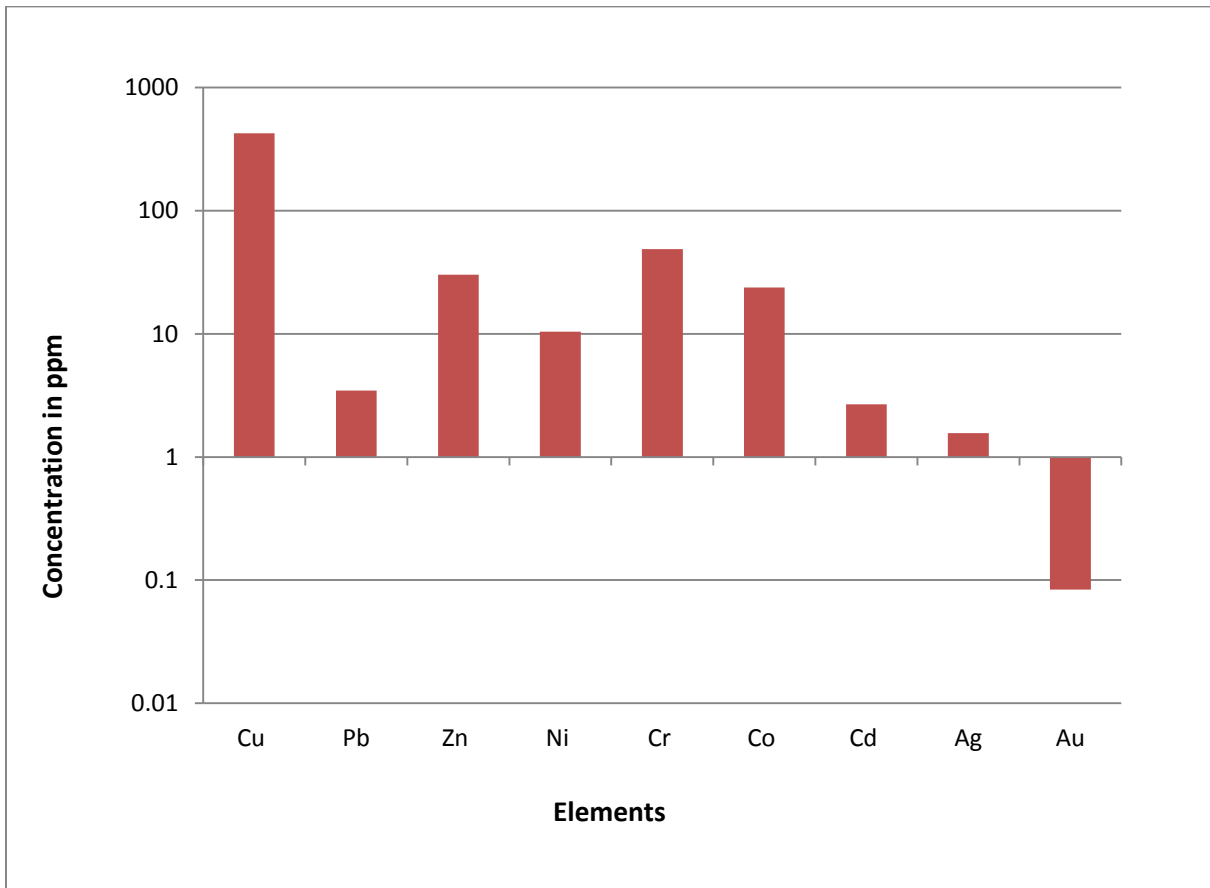
Fig.6.13. Average gold, silver and base metals concentration in bulk samples collected from the altered sulfide zones of the study area.
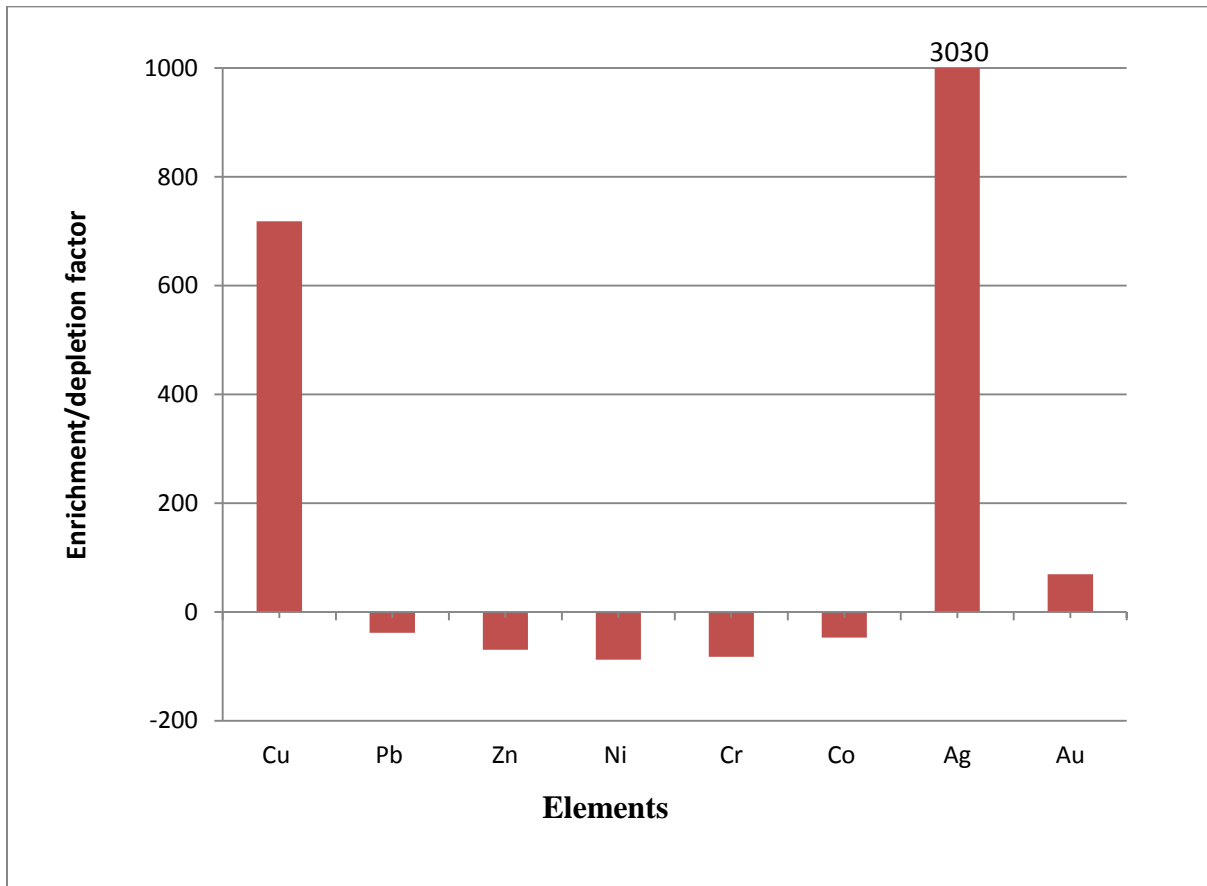
Fig.6.14. Diagram showing the enrichment and depletion of various base and precious metals in the altered sulfide zones and unaltered rocks of the study area.
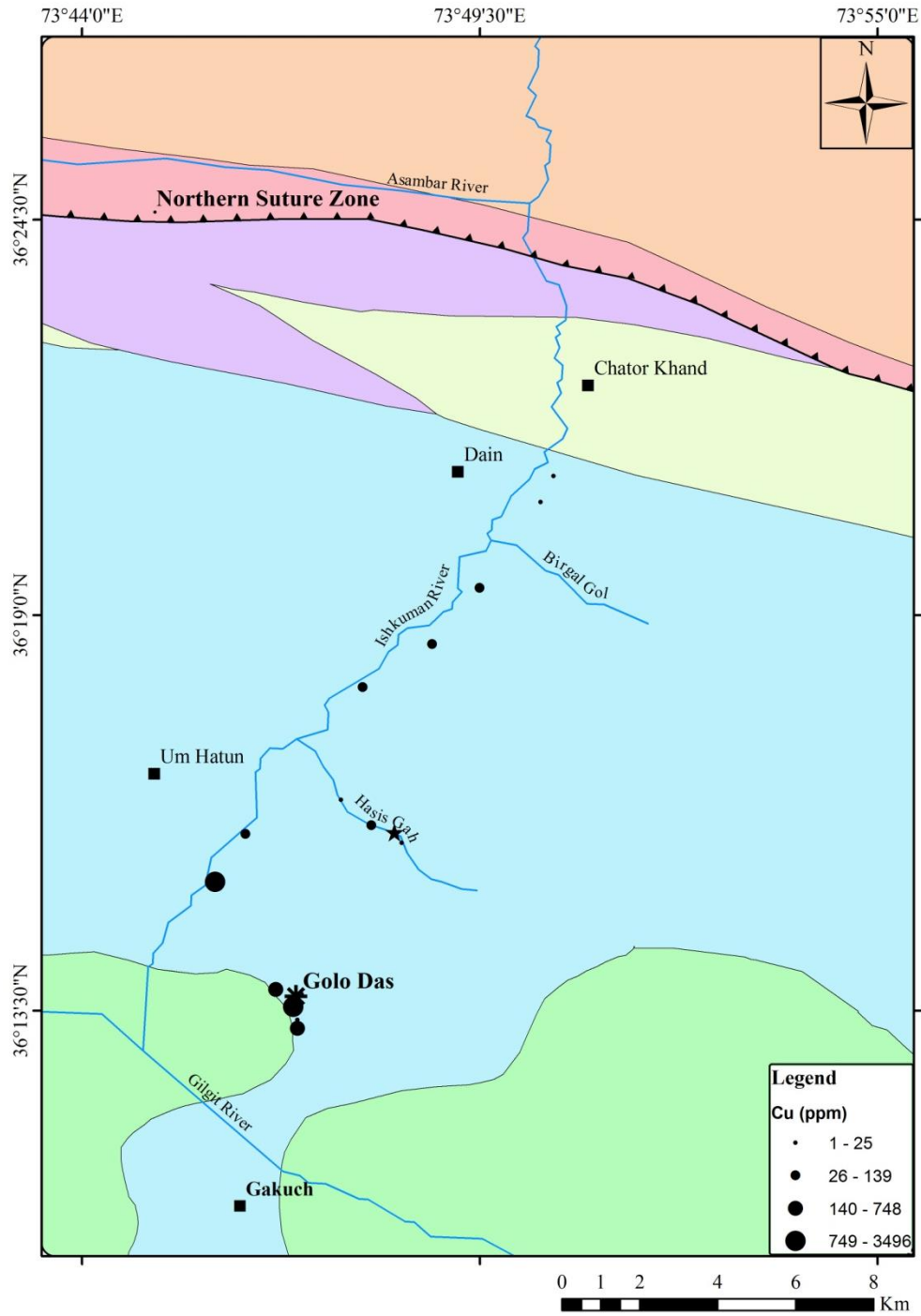
Fig.6.15(a). Geological map of the study area including Golo Das and surrounding areas showing the concentration of copper (compiled from Searle and Khan, 1996; Petterson and Treloar, 2004).
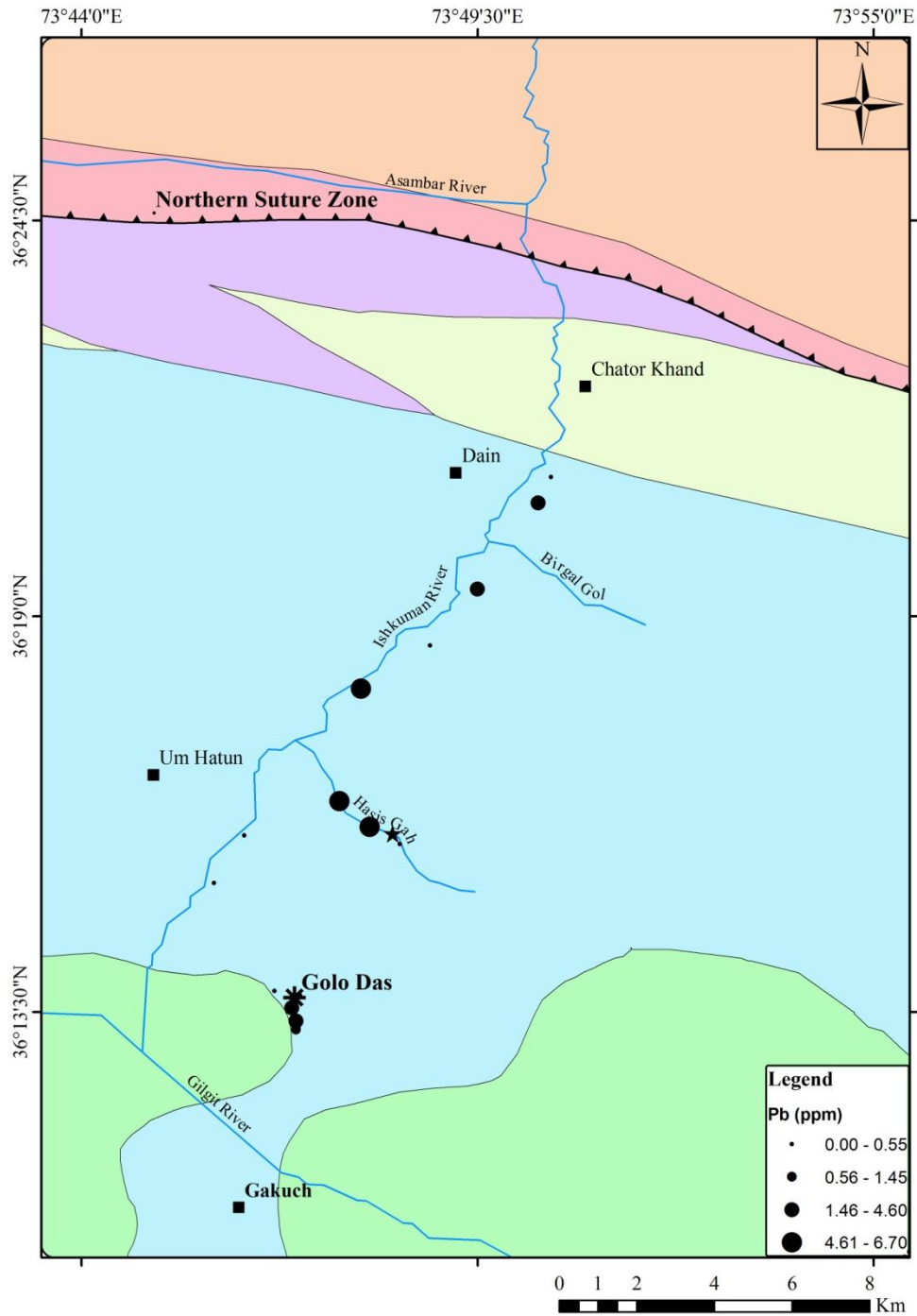
Fig.6.15(b). Geological map of the study area including Golo Das and surrounding areas showing the concentration of lead (compiled from Searle and Khan, 1996; Petterson and Treloar, 2004).
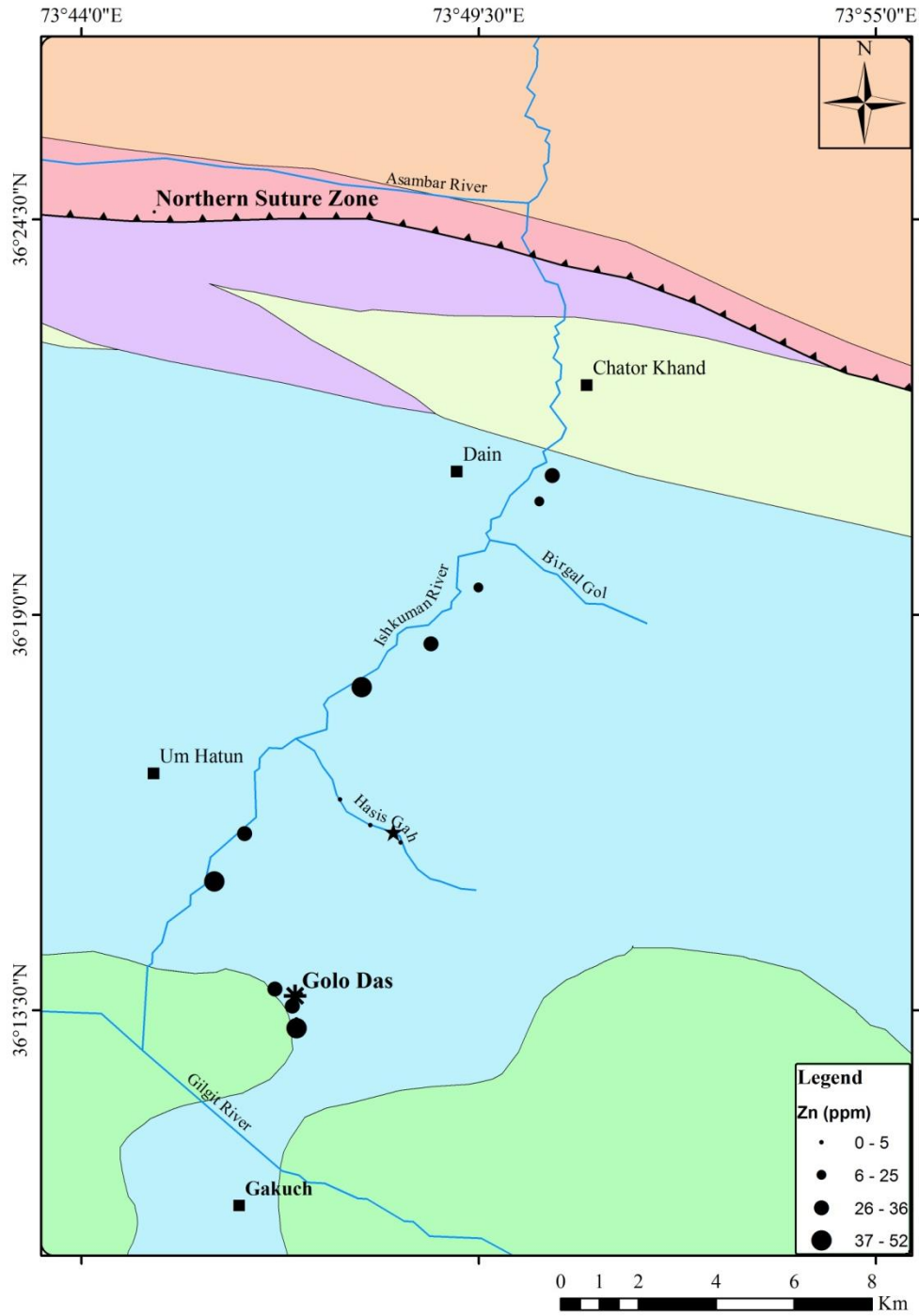
Fig.6.15(c). Geological map of the study area including Golo Das and surrounding areas showing the concentration of zinc (compiled from Searle and Khan, 1996; Petterson and Treloar, 2004).
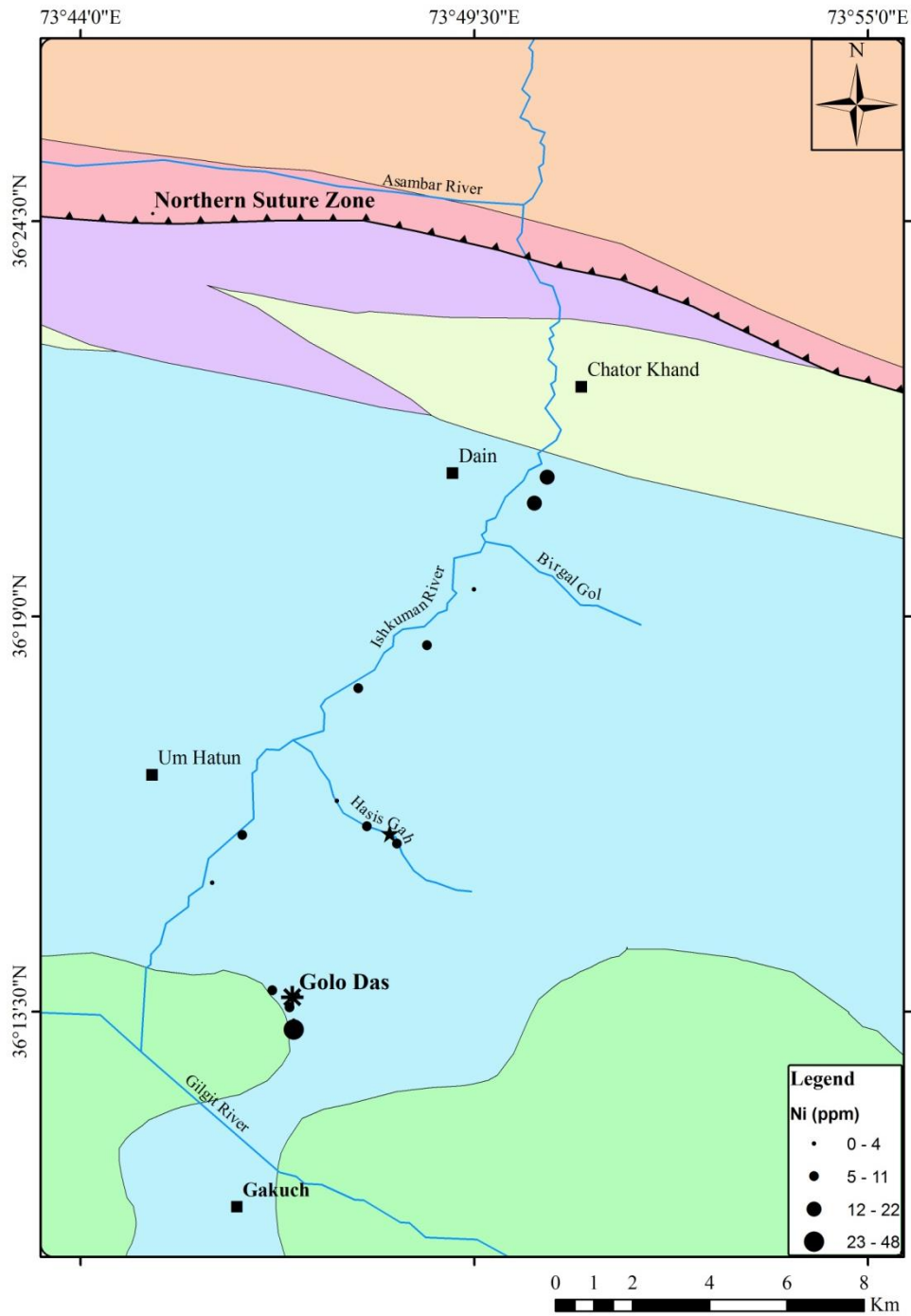
Fig.6.15(d). Geological map of the study area including Golo Das and surrounding areas showing the concentration of nickle (compiled from Searle and Khan, 1996; Petterson and Treloar, 2004).
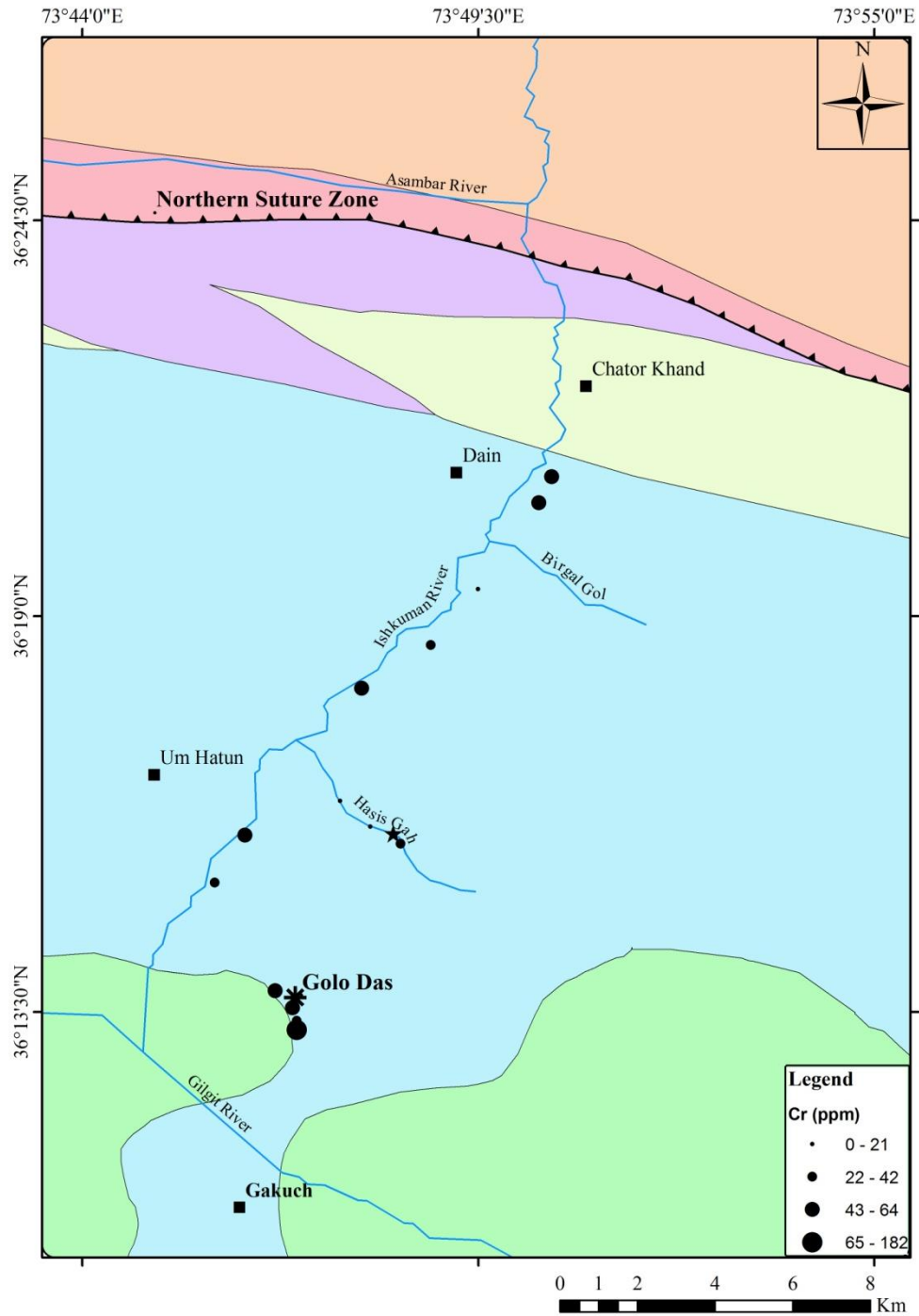
Fig.6.15(e). Geological map of the study area including Golo Das and surrounding areas showing the concentration of chromium (compiled from Searle and Khan, 1996; Petterson and Treloar, 2004).
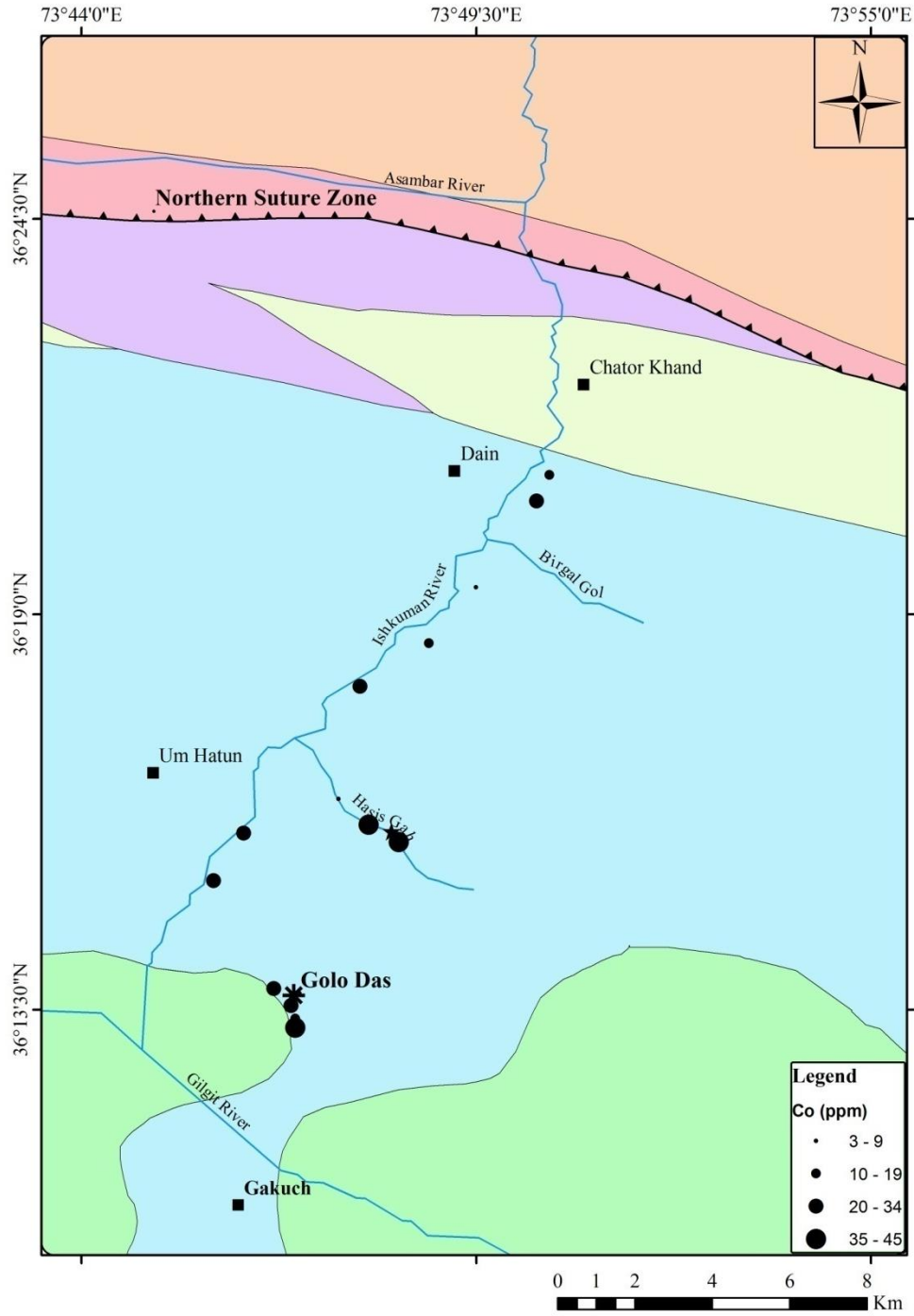
Fig.6.15(f). Geological map of the study area including Golo Das and surrounding areas showing the concentration of cobalt (compiled from Searle and Khan, 1996; Petterson and Treloar, 2004).
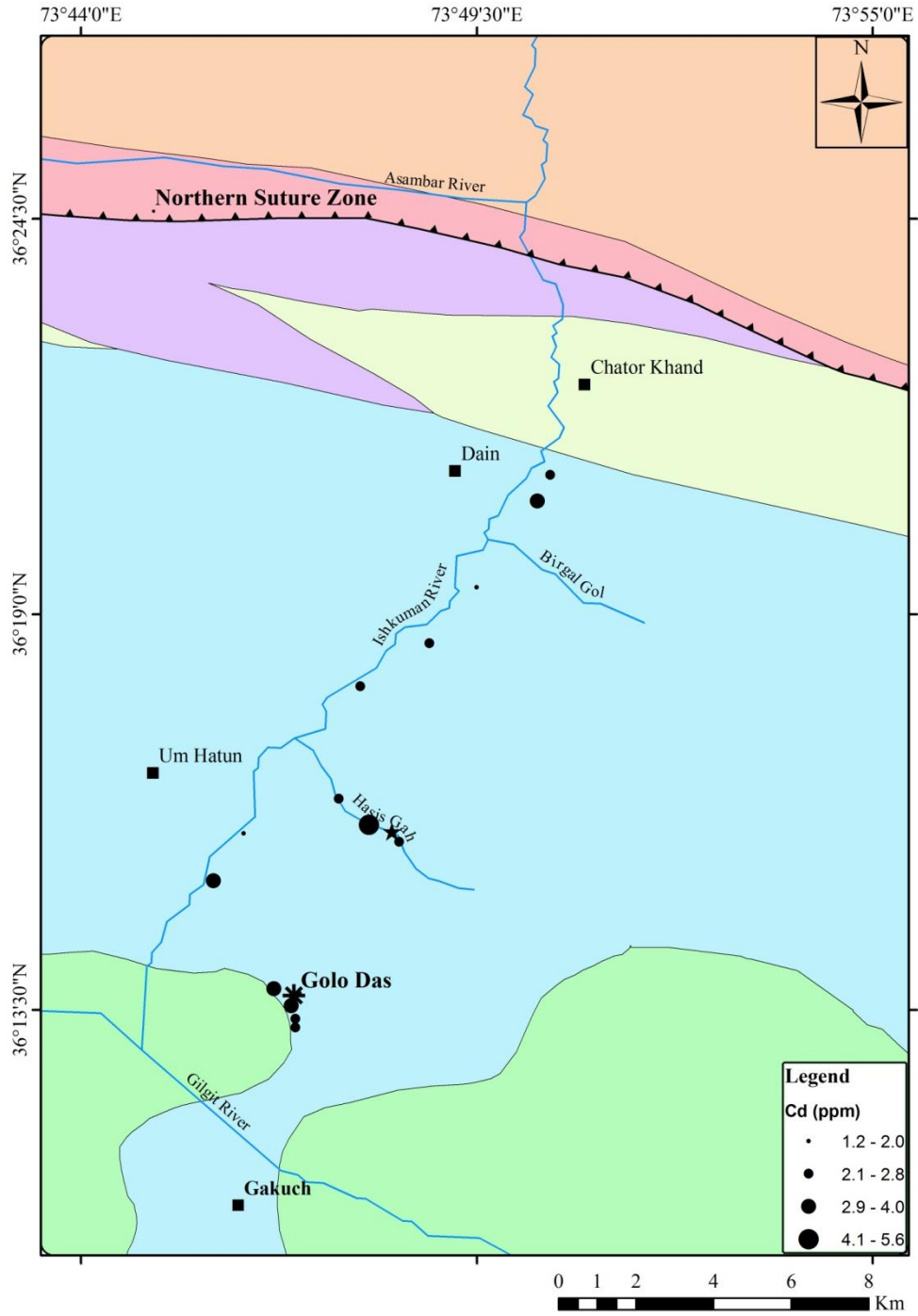
Fig.6.15(g). Geological map of the study area including Golo Das and surrounding areas showing the concentration of cadmium (compiled from Searle and Khan, 1996; Petterson and Treloar, 2004).
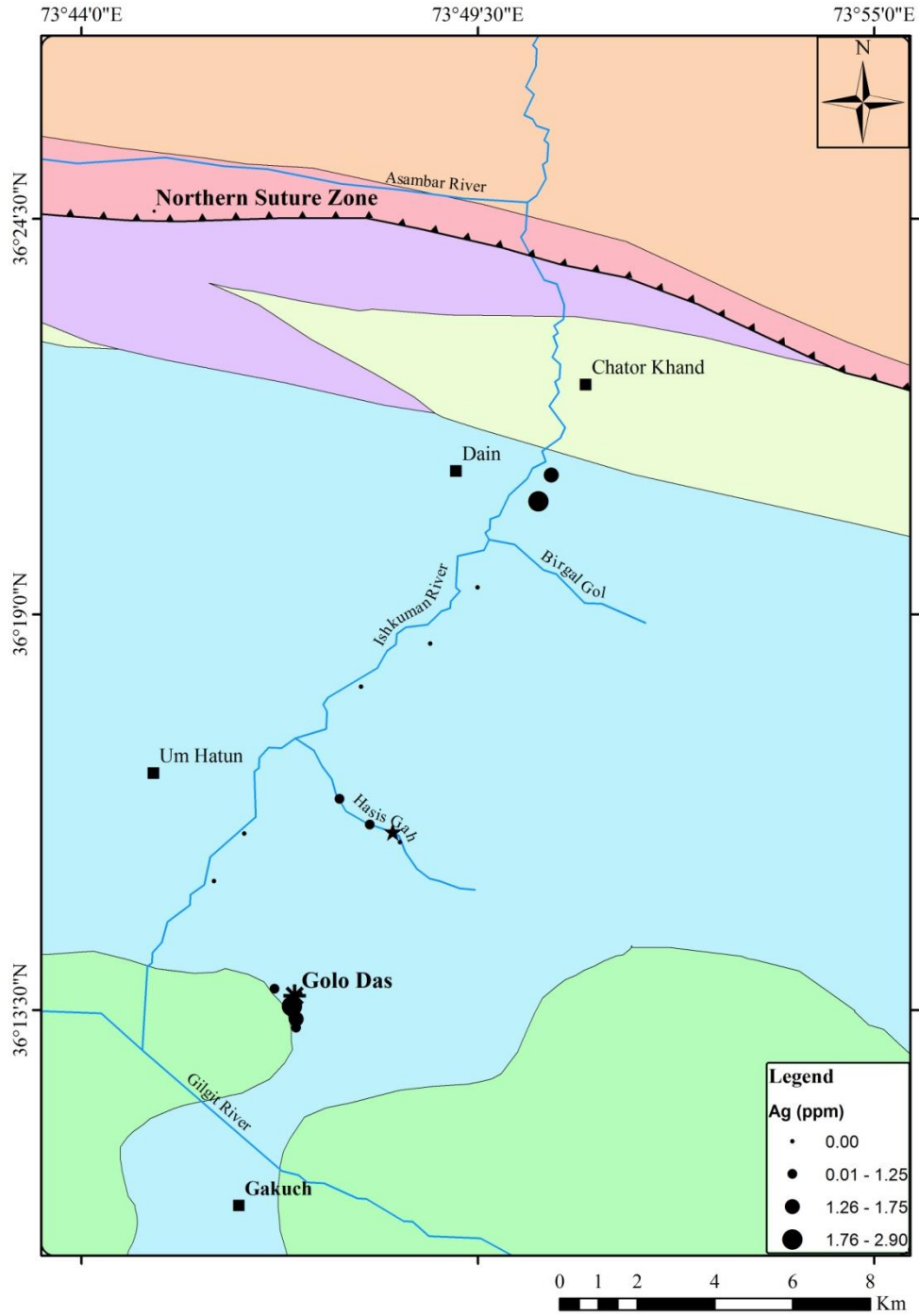
Fig.6.15(h). Geological map of the study area including Golo Das and surrounding areas showing the concentration of silver (compiled from Searle and Khan, 1996; Petterson and Treloar, 2004).
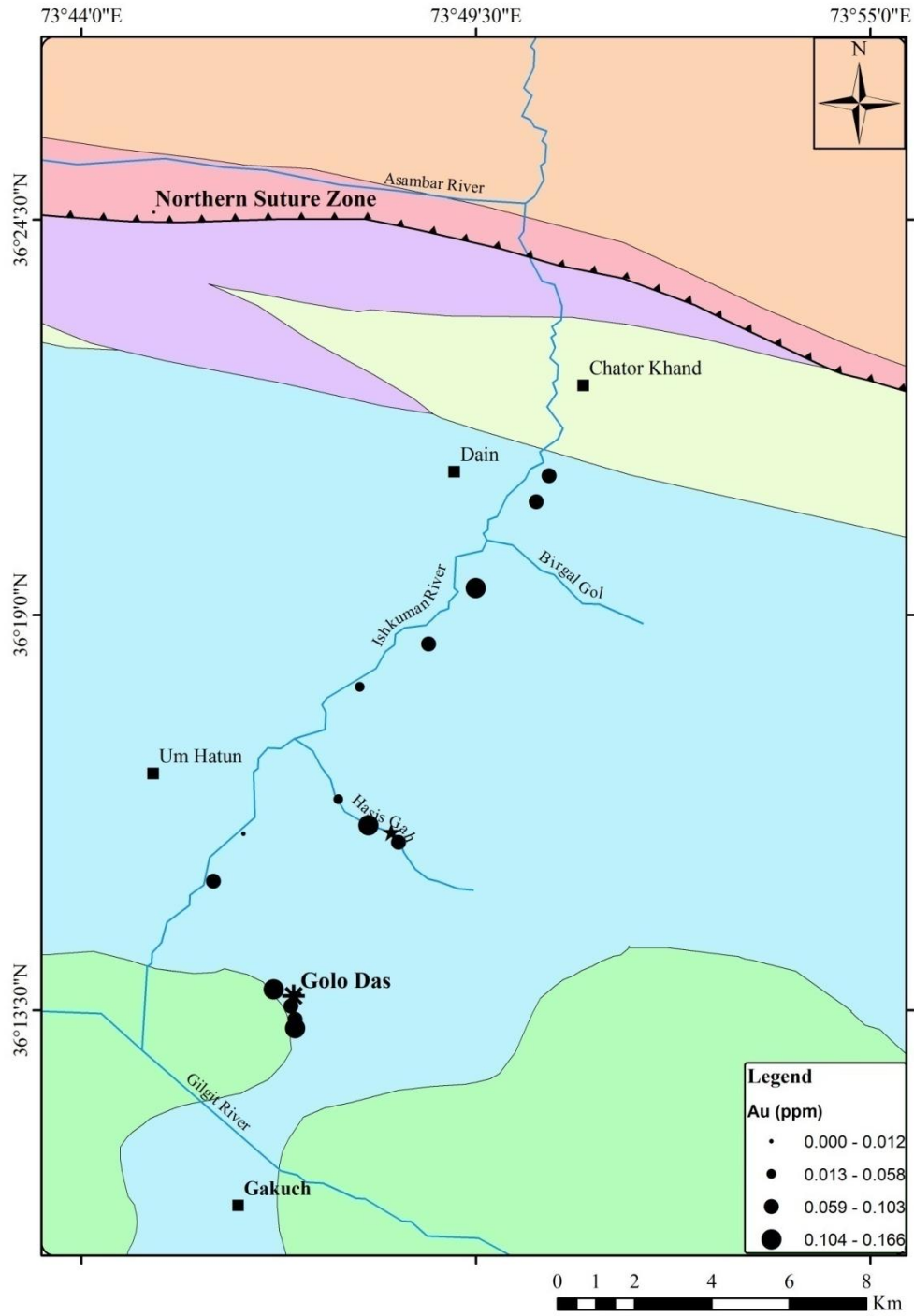
Fig.6.15(i). Geological map of the study area including Golo Das and surrounding areas showing the concentration of gold (compiled from Searle and Khan, 1996; Petterson and Treloar, 2004).

CHAPTER 7

TECTONIC SETTING OF MAGMA GENERATION

To find out the tectonic setting, magma generation of the rocks of the study area i.e., BASD volcanics, IVC volcanics and dioritic pluton, the analyzed rock samples, were collectively plotted in various discrimination diagrams which are used for finding the petrogenesis of magma in different tectonic settings. The best ternary plot used for finding the difference between calc-alkaline and tholeiitic type of magma is the AFM ternary plot after Irvine and Barager (1971) having line of divide between the two environments. In this ternary plot differentiation is made on the basis of major oxide data including total alkalis, total iron in the form of FeO and magnesium oxide present in the rock samples. The rock samples plotted on the ternary plot of AFM (Fig. 6.3) as described earlier, shows the calc-alkaline nature of all the rock types formed in typical island arc type of setup related to subduction.

Vermeesch (2006) proposed the ternary discrimination diagram (Fig. 7.1) in which the distinction is made among different tectonic environments on the basis of silicon (Si), titanium (Ti) and strontium (Sr). In this plot the trace elements used demarcated the boundaries between mid ocean ridge basalts (MORB), ocean island basalts (OIB) and island arc basalts (IAB). This ternary standard plot is the result of analysis of different rock samples collected from all the major tectonic setting and then the distinction is made by using the three elements Si, Ti and Sr to differentiate between the tectonic environment and now this is commonly used in the geochemical data analysis for plotting and comparing the results. The geochemical data of the three types of rocks (i.e., BASD volcanics, IVC volcanics and diorites) when plotted in this diagram (Fig. 7.1), all the data plot in the field of Island arc basalt (IAB).

Another type of discrimination diagram is a ternary plot of Vermeesch (2006) used for discrimination of various tectonic environment is based on trace elements like Nb, Sr and major element sodium. These three elements are used to demarcate the line of divide between mid-ocean ridge basalt (MORB), island arc basalt (IAB) and ocean island basalt (OIB) (Fig. 7.2). The rock samples when plotted in this diagram, plot in the field of IAB which is consistent with earlier observations, suggesting subduction related geotectonic environment for these rocks (Fig. 7.2). The ternary diagram (Fig. 7.3) after Mullen (1983) is generally used for differentiating

different types of tectonic environments. This diagram has all the values in its oxide weight percent with some multiples for extending the plotting field area. The three parameter used in this diagram are basically its involvement in the crystallization of magma from different sources. The Mn and Ti are readily adjusted in the structures of those minerals which are formed in the early stages of magma crystallization like in the formation of olivine and pyroxene. So there must be different patterns of fractional crystallization for the volcanic arc magmas and the oceanic basalts. The Mn, Ti and P are also immobile elements, therefore, these have been used by Mullen (1983) for the differentiation of rocks of different tectonic settings. The studied rocks when plotted in this diagram (Fig. 7.3), all the samples plot in the field of calc-alkaline basalt. Thus this discriminant diagram is typically used to differentiate between mid ocean ridges and island arc settings.

The discrimination ternary diagram (Fig. 7.4) of Meshede (1986) is also used for differentiating the rocks of different tectonic settings. In this ternary plot the incompatible elements Nb, Zr and Y are used for discrimination among basalts of different tectonic environments. The rocks of the study area when plotted in this diagram (Fig. 7.4), the samples of BASD volcanics fall in the field of N-type MORB and volcanic arc basalt while the diorite samples plot in the field of within-plate tholeiites and volcanic arc basalt (Fig. 7.4).

Wood (1980) constructed a discrimination diagram (Fig. 7.5) based on the immobile HFS elements (i.e., Th, Hf and Ta) for differentiating basalts of various tectonic settings. This diagram is best for recognizing different types of MORB, and can be applied from basic to acidic rocks and particularly good at identifying volcanic-arc basalt. The studied rock samples are plotted in this diagram (Fig. 7.5). It is clear from this diagram that all the data set plot in the field of destructive plate margin basalt.

The geochemical data of the volcanics and diorites of the study area have been used to characterize the petrology and tectonic setting of these rocks. The volcanic rocks (both deformed BASD volcanics and less-deformed/undeformed IVC volcanics) are of calc-alkaline nature. The major and trace elements distribution in the discrimination diagrams, the primordial mantle, MORB and chondrite normalized pattern suggest that the studied volcanic rocks were formed

with a strong subduction component in an island type of environment. This is consistent with the findings of the earlier workers who worked on volcanic rocks (i.e., Ghizar formation, Teru volcanic formation and Shamran volcanics) in the northern most part of the KIA (Petterson and Windley, 1991; Sullivan, 1993; Khan et al., 2004; Peterson and Treloar, 2004; Khan et al., 2009).

On the basis of chemical composition, especially MgO contents, Petterson and Windley (1991) have divided the rocks of the Chalt volcanic Group into 1) High-Mg tholeiites and 2) low-intermediate MgO calc-alkaline volcanics. Later on, Petterson and Treloar (2004) have renamed the second variety as Ghizar formation. They have further divided the Ghizar formation into 1) Ishkoman Volcanic Centre, 2) basalt-andesite sheet dominant and 3) tuff dominant volcanics. In order to understand the geochemical behavior of the studied volcanics in the context of the similar volcanic rocks exposed in the western and eastern extension of the study area, the geochemistry of the studied volcanics have been correlated with those of the earlier workers such as Petterson and Windley (1990, 1991) and Khan et al., (2004). The Table 7.1 shows the comparison of the average major and trace elements of the studied volcanics with the similar rocks of high-magnesia tholeiites (Hunza Formation) and low-intermediate MgO calc-alkaline volcanics (Ghizar formation) of Petterson and Windley (1991) and Petterson and Treloar (2004) and the Teru volcanic formation (previously known as Shamran volcanics by Pudsey et al., 1985 and Sullivan et al., 1993) of Danishwar et al. (2001) and Khan et al. (2004). The average trace element data have also been compared with the above mentioned rocks in the spider diagrams (Fig. 7.6). It is clear from the Table 7.1 and Figure 7.6 that the studied volcanics (BASD and IVC volcanics) have similar geochemical behavior as that of the Low-intermediate MgO calc-akaline volcanics (Ghizar formation) and that of the Teru volcanic formation / Shamran volcanics. The calc-alkaline nature of the volcanic rocks of the Ghizar formation as suggested by this study and also by Petetrson and Windley (1991) can, therefore, be correlated with the calc-alkaline volcanics of Teru volcanic formation / Shamran volcanics which is displaying a typical subduction zone signature for all these rocks.

These rocks are, therefore, considered a part of the Cretaceous Kohistan island arc. The volcanic rocks of the Ghizar formation of the studied area, especially the rocks of the Ishkoman

Volcanic Centre, having similar petro-chemical behavior as that of the Teru volcanic formation / Shamran volcanics, can be considered the eastern extension of the Teru volcanic formation / Shamran volcanic.

The age of the Teru volcanic formation/Shamran volcanics remained controversial. These volcanics were originally correlated with the Chalt volcanic Group and assigned mid-Cretaceous age by Pudsey et al. (1986). But later on Sullivan et al. (1993) considered the Shamran volcanics as the northern continuation of the Utror volcanic formation and assigned an early Eocene age on the basis of $^{40}Ar/^{39}Ar$ hornblende age of 58 ± 1 Ma (Treloar et al., 1989). The Shamran volcanics were also correlated with Utror and Drosh volcanics in southern and western Kohistan by Treloar et al. (1996). Khan et al. (2004) renamed the Shamran volcanics and considered these as the youngest volcanic rocks of the Kohistan arc on the basis of $^{40}Ar/^{39}Ar$. According to them the trace elements and isotopic characteristics of the Teru volcanic formation suggest that these rocks were originated in subduction related environment where the depleted mantle source was subjected to contamination by variable subduction component. However, Petterson and Treloar (2004) disagree with Danishwar et al. (2001) in renaming Shamran volcanic group as Teru volcanic formation. They consider the rocks of the Teru volcanic formation as part of the Chalt volcanic group (Ghizar formation) and are hence consistent with observations found during this study. They are of the opinion that the Shmaran volcanics group, are generally inaccessible, occurring at an altitude of >4000 m and can only be studied through loose blocks and boulders in the alluvial fan. These are the younger volcanics belonging to Yasin Group and are unconformably overlying the Chalt volcanic Group (Ghizar formation).

The diorites of the study area are also show calc-alkaline character and hence these rocks are also originated with a strong subduction component. Petterson and Windley (1991) have differentiated the Kohistan batholith in stage -1, stage-2 and stage-3 plutons. Among these the stage-2 plutons are of calc-alkaline character, having typical subdcution related calc-alkaline chemistry. The geochemical behavior of the studied diorites have, therefore, been compared with the stage-2 diorites of Petterson and Windley (1991) in Table 7.1. The trace element data for both types of diorite are plotted in the spider diagrams (Fig. 7.7). The major and trace element data of the studied diorites in the Table 7.1 and the trace element patterns in Figure 7.7 are

comparable with that of the stage-2 diorite of the Petterson and Windley (1991).   In this regard the studied diorites can be correlated with the stage-2 pluton of Kohistan batholith of Petterson and Windley (1985; 1991) for which an age of 40-85 Ma has been assigned by Zeitler (1982) and Treloar et al. (1989). According to Petterson and Windley (1991), the typical mantle is the source region for stage-2 pluton which was metasomatised by subduction related processes.

Table. 7.1. Comparision of major and trace elements data of this study with Khan et al. (2004) and Petterson and Windley (1991).

Sample	BASD volcanics (This study)	IVC volcanics (This study)	Diorites (This study)	Khan et al. 2004		Petterson and windley (1991)		Petterson and Windley (1991) High-Mg tholeiitic volcanics	Petterson and Windley (1991) Stage-2 Diorites
				42B	7_4	IK679	K681	N146	A208
SiO_2	47.30	53.20	60.54	50	54	53.8	54.2	48.7	59.68
Al_2O_3	17.45	16.87	16.39	18	17	19	16.6	11.6	16.99
TiO_2	0.60	0.38	0.57	1.7	0.7	0.75	0.62	0.42	0.73
Fe_2O_3	9.04	8.77	5.86	11	9.4	10.3	9.9	12	6.99
MnO	0.14	0.18	0.11	0.2	0.1	0.19	0.19	0.19	0.14
MgO	4.07	6.40	2.75	5.7	7	3.8	4.9	13.4	3.21
CaO	11.49	8.63	5.74	9.4	9.3	10.1	7.4	11.8	6.18
Na_2O	3.17	2.34	3.71	4.2	2.1	1.8	3.5	1.6	3.28
K_2O	0.41	0.86	3.08	0.6	1	0.12	2.01	0.25	3.74
P_2O_5	0.22	0.37	0.37	0.4	0.1	0.23	0.21	0.03	0.28
L.O.I	5.00	2.07	0.85	-	-	-	-	-	-
Total	98.89	100.10	100.14	100	101	100.1	99.53	99.99	101.22
Trace elements in ppm									
Sc	22	26	13	-	-	-	-	-	-
V	215	230	122	-	-	197	293	189	162
Co	21	45	19	-	-	-	-	-	-
Cr	85	275	66	-	-	30	21	958	24
Ni	40	84	30	-	-	9	16	267	18
Cu	76	52	128	-	-	-	-	-	-
Pb	6	5	13	-	-	-	-	-	-
Zn	82	100	76	-	-	-	-	-	-
Sr	986	638	751	832	799	1657	698	22	557
Rb	8	18	75	9.5	184	3	27	1	116
Ba	80	177	395	182	388	23	411	11	707
Th	2	3	10						
Nb	2	1	7	3.11	20	1.2	1.7	0.7	9.2
Y	22	16	23	14.7	43	20	15	9	22
Zr	48	26	105	66.8	175	100	53	34	154
Hf	7	5	5	1.9	4.8	-	-	-	-
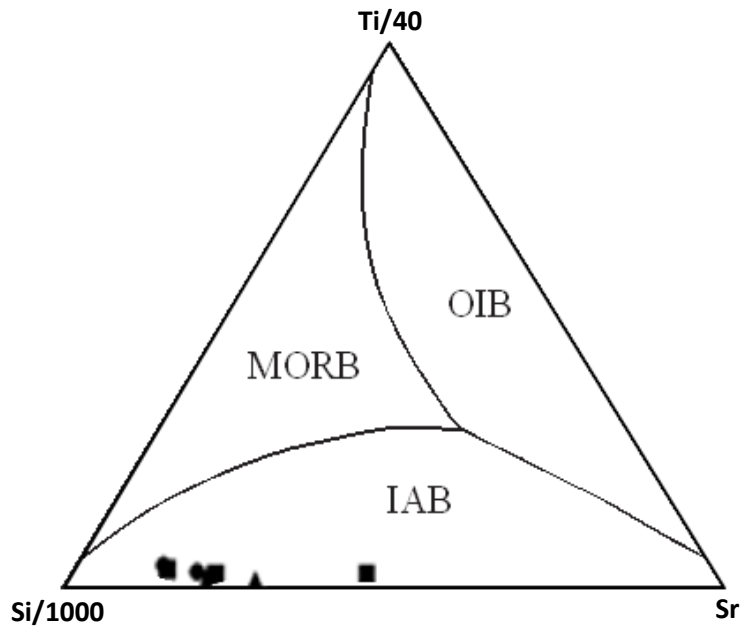
Fig.7.1. Trace elements ternary diagram for the rocks of different tectonic environments (after Vermeesh, 2006). OIB= ocean island basalts, IAB= island arc basalts, MORB= mid-oceanic ridge basalts. Symbols as shown in Figure 6.3.
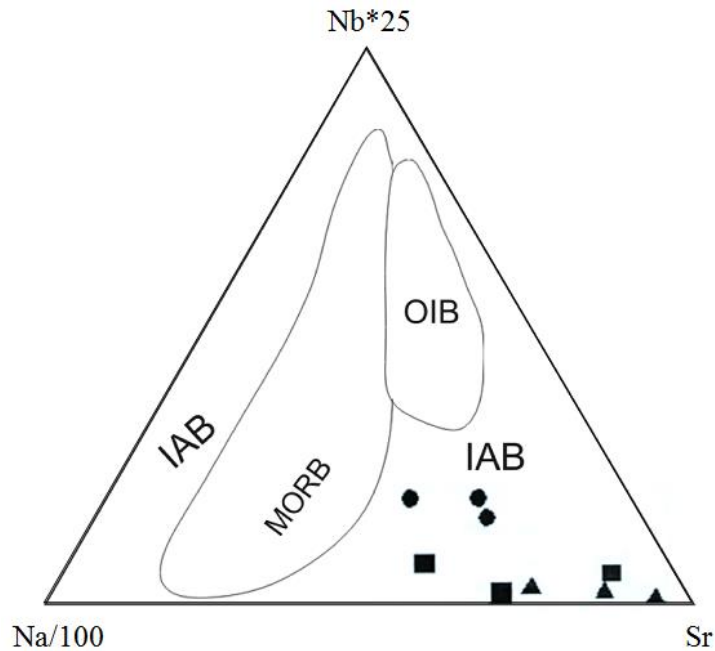
Fig.7.2. Plotting of rocks of the study area in the discrimination ternary diagram of trace elements showing different tectonic environments (after Vermeesch, 2006). IAB= island arc basalts, MORB= mid oceanic ridge basalts, OIB= ocean island basalts. Symbols as shown in Figure 6.3.
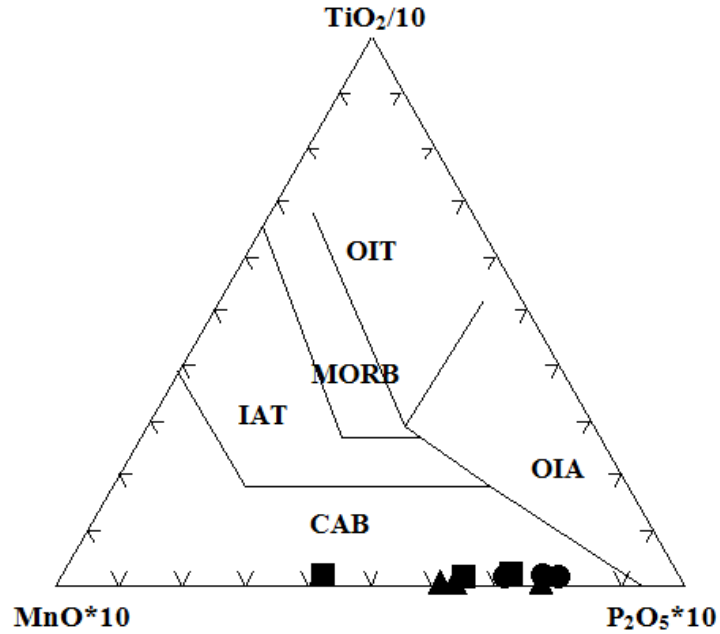
Fig.7.3. Plotting of rocks of the study area in the discrimination ternary diagram of Mullen (1983), differentiating various tectonic settings by using major oxides MnO, P_2O_5 and TiO_2. OIT= ocean island tholeiites, MORB= mid ocean ridge basalts, CAB= calc-alkaline basalts), IAT= island arc tholeiites, and OIA= ocean island arc. Symbols shown as in Figure 6.3.
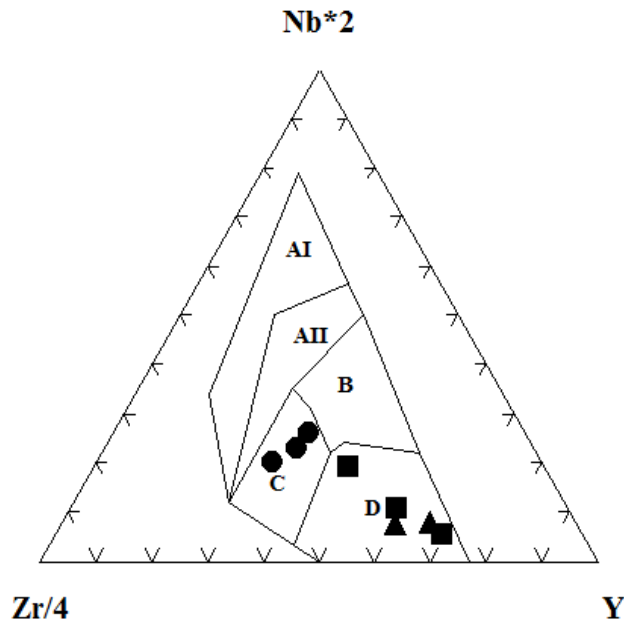
Fig.7.4. Plotting of rocks of the study area in the discrimination ternary diagram of Meschede (1986) on the basis of Zr, Nb and Y. AI= within-plate alkali basalt, AII= within-plate alkali basalt and within-plate tholeiites, B= E-type MORB, C= within-plate tholeiites and volcanic arc basalt, D= N-type MORB and volcanic arc basalt.
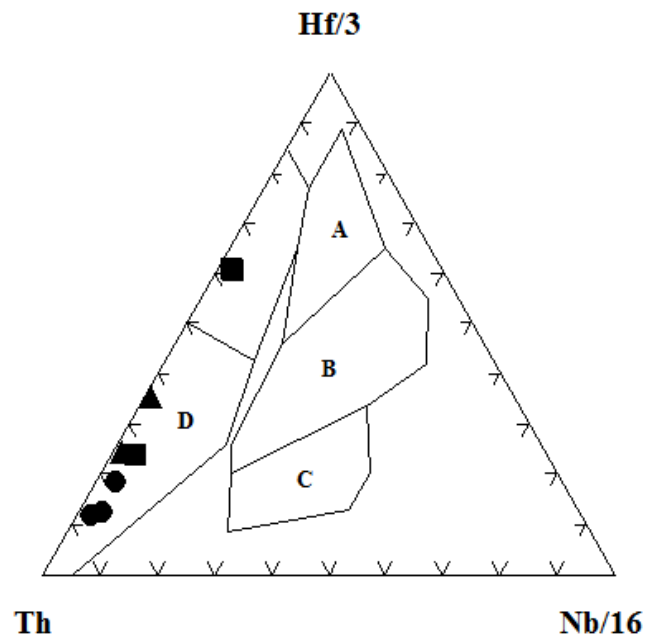
Fig.7.5. Plotting of the rocks of the study area in the discrimination diagram on the basis of Nb, Th and Hf (after Wood, 1980). A= N-type MORB, B= E-type MORB and within-plate tholeiites, C= alkaline within-plate basalts, D= destructive plate-margin basalts and differentiate.
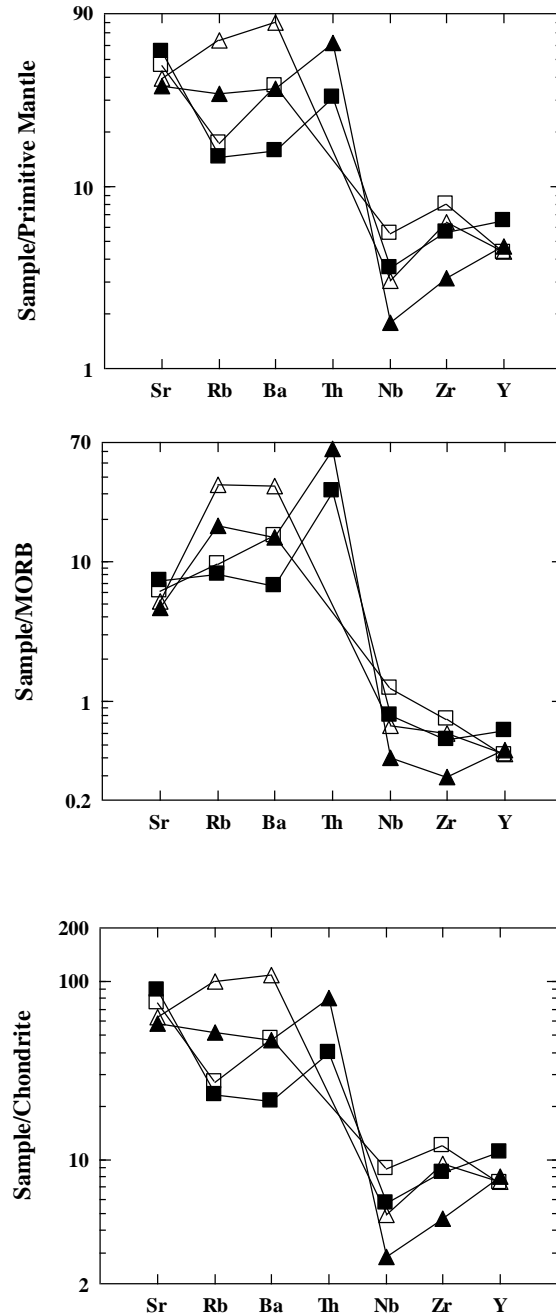
Fig.7.6. Spider variaiton diagram showing the comparision of the average trace elements of the BASD and IVC volcanics of this study with the similar composition volcanics of Teru volcanic Formaiton of Khan et al. (2004) and Ghizar Formaiton of Petterson and Windley (1991). ■= BASD (this study) , ▲= IVS volcanics (this study), □= rock sample from Khan et al. (2004) △= rock sample from Petterson and Windley (1991).
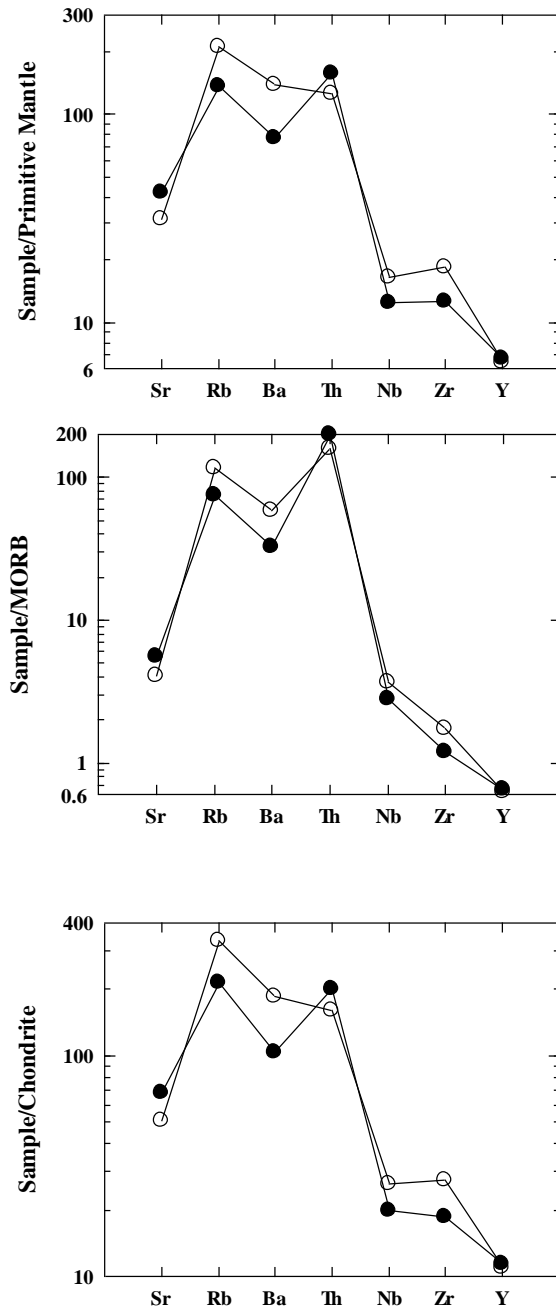
Fig.7.7. Spider variation diagram showing the comparsion of the average diorites of this study with the stage-2 diorites of Petterson and Windley (1991). ●=Diorite (this study), ○= diorite of stage-2 from Petterson and Windley (1991).

CONCLUSIONS

The following conclusions are made after the completion of this study.

- The area of study contains the rocks of the two entities, i.e., Kohistan island arc and Karakoram plate, separated by the Northern Suture zone.

- Most part of the study area is covered by the rocks of the Kohistan island arc such as the Ishkoman volcanic centre volcanics, baslat-andesite sheet dominant volcanics and diorites intruding the Ishkoman volcanic centre volcanics.

- The basalt-andesite sheet dominant volcanics are highly deformed and metamorphosed while the Ishkoman volcanic centre volcanics are undeformed/less deformed.

- Shearing along local faults is very common in these volcanics where the alteration and leaching of sulfides are common.

- Petrographically the Ishkoman volcanic centre volcanics dominantly contain plagioclase, augite and hornblende phenocrysts set in a felsophyric/cryptocrystalline groundmass.

- On the basis of variable amount of augite and hornblende phenocrysts in the Ishkoman volcanic centre volcanics, these rocks are classified as augite dominant basaltic-andesite porphyry and hornblende dominant basaltic-andesite porphyry.

- Petrographically the basalt-andesite sheet dominant volcanics are dominantly comprised of phenocryst of plagioclase and hornblende surrounded by groundmass containing chlorite, epidote and tremolit/actinolite. The plagioclase phenocrysts exhibit severe alteration in these volcanics.

- Petrographically diorites of the study area can be divided into two groups; one is having plagioclase, biotite and horblende while the other is having plagioclase, biotite and augites. The minor amount of other minerals like quartz, alkali-feldspar and epidote are also present in these rocks.

- On the basis of whole rock geochemistry, the basalt-andesite sheet dominant volcanics are classified as olivine normative basalts and the Ishkoman volcanic centre volcanics as olivine normative basaltic-andesites.

- The major and trace elements of the volcanic rocks of Iskoman volcanic centre, basalt-andesite sheet dominant volcanics and the diorites exhibit calc-alkaline nature, which are enriched in LILEs and showing strong negative anomaly for Nb and strong positive anomaly for Sr.

- The chemical characteristics of these rocks have subduction related island arc type of signature which is suggesting the formation of these rocks in the Kohistan island arc.

- Petro-chemically, the volcanic rocks, especially the Ishkoman volcanic centre volcanics, of the study area can be correlated with the rocks of the Teru Volcanic formation/Shamran volcanic exposed in the west of the study area.

- The gain and loss of gold, silver and the base metals in the altered/sulfide bearing sheared zones during alteration, could be hydrothermal alteration, suggest that there is no any economic concentration of these metals in these zones.

REFERENCES

Austromineral, 1976. Final report (feasibility study), Indus gold project: submitted to Pakistan Mineral Development Corporation by Austromineral, Vienna, Austria, 1-235.

Austromineral, 1978. Feasibility study (final report), Mineral exploration and mining development, Chitral District: submitted to Sarhad Development Authority, Peshawar Pakistan by Austromineral, Vienna, Austria, 1-289.

Bard, J.P., 1983. Metamorphic evolution of an obducted island arc: example of the Kohistan sequence (Pakistan) in the Himalayan collided range. Geological Bulletin, University of Peshawar, 16, 105-184.

Bard, J.P., Maluski, H., Matte, P., Proust, F., 1980. The Kohistan sequence, crust and mantle of an obducted island arc. Tahirkheli, R.A.K., Jan, M.Q., Majid, M, (editors), Geological Bulletin, University of Peshawar, 13, 87-94.

Beck, R.A., Burbank, D.W., Sercombe, W.J., Riley, G.W., Barndt, J.K., Bery, J.R., Afzal, J., Khan, A.M., Jurgen, H., Metje, J., Cheema, A., Shafique, N.A., Lawrence, R.D., Khan, M.A., 1995. Stratigraphic evidence for an early collision between Northwest India and Asia. Nature, 373, 55-57.

Bevins, R.E., Kokelaar, B.P., Dunkley, P.N., 1984. Petrology and geochemistry of lower to middle Ordovician igneous rocks in Wales: a volcanic arc to marginal basin transition. Proceedings of the Geologists Association, 95, 337-347.

Bignold, S.M., Treloar, P.J., 2003. Northward subduction of the Indian plate beneath the Kohistan island arc, Pakistan Himalaya: new evidence from isotopic data. Journal of Geological Society of London, 160, 377-384.

Calkins, J.A., Jamiluddin, S., Kamaluddin, B., Hussain, A., 1969. Geology and mineral resources of Chitral state, West Pakistan. Geological Survey of Pakistan, Unpublished report-Quetta.

Chatterjee, S., Goswami, A., Scotese, C.R., 2013. The longest voyage: Tectonic, magmatic, and paleoclimatic evolution of the Indian plate during its northward flight from Gondwana to Asia. Gondwana Research, 23, 238-268.

Clift, P.D., Hannigan, R., Blustajn, J., Draul., A.F., 2002. Geochemical evolution of the Dras-Kohistan arc during collision with Eurasia: evidence from the Ladakh Himalaya, India. The Island Arc, 11, 255-273.

Corfield, R.I., Searle, M.P., Green, O.R., 1999. Photang thrust sheet- an accretionary complex structurally below the Spontang ophiolite constraining timing and tectonic environment of ophiolite obduction, Ladakh Himalaya. Journal of the Geological Society, London, 156, 1031-1044.

Corfield, R.I., Searle, M.P., Pedersen, R.B., 2001. Tectonic setting, origin, and obduction history of the Spontang ophiolite, Ladakh Himalaya, NW India. Journal of Geology 109, 715-736.

Coward, M.P., Butler, R.W.H., Khan, M.A., Knipe, R.J., 1987. The tectonic history of Kohistan and its implications for Himalayan structure. Journal of Geological Society of London, 144, 377-391.

Coward, M.P., Jan, M.Q., Rex, D., Tarney, J., Thirlwall, M., Windley, B.F., 1982. Geotectonic framework of the Himalaya of N. Pakistan. Journal of Geological Society of London, 139, 299-303.

Coward, M.P., Windley, B.F., Broughton, R.D., Luff, I.W., Petterson, M.G., Pudsey, C.J., Rex, D.C., Khan, M.A., 1986. Collision tectonics in the NW Himalayas, in collision tectonics, edited by M.P. Coward and A.C. Ries. Special publication, Geological Society of London, 19, 203-219.

Cox, K.G., Bell, J.D., Pankhurst, R.J., 1979. The interpretation of igneous rocks. George, Allen and Unwin, London.

Crawford, M.B., Searle, M.P., 1992. Field relations and granitoid magmatism in the central Karakoram, northern Pakistan. Tectonophysics, 206, 171-192.

Danishwar, S., Stern, R.J., Khan, M.A., 2001. Field relations and structural constraints for the Teru volcanic formation, Northern Kohistan Terrane, Pakistani Himalayas. Journal of Asian Earth Sciences, 19, 683-695.

Debon, F., 1995. Incipient india-Eurasia collision and plutonism: The lower Cenozoic Batura granites (Hunza Karakorum, north Pakistan), Journal of Geological Society of London, 152, 785-795.

Debon, F., Le Fort, P., Dautel, D., Sonet, J., Zimmermann, J.L., 1987. Granites of western karakoram and northern Kohistan (Pakistan): A composite Mid-Cretaceous to upper Cenozoic magmatism. Lithos, 20, 19-40.

Ding, L., Kapp, P., and Wan, X., 2005, Paleocene-Eocene record of ophiolite obduction and initial India-Asia collision, south central Tibet: Tectonics, v. 24, p. TC3001, doi: 10.1029/2004TC001729.

Fraser, J., Searle, M.P., Parrish, R., Noble, S., 1999. U-Pb geochronology on the timing of metamorphism and magmatism in the Hunza Karakoram. Terra Nostra, 99/2, 45-46.

Gaetani, M., Le fort, P., Tanoli, S., Angiolini, L., Nicora, A., Sciunnach, D., Khan, A., 1996. Reconnaissance geology in the upper Chitral, Baroghil and Karamber districts (northern karakoram Pakistan). Geology Rundsch, 85, 683-740.

Halfpenny, R., Mazzucchelli, R.H., 1999. Regional multi-element drainage geochemistry in the Himalayan mountains, northern Pakistan. Journal of Geochemical Exploration, 67, 223-233.

Hamidullah, S., Jan, M.Q., 1986. Preliminary petrochemical study of the Chilas complex, Kohistan island arc, Northern Pakistan. Geological Bulletin, University of Peshawar, 19, 157-182.

Hanson, C.R., 1989. The northern suture in the Shigar Valley, Baltistan, northern Pakistan, in Malinconico, L.L.J. and Lillie, R.J., eds., Tectonics of the Western Himalayas, Geological Society of America, Special paper, 232, 203-215.

Hayden, H.H., 1914. Notes on the geology of Chitral and Gilgit and the Pamirs. Records of the Geological survey of India, 45, 271-335.

Hofmann, A.W., 1988. Chemical differentiation of the earth: The relationship between mantle, continental crust, and oceanic crust. Earth and Planetary Science letters, 90, 297 - 314.

Irvine, T.N., Barager, W.R.A., 1971. A guide to the chemical classification of the common volcanic rocks. Canadian Journal of Science, 8, 523-548.

Ivanac, J.F., Traves, D.M., King, D., 1956. The geology of the northwest portion of Gilgit agency. Records of Geological Survey of Pakistan, 8 (2), 3-26.

Jan, M.Q., 1988. Relative abundances of minor and trace elements in mafic phases from the southern part of the Kohistan arc. Geological Bulletin, University of Peshawar, 21, 15-25.

Jan, M.Q., 1990. Petrology and geochemistry of the southern amphibolites of the Kohistan arc, N. Pakistan. In: Sharma, K.K. (ed.) Geology and geodynamic evolution of the Himalayan collision zone. Physics and Chemistry of Earth, 17, 71-92.

Jan, M.Q., Howie, R.A., 1981. The mineralogy and geochemistry of the metamorphosed basic and ultrabasic rocks of the Jijal complex, Kohistan, NW Pakistan. Journal of Petrology, 22, 85-126.

Jefferry, P. G., Hutchison, D., 1986. Chemical Methods of rock analysis. Pergamon press, New York.

Kazmi, A.H., Jan, M.Q., 1997. Geology and Tectonics of Pakistan. Graphic publishers, Karachi, Pakistan.

Khan, M.A., Habib, M., Jan, M.Q., 1985. Ultramafic and mafic rocks of Thurly Gah and their relationship to the Chilas complex, N. Pakistan. Geological Bulletin, University of Peshawar, 18, 83-102.

Khan, M.A., Jan, M.Q., Weaver, B.L., 1993. Evolution of the lower arc crust in Kohistan: Temporal arc magmatism through early, mature and intra-arc rift stages, in Himalayan Tectonics, edited by P.J Treloar and M.P Searle. Journal of Geological Society of London, Special Publication, 74, 123-138.

Khan, M.A., Jan, M.Q., Windley, B.F., Tarney, J., Thirlwall, M.F., 1989. The Chilas mafic-ultramafic igneous complex: The root of the Kohistan island arc in the Himalaya of northern Pakistan. Special Paper, Geological Society of America, 232, 75-94.

Khan, S.D., Stern, R.J., Manton, M.I., Copeland, P., Kimura, J.I., Khan, M.A., 2004. Age, geochemical and Sr-Nd-Pb isotopic constraints for mantle source characteristics and

petrogenesis of Teru Volcanics, Northern Kohistan Terrane, Pakistan. Tectonophysics, 393, 263-280.

Khan, S.D., Walker, D.J., Hall, S., Burke, K., Shah, M.T., Stockli, L., 2009. Did Kohistan-Ladakh island arc collide first with India? Geological society of America Bulletin, 121 (3/4), 366-384.

Khan, T., 1994. Evolution of the "Upper and Middle Crust in Kohistan Island Arc", North Pakistan. Unpublished Ph.D thesis, National Centre of Excellence in Geology, University of Peshawar, 1-225.

Khan, T., Kausar, A.B., Takahashi, Yut., Takahashi, Yuh., 1995. Geochemistry of mafic and ultramafic rocks of the Chilas Complex, Chilas, northern Pakistan. Geological Research Bulletin, Geoscience Laboratory, Geological Survey of Pakistan, 1, 15-22.

Khan, T., Murata, M., Karim, T., Zafar, M., Ozawa, H., Rehman, H.U., 2007. A cretaceous dike swarm provides evidence of a spreading axis in the back-arc basin of the Kohistan paleo-island arc, northwestern Himalaya, Pakistan. Journal of Asian Earth Sciences, 29, 350-360.

Khan, T., Murata, M., Zafar, M., Rehman, H.U., 2011. Petrogenetic comparison of the mafic dykes in the Kohistan paleo-island arc-back-arc system, Himalayas of North Pakistan. Dyke Swarms: keys for Geodynamic interpretation, Springer, 437-455.

Khan, T., Shirahase, T., 1996. Evolution of the Kohistan terrane with reference to Jaglot Group and the Chilas Complex, Gilgit-Chilas, northern Pakistan. proceeding of Geoscience Colloquium, Geoscience Laboratory, Geological Survey of Pakistan, 15, 15-36.

Klootwijk, C.T., Peirce, J.W., 1979. India's and Australia's pole path since the Late Mesozoic and India-Asia collision. Nature, 282, 1-3.

Le Bas, M.J., Lemaitre, R.W., Streckeisen, A., Zanettin, B., 1986. A chemical classification of volcanic rocks based on the total alkali silica diagram. Journal of Petrology, 27(3), 745-750.

Meschede, M., 1986. A method of discriminating between different types of mid-oceanic ridge basalts and continental tholeiites with the Nb-Zr-Y diagram. Chemical Geology, 56, 207-218.

Molnar, P., and Tapponnier, P., 1975. Cenozoic tectonics of Asia-Effects of a continental collision: Science, V, 86, PP 1093-1102.

Mullen, E.D., 1983. Mno/TiO$_2$/P$_2$O$_5$: A minor element discriminant for basaltic rocks of oceanic environments and its implications for petrogenesis. Earth and Planetary Science Letters, 62, 53-62.

Pakistan Mineral Development Corporation, 2001. Geochemical exploration and evaluation of gold and base metals, northern areas, Pakistan. Final Report. PMDC, Volume 1-4.

Pearce, J.A., Cann, J.R., 1971. Ophiolite origin investigated by discriminant analysiss using Ti, Zr and Y. Earth and Planetary Science Letters, 12, 339-349.

Pearce, J.A., Cann, J.R., 1973. Tectonic setting of basic volcanic rocks determined using trace element analyses. Earth and planetary Science Letters, 19, 290-300.

Petterson, M.G., Treloar, P.J., 2004. Volcanostratigraphy of arc volcanic sequences in the Kohistan arc, North Pakistan: volcanism within island arc, back-arc-basin, and intra-continental tectonic settings. Journal of Volcanology and Geothermal Research, 130, 147-178.

Petterson, M.G., Windley, B.F., 1985. Rb-Sr dating of the Kohistan arc batholith in the Himalaya of N. Pakistan. Earth and Planetary Science Letters, 74, 54-75.

Petterson, M.G., Windley, B.F., 1991. Changing source regions of magmas and crustal growth in the Trans-Himalayas: evidence from the Chalt volcanics and Kohistan batholith, Kohistan, northern Pakistan. Earth and Planetary Science Letters, 102, 326-341.

Pudsey, C.J., 1986. The northern suture, Pakistan: Margin of a Cretaceous island arc. Geological Magazine, 123, 405-423.

Pudsey, C.J., Schroider, R., Skelton, P.W., 1985. Cretaceous (Aptian/Albian) age for island arc volcanics. Kohistan, N. Pakistan. Contribution to the Himalayan Geology, 3, 150-168.

Rehman, H.U., Seno, T., Yamamoto, H., Khan, T., 2011. Timing of collision of the Kohistan-Ladakh Arc with India and Asia: Debate. Island Arc, 20, 308-328.

Reuber, I., 1986. Geometry of accretion and oceanic thrusting of the Spongtang Ophiolite, Ladakh-Himalaya. Nature, 321, 592-596.

Rex, A.J., Searle, M.P., Timul, R., Crawford, M.B., Prior, D.J., Rex, D.C., Barnicoat, A., 1988. The geochemical and tectonic evolution of the central Karakoram, north Pakistan. Philos. Trans. Royal Society of London, seires, A, 326, 229-255.

Rowley, D.B., 1996. Age of initiation of collision between India and Asia: a review of stratigraphic data. Earth and Planetary Science Letters, 145, 1-3.

Saunders, A.D., Tarney, J., 1991. Back-arc basins. In: Floyd, P.A. (eds.) Oceanic basalts. Blackie and Nostrand Teihold, 219-263.

Scharer, u., Xu, R.H., Allegre, C.J., 1984. U-Pb geochronology of Gandase, Transhimalya.Plutonism in the Lahasa-Xigaze region, Tibet. Earth and Planetary Science letters, 69, 311-320.

Searle, M.P., 1991. Geology and tectonics of the Karakoram mountains. Wiley, chichester, 1-358.

Searle, M.P., 1999. Extensional and compressional faults in the Everest-Lhotse massif, Khumbu Himalaya, Nepal. Journal of Geological Society, London, 156, 227-240.

Searle, M.P., Khan, M.A., 1996. Geological Map of North Pakistan and Adjacent Areas of Northern Ladakh and Western Tibet, Scale 1:650,000. Oxford University, Oxford, England.

Shah, M.T., 1991. Geochemistry, mineralogy and petrology of the sulfide mineralization and associated rocks in the area around Besham and Dir, Northern Pakistan. Unpublished Ph.D thesis, University of South Carolina Columbia.

Shah, M.T., Majid, M., Hamidullah, S., Shervais, J.W., 1992. Petrochemistry of amphibolites from Shergarh Sar area, Allai Kohistan, N. Pakistan. Kashmir Journal of Geology, 10, 123-139.

Shah, M.T., Shervais, J.W., 1999. The Dir-Utror metavolcanic sequence, Koistan arc terrance, northern Pakistan. Journal of Asian Earth Sciences, 17, 459-475.

Sharma, K.K., Gupta, K.R., 1983. Calc-alkaline island arc volcanism in Indus-Tsangpo Suture zone. In: Sharma, K.K. (Ed.) Geology and Geodynamic Evolution of the Himalayan collision zone. Part-2, Physics and Chemistry of the Earth, 18, 71-78.

Shervais, J. W., 1982. Ti-V plots and the petrogenesis of modern and ophiolitic lavas. Earth and Planetary Science Letters, 59, 101-118.

Smith, R.E., Smith, S.E., 1976. Comments on the use of Ti, Zr, Y, Sr, K, P, and Nb in classification of basaltic magmas. Earth and Planetary Science Letters, 32, 114-120.

Stolz, A.J., Jochum, K.P., Spettel, B., Hofmann, A.W., 1996. Fluid and melt related enrichment in the subarc mantle: evidence from Nb/Ta variations in island-arc basalts. Geology, 24, 587-590.

Sullivan, M.A., Windley, B.F., Saunders, A.D., Haynes, J.R., Rex, D.C., 1993. A palaeogeographic reconstruction of the Dir Group: evidence for magmatic arc migration within Kohistan, N, Pakistan. Geological society special publication, 74, 139-160.

Sun, S.S., 1980. Lead isotopic study of young volcanic rocks from mid-ocean ridges, ocean islands and island arcs. Philosophical Transactions of the Royal Society, A297, 409-445.

Sweatman, T.R., Clavarino, J.G., Dawney, R.L., 1995. Drainage geochemical exploration and mineral potential of Northern Pakistan. Third report by Rex Sweatman and Associates for Australian Agency for International Development.

Tahirkheli, R.A.K., 1974. Alluvial gold prospects in the North-west west Pakistan. National Centre of Excellence in Geology, University of Peshawar, Information Release No.7. 1-50.

Tahirkheli, R.A.K., 1979. Geology of Kohistan and adjoining Eurasian and Indo-Pakistan continents, Pakistan. Geological Bulletin, University of Peshawar, 11, 1-30.

Tahirkheli, R.A.K., 1982. Geology of the Himalaya, Karakoram and Hindukash in Paksitan. Geological Bulletin, University of Peshawar, 15, 1-50.

Tahirkheli, R.A.K., 1994. A macro-over view of geology of Pakistan. Paper presented at international round table conference on foreign investment in exploration and mining in Pakistan. 1-13.

Tahirkheli, R.A.K., Jan, M.Q., 1979. Geology of Kohistan, Karakoram Himalaya, northern Pakistan. Geological Bulletin, University of Peshawar, 11, 1-187.

Tahirkheli, R.A.K., Jan, M.Q., 1984. The geographic and geologic domains of the Karakoram, International Karakoram Project, (K.J. Miller, ed.). Royal Geological Society of London, 2, 57-70.

Tahirkheli, R.A.K., Mattauer, M., Proust, F., Tapponnier, P., 1979. The India-Eurasia suture zone in northern Pakistan: Synthesis and interpretation of recent data at plate scale, in Geodynamics of Pakistan, edited by A. Farah and K.A. Dejong. Geological survey of Pakistan, 125-130.

Taylor, S.R., Mclennan, S.M., 1985. The continental crust: its composition and evolution. Blackwell, Oxford.

Thompson, R.N., 1982. British Tertiary volcanic province. Scottish Journal of Geology, 18, 49-107.

Treloar, P.J, O'Brien, P.J., Parrish, R.R., Khan, M.A., 2003. Exhumation of early Tertiary coesite bearing eclogites from the Pakistan Himalaya. Journal of the Geological Society, London, 160, 367-376.

Treloar, P.J., Petterson, M.G., Jan, M.Q., Sullivan, M.A., 1996. A re-evaluation of the stratigraphy and evolution of the Kohistan arc sequence, Pakistan Himalaya: implications for magmatic and tectonic arc-building processes. Journal of the Geological Society, London, 153, 681-693.

Treloar, P.J., Rex, F.C., Guise, P.G., Cowar, M.P., Searle, M.P., Windley, B.F., Petterson, M.G., Jan, M.Q., Luff, I.W., 1989. K-Ar and Ar-Ar geochronology of the Himalayan collision in NW Pakistan. constraints on the timming of suturing, deformation, metamorphism and uplift. Tectonics, 8, 881-909.

Vermeesch, P., 2006. Tectonic discrimination diagrams revisited. Geochemistry, Geophysics, Geosystems, 7(6), 1-68.

Wilson, M., 1989. Igneous petrogenesis. Unwin Hyman, London.

Winchester, J.A., Floyd, P.A., 1977. Geochemical discrimination of different magma series and their differentiation products using immobile elements. Chemical Geology, 20, 325-343.

Wood, D.A., 1980. The application of a Th-Hf-Ta diagram to problems of tectonomagmatic classification and to establishing the nature of crustal contamination of basaltic lavas of the British Tertiary volcanic province. Earth and Planetary Science letters, 50, 11-30.

Wood, D.A., Joron, J.L., Treuil, M., 1979. A re-appraisal of the use of trace elements to classify and discriminate between magma series erupted in different tectonic settings. Earth and Planetary Science Letters, 45, 326-336.

Yin, A., 2006. Cenozoic tectonic evolution of the Himalayan orogen as constrained by along-strike variation structural geometry, exhumation history, and foreland sedimentation. Earth-Science Reviews, 76, 1–131.

Yin, A., Harrison, T.M., 2000. Geologic evolution of the Himalayan-Tibetan orogeny. Annual review of Earth and Planetary Sciences, 28, 211-280.

Zanchi, A., Gaetani, M., 1994. Introduction to the geological map of north karakoram terrain from the Chapursan valley to Shimshal pass 1:150,000 scale. Rivista Italian dt Paleontolgia I Stratigraphia, 100, 125-136. London.

Zeitler, P.K., 1982. Uproofing history of a suture zone in the Himalaya of Pakistan by means of fission-track annealing ages. Earth and Planetary Science letters, 57, 227-240.

Ziabrev, S.V., Aitchison, J.C., Abrajevitch, A., Badengzhu, Davis, A.M., Luo, H., 2004. Bainang Terrane, Yarlung-Tsangpo suture, southern Tibet: a record of intra-Tethyan subductin on the roof of the world. Journal of the Geological Society, 161(3), 523-538.